The University of Michigan • Office of Research Administration
Ann Arbor, Michigan

SENSITIVITY OF THE CREEP-RUPTURE PROPERTIES OF WASPALOY SHEET TO SHARP-EDGED NOTCHES IN THE TEMPERATURE RANGE OF 1000°-1400°F

by

David J. Wilson
James W. Freeman
Paul D. Goodell

Report 04368-14-T February 1968

Progress Report to:

National Aeronatuics and Space Administration
Washington, D. C. 20025
Project 04368 - Grant NsG-124-61

TABLE OF CONTENTS

TABLE OF CONTENTS

LIST OF TABLES

LIST OF FIGURES

LIST OF FIGURES, continued

LIST OF FIGURES, continued

SUMMARY

A study was made of the scope and cause of the edge-notch sensitivity exhibited by nickel-base superalloy sheet material in creep-rupture in the intermediate temperature range. Heat treatment variations of Waspaloy were used to enable the evaluation of the influence of microstructural and mechanical property variation on the notch sensitivity at 1000°, 1200° and 1400°F of 0.026-inch thick material. In addition, exploratory tests on the influence of sheet thickness on the notch sensitivity were undertaken.

The results showed that the microstructural variations produced by heat treatment influenced the plastic deformation characteristics, which seem to control the notch sensitivity most directly. The notch sensitivity appears to fall in the general range where plastic flow is limited by low yielding and/or creep deformation.

Rupture of both smooth and notched specimens occurred by intergranular crack initiation and growth, apparently by creep, until abrupt transgranular failure occurred due to the increase in stress on the reduced load-bearing area. The time-to-rupture was governed by all of these fracture processes. However, the initiation and growth of the intergranular cracks consumed most of the time leading to rupture. Also, it was evident that for a given stress and temperature, the difference in rupture times for smooth and notched specimens (i.e., the notch sensitivity) was determined primarily by the times for the first stages of intergranular cracking.

Relaxation of the stresses around the notches was a critical factor affecting the intergranular failure process and, thus, the notch sensitivity. The relaxation resulted from deformation by yielding and by subsequent creep. On the other hand, excessive creep could promote intergranular cracking. The interaction of these two effects apparently resulted in the notch sensitivity being dependent upon the time-dependence of the processes contributing to the ductility of the material, as well as to the actual level

of ductility itself.

The limited study of 0.050-inch thick specimens did not show the increase in notch sensitivity with time that was exhibited for the 0.026-inch thick materials. Additional research is needed to establish if this is a stress-strain state relaxation phenomenon, or if surface effects are involved.

INTRODUCTION

Results are presented for an investigation now underway to determine the scope and causes of the severe time-dependent, edge-notch sensitivity of nickel-base superalloy sheet materials at 1000° and 1200°F. The alloys studied were the most promising ones derived from a survey investigation (ref. 1) of sheet materials for supersonic transport (SST) construction. The sensitivity to notches is so severe that failures had been observed in less than 1000 hours at 1000°F under stresses of 40,000 psi; this stress was a conservative design stress based on tensile-yield strength criteria rather than on the much higher creep-rupture strengths. Failures in such short time periods due to exposure at low stresses and low temperatures for the alloys were entirely unexpected because smooth specimen rupture strengths were well over 100,000 psi, and the ratios of smooth specimen strengths to notched specimen strengths (N/S ratio) in tensile tests were high. There was no reason to expect that such "stable" materials as the superalloys would show a marked time-dependent decrease in N/S ratio at all, and especially not in the short time periods observed.

The occurrence of time-dependent, edge-notch sensitivity had not been establsihed previously. The original concept of the SST materials program was based on the short-time tensile properties and their retention without embrittlement during exposure. It had not been anticiapted that it would be necessary to consider a "creep-rupture" type notch sensitivity phenomenon to consider. However, once this phenomenon became known, it was important to establish the causes and scope of the problem for the following reasons:

1. The most stable and heat-resistant alloys available would be severely temperature-limited unless means could be found to avoid the notch sensitivity.

2. A serious question was now raised as to whether or not time-dependent stress concentration sensitivity in the

intermediate temperature range (that is, between the points where short-time strength characteristics and creep characteristics control design) might not be far more important than had been recognized.

3. It is possible that this same phenomenon could occur in other alloys at temperatures below the range where creep-rupture properties govern design stresses.

BACKGROUND

Extensive research on the part of many laboratories has been carried out to determine the potential usefulness of various alloys in sheet form for building the SST. In an early evaluation program (ref. 1), the three superalloys which had the most promising properties for a Mach 3 transport were René 41, Waspaloy and Inconel 718. This selection was based on exposure up to 650°F for 1000 hours under a stress of 40,000 psi, followed by tensile tests at from -110°F to 650°F, using both smooth and edge-notched specimens. The results were evaluated on the basis of stability of strength properties and retention of resistance to catastrophic crack propagation in the tensile tests after exposure.

In the investigation of superalloys, the University of Michigan had the additional responsibility of conducting survey tests which would indicate their upper temperature of usefulness. This was done by increasing the exposure temperature to 800°, 1000° and 1200°F, under a stress of 40,000 psi for 1000 hours, with the intention of subsequently conducting tensile tests to determine retention of strength and resistance to catastrophic crack propagation. Several of the notched specimens failed unexpectedly during exposure at 1000°F in less than 1000 hours. These failures resulted from the initiation and development of intergranular cracks at the notches. The failures were erratic and some specimens survived exposure without failure. During subsequent tensile tests of these unfailed specimens, no significant change in tensile properties were found to have

resulted from exposure.

The failures of notched specimens during exposure at 1000°F suggested that there could be a marked time dependence of strength even though the temperatures were far below those at which it would be expected. Subsequent characterization of the sensitivity to edge notches revealed a marked time dependence at 1000° and 1200°F. Figure 1 is an example taken from a prior report. It was also found that while sharp notches were originally used to simulate cracks, in many cases the notches did not have to be very sharp to induce premature fracture at relatively low loads.

The time-dependent notch sensitivity could be the property limiting the upper temperature at which the superalloys could be used in sheet form, particularly for SST applications. At least no data had indicated that stressed exposure at elevated temperatures which did not cause cracking, also did not significantly change the tensile properties or catastrophic crack propagation resistance. While time-dependent stress concentration sensitivity is important in superalloys, it is perhaps more important to know if it also occurs, unrecognized, in other alloys in the intermediate temperature range where design stresses are based on tensile-yield strengths, but where limited creep can occur.

BASIS OF RESEARCH

The experimental program being reported was based on the concept that the notch sensitivity would be closely related to certain microstructural and/or mechanical properties. Thus, in seeking to determine the scope and causes of this behavior, the research utilized Waspaloy and Inconel 718, between which extensive variation of significant microstructural features (and, therefore, mechanical characteristics) were generated by appropriate solution and aging treatments. Variations in test conditions, particularly the extension of the test temperature to 1400°F, were also expected to help delineate the causes by shifting the strength-controlling property more towards creep.

The two alloys studied in this investigation belong to the same family. However, they have marked metallurgical differences. The dispersion hardening phase in Waspaloy is $Ni_3(Al, Ti)$, known as γ', whereas, in Inconel 718, this phase contains a significant proportion of Cb. The presence of Cb in Inconel 718 results not only in a sluggish γ' reaction when compared to the other alloy, but also in substantial differences in the carbide phase and in other minor phases.

Because of the extensive differences between the alloys chosen for this investigation and for ease of presentation, the results are presented in two reports. The present report will deal with the results obtained from the study of Waspaloy, while a second report will consider Inconel 718.

Both the solution and aging treatments of Waspaloy have a significant influence on the resulting microstructure, particularly on the amount and distribution of the carbide and γ' phases. The following four solution treatments were selected for this investigation:

1. A high-temperature heat treatment to insure complete solution of the γ' and $M_{23}C_6$ carbide:
   1/2 hour at 2150°F

2. A solution treatment to dissolve the γ' and the majority of the $M_{23}C_6$, but low enough to prevent grain growth:
   1/2 hour at 1975°F

3. An intermediate solution treatment to dissolve the γ', with only limited solution of the $M_{23}C_6$ carbide:
   1/2 hour at 1900°F

4. A low-temperature solution treatment to partially dissolve the γ', with only slight solution of $M_{23}C_6$:
   1/2 hour at 1825°F

Two separate aging treatments: 16 hours at 1400°F and 10 hours at 1700°F, were applied after each of these solution treatments. The aging treatments were designed to produce γ' particles whose average size would vary by an order of magnitude. The aging treatment at 1400°F was chosen so that, when applied with the 1975°F heat treatment, the combination would be

typical of commercial practice.

Very little rupture data have been obtained on sheet specimens of superalloys at temperatures above 1200°F. Since short-time, high-temperature applications for sheet materials will undoubtedly arise, it was considered important to determine their degree of sensitivity to stress concentrations at temperatures higher than 1200°F. Furthermore, the extension of testing above 1200°F would result in lower creep resistance and cause creep processes to be the predominant factors governing strength. In order to determine the degree of notch sensitivity under these conditions, the material in the standard heat treated conditions, namely solution treated 1/2-hour at 1975° and aged 16 hours at 1400°F, was tested at 1400°F.

The initial survey of the properties of René 41, Waspaloy (ref. 2) and Inconel 718 (ref. 3) sheet material, the presence of dull notches was found, in many instances, to be nearly as detrimental to rupture properties as sharp-edged ones. Limited unpublished results (see fig. 2) have shown that notch sensitivity does not occur in round bars of René 41 tested at 1200°F; in fact, a slight degree of notch strengthening was observed. The principal difference between the round and sheet specimens lies in the distribution of stresses at the root of the notch. Edge notches result essentially in a condition of biaxial stress in thin-sheet specimens, as opposed to one of triaxial stress in round specimens. In addition, for a given nominal stress, the effective stress (non-hydrostatic) capable of producing deformation at the root of the notch in the triaxial-stress state is lower than in the biaxial-stress state. It is not known at present the degree to which the differences in the notch sensitivity observed are due to the differences in stress (or strain) states or to the relative stress level of the two types of samples. In the current research, a limited study of the effect of stress state was evaluated, in that two conditions of heat treatment of Waspaloy were tested in two sheet thicknesses (0.026- and 0.050-inch thick sheet).

EXPERIMENTAL MATERIAL

The commercially-produced Waspaloy used in this study was received in the form of 0.026-inch thick and 0.050-inch thick sheet. The sheet was reported to have been cold reduced 23 to 25 per cent subsequent to a solution treatment, and to have the following compositions:

Element	Weight Per Cent 0.026-inch thick	0.050-inch thick
Nickel (by difference)	57.95	57.90
Chromium	19.33	19.47
Cobalt	13.52	13.72
Molybdenum	4.16	4.25
Titanium	2.95	2.89
Aluminum	1.35	1.39
Carbon	0.06	0.08
Boron	0.005	0.006
Zirconium	0.03	0.02
Iron	0.55	0.18
Sulphur	0.007	0.007
Manganese	<0.01	0.01
Silicon	0.05	0.07
Copper	0.03	<0.01

Specimen blanks were cut in the longitudinal direction from these cold-rolled sheet materials prior to heat treatment.

EXPERIMENTAL PROCEDURES

The experimental procedures are summarized in the following sections.

Heat Treatment

The heat treatment of the material consisted of a high-temperature

solution treatment followed by a lower-temperature aging treatment. The solution treatment was carried out on each specimen blank in an argon atmosphere. Subsequent air-cooling of these blanks was rapid enough to sufficiently suppress γ' precipitation so that the particle size could be controlled by the aging treatment. Aging was carried out in batches of 10 or 12 samples; following this, the specimens were air cooled.

The 0.026-inch thick sheet was heat treated under the following eight different conditions:

	Solution Treatment	Aging Treatment
1.	1/2 hour at 1825°F	16 hours at 1400°F
2.	1/2 hour at 1825°F	10 hours at 1700°F
3.	1/2 hour at 1900°F	16 hours at 1400°F
4.	1/2 hour at 1900°F	10 hours at 1700°F
5.	1/2 hour at 1975°F	16 hours at 1400°F
6.	1/2 hour at 1975°F	10 hours at 1700°F
7.	1/2 hour at 2150°F	16 hours at 1400°F
8.	1/2 hour at 2150°F	10 hours at 1700°F

In the case of the 0.050-inch thick material, only the solution treatment at 1975°F was used, but both the 16 hours at 1400°F and the 10 hours at 1700°F aging treatments were studied. After the heat treatment, the specimen blanks were machined into either smooth or sharp edge-notched specimens prior to testing.

Test Specimens

Smooth Specimens: The smooth specimen configuration is shown in figure 3. These specimens were prepared from rectangular bundles of specimen blanks by a milling operation. Approximately ten specimens were machined at one time using a fixture to clamp the blanks together, thereby assuring accurate alignment throughout the milling operation.

Notched Specimens: The research utilized a sharp edge-notched specimen of $K_t = 20$ (see fig. 3) which was designed to simulate, in some

respects, an actual crack in the specimen. As was the case with the smooth specimens, ten blanks were machined at one time using a fixture to maintain alignment. The reduced section of the specimen was first milled to size. The notches were then ground almost to size using an alundum wheel having a 60-degree included angle. The notch root radii of the specimens of low and intermediate acuity were lapped to final dimensions. The final radii of the sharp notches were obtained by drawing a sharp carbide tool through the notches. Root radii and net section widths were then measured using a 50X optical comparator.

Testing Methods

The mechanical characteristics were evaluated mainly at 1000° and 1200°F, with one heat treatment tested at 1400°F. The testing program consisted of the determination of tensile and creep-rupture properties of both smooth and sharp edge-notched specimens. Structural examination of the heat treated materials was carried out by optical microscopy, electron microscopy, and X-ray diffraction of extracted residues.

Creep-Rupture Tests

The creep-rupture tests were conducted in individual University of Michigan creep testing machines. In these units, the stress is applied through a third-class lever system having a lever to arm ratio of about 10 to 1. The specimen was gripped by means of pins which were passed through each end of the specimen and into holders fitting into a universal joint-type assembly for uniaxial loading. Heating was provided by a resistance furnace which fitted over the specimen and holder assembly.

Strain measurements were taken on smooth specimens by means of a modified Martens optical extensometer system. Pairs of extensometer bars were attached to collars clamped onto the gage section of the specimens. The stems of mirror assemblies were placed between these pairs, which reflected an illuminated scale located about five feet in front of the creep unit. The differential movements of the top and bottom pairs of bars caused a rotation of the mirrors, which was observed through a telescope

mounted next to the illuminated scale. As the specimen elongated, very small movements of the extensometer bars were magnified by the resulting optical level, and were converted into a large change in the reflected scale reading. This system permitted the detection of a specimen strain of about 10-millionths of an inch.

Strain measurements were made as each weight was applied during loading. Creep strain was read periodically throughout the test. When failure occurred, an automatic timer, measuring the rupture time to one-tenth of an hour, was activated by the fall of the specimen holder.

Three thermocouples were attached to each of the creep-rupture specimens at the center and at either end. All of the thermocouples were shielded from direct radiation. Prior to starting a test, the furnace was heated to within 50°F of the desired temperature. The specimen was then placed in the hot furnace and brought up to the test temperature and distribution in a period of not more than four hours. ASTM-recommended practices were followed in the control of test temperature and distribution.

Tensile Tests.

Tensile tests were conducted in order to facilitate the selection of suitable stress levels for the creep-rupture tests. However, it became evident from this investigation that the time-independent, tensile properties do affect the time-dependent notch sensitivity.

All of the tensile tests were conducted with a 60,000-pound capacity, hydraulic tensile machine. Smooth specimens were tested at a cross head speed of approximately 0.01-inch per minute up to about 2 per cent deformation. The strain rate was then increased to about 0.05-inch per inch per minute until failure. Notched specimens were loaded at a rate of 1000 psi net section stress per second.

Strain measurements were made on the smooth specimens by means of the extensometer system which was described in the previous section on Creep-Rupture Tests.

Structural Examinations

Optical Microscopy

The study of the structures was carried out by conventional methods employed for microscopic examination. Samples cut from the sheet specimens were mounted in plastic and their flat surfaces were polished. Polishing was achieved by wet grinding on a rotating cap through a series of silicon carbide papers, finishing at 600-mesh grit. Final polishing was accomplished on a cloth-covered rotating lap using fine diamond compound and then on a vibratory polisher in an aqueous media of Linde "B" polishing compound.

The specimens were etched electrolytically in "G" etch, an etchant developed by Bigelow, Amy and Brockway (ref. 4). Etching was conducted at 1-1/2 volts and a current density of approximately 0.2 amperes per square inch for a period of 10-20 seconds. The composition of the etchant is as follows:

"G" Etch

H_3PO_4	(85%)	12 parts
H_2SO_4	(96%)	47 parts
HNO_3	(70%)	41 parts

Conventional methods for general optical examination and photomicrography were employed.

Electron Microscopy

The materials were studied using a JEM electron microscope. Both replica and transmission techniques were utilized.

Collodion replicas mounted on copper grids for examination in the microscope were prepared from the surface of the specimens, which had been etched with "G" etch. The replicas were shadowed with chromium to increase the contrast and reveal surface contours. The replicas were then examined in the electron microscope which was operated at 80 KV.

A study by transmission electron microscopy was made of thinned samples cut from the heat treated specimens. Thinning was accomplished

by grinding on wet silicon carbide papers followed by electropolishing. These techniques are described more fully in a recent report by Wilson, et. al. (ref. 5). The electrolyte used in this case was a chilled mixture of 6 per cent perchloric acid and 94 per cent acetic acid. By electropolishing with an applied voltage of 35 volts, satisfactory results were obtained. The grain boundaries and the grains themselves were thinned at approximately the same rate, thus permitting study of all of the microstructural details of the alloy. The thin films were studied and photographed in the electron microscope operated at 100 KV.

X-Ray Diffraction

X-ray diffraction analysis of extracted residues was used for the identification of minor phases. The residues were extracted from solid samples by immersion in a bromine-alcohol solution. The extract was centrifuged and the residue washed repeatedly with alcohol until the supernatant liquid was clear. The extract was then dried and formed into a thin wire using a Duco Cement binder. X-ray exposures were conducted using a 144.6 mm diameter Debye camera and nickel-filtered copper radiation for a period of four hours. The line positions were determined on an optical comparator and the "d" values were calculated. The patterns were then analyzed by comparison with standard patterns available from the literature and, in particular, from the ASTM Powder Data File.

EXPERIMENTAL DATA

The experiments provided data on short-time tensile properties and survey type creep-rupture properties. The intent of these tests was to obtain data showing the change in notch sensitivity with changes in mechanical properties as controlled by microstructural characteristics. To accomplish this, heat treatments over a range of temperatures were used. Limited data on sheet thickness were also obtained to provide information on stress state.

Short-Time Tensile Properties

The tensile tests of the 0.026-inch thick material (see table 1 and fig. 4) showed that the tensile strength for both smooth and notched specimens at 1000°F decreased with increasing temperature of solution treatment. Also, for a given solution treatment, aging at 1400°F produced higher strengths than aging at 1700°F.

The notched specimens had lower strengths than the smooth ones. The N/S ratios ranged from 0.73 to 0.86 with the materials aged at 1700°F having the lower N/S ratios. There was very little effect of solution temperature on N/S ratio at each aging temperature.

Smooth specimens tested at 1200°F had tensile strengths similar to those obtained at 1000°F. Only the standard heat treated material was tested at 1400°F and it showed a decrease in strength due to the increase in test temperature.

At this point it should be noted that the tensile data appear to be incomplete. This resulted from the fact that the research initially planned was concentrated on the creep-rupture properties. It was thought at that time that tensile tests would be used only as an aid in selecting stresses for the creep-rupture tests.

The yield strengths varied with the heat treatment, generally in a way similar to the tensile strengths. However, certain effects should be noted:

1. The ratio of YS/TS was lower after aging at 1700°F than after 1400°F.
2. The yield strengths were practically the same at 1200°F as they were at 1000°F.
3. The standard heat treatment had a somewhat higher YS/TS ratio at 1400°F than at the lower temperatures.

The elongation and reduction of area values after testing at 1000° and 1200°F were relatively high, except for rather low values when solution treated at 1825°F and especially when aged at 1400°F. The material solution treated at 1975°F and aged at 1400°F decreased in ductility with

increasing test temperature to rather low values at 1000°F. The two cases of low elongation corresponded to the highest observed N/S tensile strength ratios.

Rupture Properties of 0.026-inch Thick Sheet

The results of the rupture tests of smooth specimens are presented in table 2; those for the notched specimens are presented in table 3. For each heat treatment only enough tests were run to determine the general position and shape of the stress-rupture time curve. Several tests were discontinued when it became apparent that either the specimens would not rupture until an excessive amount of time had elapsed, or that the trends in the results had been sufficiently established.

The results obtained from the smooth and notched specimens at 1000° and 1200°F are presented graphically in the form of rupture curves in figures 5 to 8. From a comparison of these, together with figures 9 to 12 and table 4, the following observations can be made:

1. The smooth specimen strengths at 1000°F follow the same general trends at short times as were exhibited in the tensile tests (see figs. 5 to 9). All of the rupture curves have slight slopes. The strength levels for the materials solution treated at 1975° and 2150°F and aged 16 hours at 1400°F also decreased with increasing rupture times somewhat more rapidly than the other materials. (It is emphasized that the stress scale for figure 9 is expanded more than is usual for stress-rupture time curves in order to separate the curves for the various heat treatments.

2. For the materials aged 16 hours at 1400°F, the rupture time curves for the notched specimens at 1000°F (see figs. 5 to 8) undergo a drastic increase in slope at time periods which varied with the heat treatment. Since for the time of the tests the rupture curves for the smooth specimens do not exhibit similar breaks, the notch sensitivity of these materials increased rapidly at times beyond those at which the break occurred.

Within the scatter of data, the slopes of the rupture curves subsequent to the break appear to be approximately the same for all of the solution treated materials (see fig. 10). The long-time notch strengths are therefore dependent on the time at which the break occurs.

The time at which the break occurred increased markedly with increasing solution temperature.

Solution Treatment (°F)	Time for "Breaks" in Stress-Rupture Time Curves (hours)
1825	110
1900	280
1975	700
2150	2500

3. Compared with aging at 1400°F, aging at 1700°F apparently reduced the notch sensitivity at 1000°F to a marked degree. At least this was the case for the two solution treatments: 1900° and 2150°F, which were tested at 1000°F after aging 10 hours at 1700°F (see figs. 6 and 8). In contrast to the results of the materials aged 16 hours at 1400°F, no breaks were found in the curves for the materials aged 10 hours at 1700°F within the time limits of the tests.

4. Whether or not breaks occurred in the rupture curves for the notched specimens at 1000°F had a very marked effect on the extrapolated notch strength levels at long times and, hence, on the notch sensitivity. Within the limits of the data available, one possible correlation exists that can be used to clarify and correlate the occurrence of breaks in the rupture curve with the nature of the material tested. The breaks in the rupture curves for the notched specimens appear to occur when the loading stress (based on the net section at the base of the notch) approximately equals the 0.2 per cent yield strength as determined in the smooth specimen tensile tests.

5. The stress-rupture time data at 1200°F (see figs. 5, 8, 11 and 12) had the following features:

a. The stress-rupture time curves at 1200°F in all but one case (those for the material solution treated at 2150°F and aged at 1400°F) did not undergo drastic increases in slope for either notched or smooth specimens. In fact, the notched specimen rupture curve for the material solution treated at 1900°F and aged at 1400°F (see fig. 6) exhibited an upward break, i.e., a decrease in slope, at approximately 200 hours.

b. The material heat treated at 2150°F and aged at 1400°F underwent a drastic increase in slope at about 100 hours when tested as either smooth or notched specimens (see fig. 8). Although the curves are incomplete, it is apparent that the strength levels fell rapidly with time. The specimens fractured in the loading pin holes in three of the four tests. Obviously, the material was extremely stress-concentration sensitive at the pin holes, possibly because of a lower temperature in this area than in the gage section.

c. Depending upon the heat treatment, testing at 1200°F resulted in decreasing as well as increasing notch sensitivity with time. The notched specimen curves for the material solution treated at 1825° or 1900°F were either parallel or convergent to the curves for the smooth specimens. Those tested after the 1975° and 2150°F solution treatments were divergent, with the degree of divergence greater for the 1400°F aging treatment than for the 1700°F aging treatment. Variations of the notch sensitivity with rupture time for solution treated materials aged at 1400°F (see fig. 13) clearly exhibited the wide range of behavior observed.

d. When the rupture curves for smooth specimens at 1200°F were plotted together (see fig. 11), it was evident that the curves of three materials had considerably less slope than the others. The three materials which showed less slope (i.e., 2150°F+1700°F; 1975°F+1400°F; and 1975°F+1700°F) were all tested above or close to the yield strength. As in the tests at

1000°F on notched specimens, the data suggest that stresses below the yield strength may also have a slight tendency to shorten rupture life even for smooth specimens. Presumably, the steeper curves for the other materials were due to the fact that the stress levels were generally below the yield strength. Whether the level of the yield stress is related to to the extreme sensitivity of the material solution treated at 2150°F and aged at 1400°F cannot be established. Other factors may be involved which are not evident, especially since the specimens fractured in the loading pin holes.

Rupture tests were carried out at 1400°F on the material in the standard condition of heat treatment (i.e., 1/2 hour at 1975°F + 16 hours at 1400°F). These results together with those obtained at 1000° and 1200°F (see fig. 14) show that the material exhibited marked notch sensitivity at 1000° and 1200°F, but not at 1400°F. The notch to smooth strength ratio at both 1000° and 1200°F decreased with time (see fig. 13) to a value at least as low as 0.56. On the other hand, at 1400°F the stress-rupture time curve for the notched specimens converged with the curve for the smooth specimends so that the notch to smooth ratio increased from 0.78 at one hour to 1.0 at 1000 hours. On the basis that a short time at a high temperature is equivalent to a long time at a lower temperature, these results suggest that the N/S ratio could reverse from a decrease to an increase at longer times than those of the tests in this investigation at temperatures below 1400°F.

Creep Resistance

All of the tests on smooth specimens were instrumented to measure creep. The minimum creep rates (see table 2) are plotted as stress-creep rate curves in figure 5. The curves for the tests at 1000°F show variations in creep rates and, hence, in creep resistance with heat treatment. For a given solution treatment, the aging treatment had only a relatively small influence on the creep resistance. The creep resistance was slightly

higher after aging at 1400°F than after aging at 1700°F. The creep resistance increased with decreasing solution temperature. The stress/minimum-creep-rate curves for the material solution treated at 2150°F, especially for the 1400°F aging treatment, were steeper than for the other heat treated materials.

When tested at 1200°F, the relationship between minimum creep rates and heat treatment was more variable than at 1000°F. Within the range of stresses studied, the materials aged at 1700°F did, however, have lower creep resistance.

The stress-creep-rate curves at 1400°F for the material in the standard condition of heat treatment, when compared with the results obtained at 1000° and 1200°F (see fig. 16), indicated that temperature had a marked effect. The slopes of the curves increased with increasing temperature, particularly in the range of 1200° to 1400°F. In addition, within the range of minimum creep rates considered, the creep resistance decreased a greater amount for an increase in temperature from 1200°F to 1400°F than from 1000°F to 1200°F.

Ductility in Creep-Rupture Tests

There is a rather general belief that the elongation and reduction in area values in rupture tests are related to notch sensitivity. Consequently, considerable effort was spent on evaluation of these characteristics in relation to the notched and smooth specimen rupture strengths. In doing so, it became evident that the elongation occurring in each of the various stages of creep should also be presented.

The majority of the elongation of the smooth specimens in the tests at 1000°F (see table 5) occurred during loading. As the loading stresses were above the yield strength, the deformation on loading can be considered identical to that occurring up to the same stress in a tensile test. The amount of deformation on loading, and hence the total elongation, decreased with increasing rupture time (corresponding to the decrease in the load to yield strength ratio). For one material solution treated at 1825°F and

aged at 1400°F, considerable elongation occurred in second stage creep in addition to the deformation occurring on loading. Although the amount of elongation which occurred in this stage was relatively small for the other heat treatments, in all cases the time period for second stage accounted for the majority of the time to rupture.

Most evident from the curves for the variation of elongation with rupture time at 1000°F (see fig.17) is the relatively high elongation for the materials aged at 1700°F compared with those aged at 1400°F. Since only two test points existed for the majority of heat treatments, it was impossible to establish the exact shapes of the curves. Therefore, the straight lines of figure 17 have no interpolative significance. Based on three test points, the slope of the curve for the material solution treated at 1825°F and aged at 1400°F apparently decreases with time, whereas the slope for the curve for the 2150°F heat-treated material increases with time.

For the tests at the lower stress levels at 1200°F (see table 6), the majority of the elongation which occurred did so during creep subsequent to loading, this being reflective of loading stresses generally below the yield strengths. In these tests, the majority of the elongation occurred in third stage creep (in sharp contrast to the little or no third stage creep in the tests at 1000°F). The time to rupture was therefore comprised predominantly of the time periods for second and third stage creep.

The curves of elongation with rupture time at 1200°F (see fig.18) show high values of elongation for the materials aged at 1700°F compared with those aged at 1400°F. The elongation for the material solution treated at 2150°F and aged at 1400°F was probably extremely low. The failure of the specimens in the pin holes did not, however, allow an adequate determination of the ductility after this heat treatment.

For the materials aged at 1400°F, the elongations both increased and decreased with rupture time. Most striking was the trough, or minimum in elongation, exhibited by the material solution treated at 1975°F.

The material solution treated at 1975°F, aged at 1400°F, and tested at 1400°F gave the elongation values shown in table 7. In these tests, the majority of elongation occurred in third stage creep. The rupture time was predominantly comprised of the time periods for second and third stage creep. When the values of the elongation at 1400°F were compared with those obtained at 1000° and 1200°F (see table 7) for the same heat treatment, the following pattern of changes in elongation was evident:

1. Elongation decreased with rupture time at 1000°F.
2. Elongation decreased and then increased with rupture time at 1200°F.
3. Elongation increased with rupture time at 1400°F.

The apparent occurrence of a rupture time-temperature dependent trough, or minimum in ductility, will be discussed further in the following section.

Temperature-Time Rupture Characteristics

It is well known that in many instances the effects of long-time exposure under constant load at a relatively low temperature can be simulated by a shorter-time exposure at a higher temperature. In the following sections, the rupture characteristics (i.e., smooth and notched specimen rupture strengths, rupture strength ratios, and ductility) are considered within this context.

Smooth and Notched Specimen Rupture Strengths

Several empirical methods are used to correlate the rupture times of materials tested at a number of different temperatures. The method used most widely is that of Larson-Miller (ref. 6). The correlation is achieved by the use of a parameter (P) which is plotted against log stress. P is defined by:

$$P = T(C + \log t)$$

where,

T = Absolute temperature, °R
t = time for rupture at temperature T, hours
C = Constant

For a given material and range of test temperatures or rupture times, the value of C is estimated from a plot of Log t against 1/T for constant stress levels. The isostress lines should converge at a common point on the log and axis at infinite T, thereby defining the value of C. From the graphs (Log t versus 1/T), the most appropriate values (i.e., mean value of the intercepts of isostress lines with the line for 1/T = 0) for the constant C for the smooth and notched specimens were 20 and 14, respectively. Although the convergence of the curves was poor and the data limited, the use of the parameter method offered a simple means of analyzing the data in relation to the notch sensitivity.

From the rupture curves (see figs. 5-8 and 14) and the parametric curves for the rupture tests of smooth specimens (see fig. 19), the following factors are evident:

1. The material solution treated at 1825°F and aged at 1400°F had the highest rupture strength level within the range of testing times at 1000° and 1200°F.

2. The strength of the material solution treated at 2150°F and aged at 1400°F was low at 1000°F. Both of the tests conducted at 1200°F failed in the pin holes. A notched specimen of this material also fractured in the pin hole, indicating a high degree of stress concentration sensitivity somewhat below 1200°F.

3. For the material in the standard condition of heat treatment, there is a tendency for the strength level to decrease more rapidly at parameter values greater than about 38 to 39 (this corresponds roughly to 1500 hours at 1200°F, or 5 hours at 1400°F). There is no evidence to prove that a similar drop in strength does not occur for the other materials. It should also be noted that the curves for the various materials (with the exception of those solution treated at 2150°F and aged at 1400°F)

generally tended to converge with increasing values of P. Therefore, there is some question as to whether the curves of figure 11 actually cross, or if there are changes in slope such that they converge for the various heat treatments.

The parametric curves for the rupture tests of the notched specimens (see fig. 20) showed more variability than those for the smooth specimens. However, the following factors were evident:

1. For an aging temperature of 1400°F, solution treatment at 1825°F resulted in the highest notched specimen strength at 1000° and 1200°F. The notched specimen strength of the material solution treated at 2150°F apparently decreased rapidly with increasing parameter.

2. All of the materials aged at 1400°F showed an initial rapid decrease in strength levels with increasing P. However, with further increase in P, the curves showed a distinct decrease in slope (this is not evident within the limits of test results for the material solution treated at 2150°F, possibly because of the pin hole failure). The occurrence of a decrease in slope suggested that upward breaks occur in the rupture curves, and examination of the rupture curves tended to confirm this:

   a. The rupture curves at 1200°F for the materials solution treated at 1825°F and 1900°F (see figs. 5 and 6) had considerably less slope than those beyond the breaks at 1000°F. In order to prevent the occurrence of lower rupture strengths at 1000°F than at 1200°F, the results would require that an upward break occur at longer times than the tests conducted to date at 1000°F. If this is indeed the case, the upward breaks should also be evident at shorter times at higher temperatures. A break of this type (see fig. 6) was in fact observed at approximately 200 hours for the material solution treated at 1900°F and tested at 1200°F. The number of tests at 1200°F for the material solution treated at 1825°F were insufficient to show whether or not an upward break occurred.

b. For the material solution treated at 1975°F (see fig. 14), the notched specimen rupture curve had considerably less slope at 1400°F than at 1200°F. This suggests that an upward break should occur, but at a value of P higher than was the case for the lower solution treatments. Again the number of tests at a given temperature were insufficient to actually show the presence of an upward break.

c. Within the limits of the results for the material solution treated at 2150°F (i.e., the limited data points and a pin hole failure for the longest time test at 1200°F), there was no evidence for the occurrence of an upward break (see fig. 8).

The parametric representation of the results and the individual rupture curves indicate that an upward break possibly occurs at longer times than those considered for the notched specimen tests at 1000°F. In addition, it is apparent that such an upward break would occur at shorter times, the lower the temperature of solution treatment. Additional support for the contention that upward breaks do occur is evident from the results of a study, previously reported, of a nickel-base superalloy sheet, Inconel 718 (ref. 3). Here, upward breaks were shown to occur in the notched specimen rupture curves for this alloy at a test temperature of 1200°F.

Notch to Smooth Rupture Strength Ratios (N/S)

In the previous section, changes in rupture strengths were reviewed with respect to associated variations in time and temperature. Rupture time-temperature parameter analysis, as well as evaluation of the rupture curves, indicated that there was a general tendency for the notched specimen rupture curves to increase in slope and then, at longer times, to decrease in slope, while the smooth specimen rupture curves exhibited only gradually varying slopes. In making this analysis, the data for notched and smooth specimens were treated separately; thus, the corresponding relationships for the degree of notch sensitivity (i.e., the N/S ratio) are not readily apparent. The N/S ratios were established as the ratio of the

notched specimen rupture strength (for rupture times as determined by the actual tests) to the stress for rupture of a smooth specimen for the same rupture time (as determined from the smooth specimen rupture time curve).

The constant for the parameter was different for the correlation of the notched and smooth specimen rupture test results. To display the N/S values with time and temperature (see figs. 21 and 22), the parameter with an average constant value of 17 was used. This method of presenting N/S values should be considered no more than a matter of convenience. However, the results do suggest a distinct correlation between notch sensitivity and the rupture time-temperature relationship:

1. Before considering the parameter analysis of the data, it should be recalled that the N/S ratio for the material in the standard condition of heat treatment decreased with increasing time at 1000° and 1200°F (see figs. 13 and 14), while this ratio increased with time at 1400°F. This suggested that if time tests longer than those of this investigation were conducted at temperatures below 1400°F, the N/S ratio could reverse from a decreasing trend to an increasing one.

2. Examination of the changes in notch sensitivity with increasing time and temperature for the other materials aged at 1400°F (see figs. 5 to 8, 13 and 21) showed that these results were not inconsistent with a general pattern of decreasing N/S ratio followed by an increase. From examination of this data, the following effects were noted:

   a. The marked increase in notch sensitivity (beginning at 0.2 per cent offset yield strength) occurred at longer times at 1000°F, the higher the temperature of solution treatment.

   b. The N/S ratio reached a minimum at lower values of the parameter, the lower the solution temperature.

3. Although the test results which were available for the materials aged at 1700°F were limited, a number of factors were evident when the time-temperature dependence of the N/S ratio (see fig. 22) was considered:

a. Within the times and temperatures studied, the degree of notch sensitivity did not vary markedly. The N/S ratios of the rupture tests were generally greater than the minimum values determined in the tensile tests at 1000°F. Since the stresses applied to the specimens were both above and below the 0.2 per cent offset yield strength of the material, it is apparent that at least no marked increase in notch sensitivity occurred when the loading stresses were below the yield strength.

b. The results for the material solution treated at 1900°F showed a minimum in the curve of the N/S ratio as a function of P. However, this minimum was much less pronounced than that which occurred for the materials heat treated at 1400°F (see fig. 21). The results for the materials in the other solution treated conditions and aged at 1700°F were insufficient to establish whether or not a minimum in the N/S ratio occurred; the results did not eliminate this possibility, however.

Rupture Ductility

It was shown previously that the rupture elongation in the smooth specimens of the material in the standard condition of heat treatment decreased with time at 1000°F, decreased and subsequently increased with time at 1200°F, and increased with time at 1400°F. These changes in elongation can be represented as a function of the parameter P (see fig.23); in this case, a value of C = 20 was used since this was the appropriate value for the description of the smooth specimen rupture strengths. The elongation values were in the form of a "trough", with a minimum in ductility in the region of P = 37. Further examination of the possible existence of ductility troughs for the other heat-treated conditions and of the contribution of the elongation in the various stages of creep to the formation of the trough resulted in the following observations:

1. For the material in the standard condition of heat treatment, the ductility trough occurred because of the large contributions of the deformation on loading (at low P-values) and the deformation in the third

stage of creep (at high P values) to the total elongation (see fig. 26). The elongation on loading decreased rapidly as the load to yield stress ratio decreased, i.e., with increasing values of P. In contrast, the elongation which occurred in third stage creep was zero for low values of P, but increased at higher values.

2. Examination of the changes in ductility with increasing time and temperature for the other materials aged at 1400°F (see figs. 24-27) also showed the presence of troughs. In general, then, these troughs were due to the balance of contributions to the total elongation of the deformation on loading and the deformation in third stage creep. In one case, material solution treated at 1825°F and aged at 1400°F (see fig. 24) exhibited a trough that was apparently due to a minimum in the amount of deformation which occurred in second stage creep at intermediate values of the parameter. Since for every other heat treatment the amount of second stage creep did not exhibit such a minimum (and also since difficulty was encountered in distinguishing the end of the period of second stage creep for the point at P = 36), the second or dotted alternative shown in figure 24 probably occurred.

3. The limited data for the materials aged 10 hours at 1700°F made it difficult to establish whether or not a ductility trough occurred for these materials. However, by the amounts of deformation in each of the creep stages (see figs. 28 and 29) it was possible to derive appropriate total elongation versus parameter. Curves for the total elongation derived by this method (see figs. 28 and 29) indicated that at least no pronounced ductility trough was present. The results do, in fact, suggest only an inflexion in the total elongation curve. The elimination of a pronounced trough by aging at 1700°F compared with aging at 1400°F apparently resulted because larger amounts of third stage creep occurred at lower values of the time-temperature parameter.

4. The reduction in area which occurred in the rupture of smooth specimen tests (see table 2) was also considered in terms of the time-

temperature parameter. Generally, the variations in reduction of area with changes in the parameter were analogous to the variations in elongation (see fig. 23). The minimum in the trough, however, occurred over a wider range in P values, and the increase in reduction in area subsequent to the minimum was less marked than for elongation.

Effect of Sheet Thickness on the Mechanical Properties

To obtain an indication of the influence of sheet thickness on the mechanical properties of the alloy, sheet material 0.050-inch thick was added to the investigation. Creep-rupture tests at 1000° and 1200°F were carried out on notched and smooth specimens which had been solution treated 1/2-hour at 1975°F and aged 16 hours at 1400°F, or 10 hours at 1700°F. The following sections consider the results of these tests along with the results previously discussed for the 0.026-inch thick material tested in the same conditions of heat treatment.

Tensile Properties at 1000°F.

Tensile tests were conducted at 1000°F to aid selection of initial test stresses for the creep-rupture tests. The results are given below along with the results for the 0.026-inch thick sheet previously discussed.

Heat Treatment °F	Sheet Thickness	Tensile Strength	0.2% Offset Yield Strength	YS/TS	Elong. %	R.A. %
½ hr-1975 + 16 hrs-1400	0.026	161.0	115.0	0.71	33.4	32
	0.050	158.5	109.0	0.69	38.0	33
½ hr-1975 + 10 hrs-1700	0.026	148.5	94.9	0.64	36.0	28
	0.050	139.8	79.5	0.57	34.0	36

The thicker material had strengths, particularly yield strengths, slightly lower than the 0.026-inch thick material. Because the two materials were from different heats, however, these differences could have arisen from slight compositional or heat treatment variations. Therefore, it is by no means definite that dimensional effects were responsible for the observed differences.

Creep-Rupture Properties

In the creep-rupture tests (see table 8 and fig. 30), the strength levels shown by the smooth specimens of the 0.050-inch thick material were very slightly higher than those for the thinner material tested under comparable conditions. On the other hand, there were very large differences in the rupture strengths of the notched specimens between the two thicknesses.

1. Within the range of testing time at 1000°F, the strength of the 0.050-inch thick material aged at 1400°F was higher than that of the thinner material. In order to cause rupture within the testing times investigated, it was necessary to apply stresses above the net section yield strength. Based on the results for the 0.026-inch thick material, it would be necessary for the stress to be less than the yield strength for a break to occur. Therefore, it is not known if a break would occur at longer times when the stresses are below the yield strength. When tested at 1200°F, the 0.050-inch thick material aged at 1400°F had much higher notch-rupture strengths than the 0.026-inch thick material. The notch to smooth ratio for the 0.050-inch thick material was in the range of 0.80 to 0.87 for tests at 1000° and 1200°F (see fig. 31). In contrast, the strength ratio for the 0.026-inch thick material decreased from 0.85 at 1000°F to 0.56 at 1200°F (within the range of test times studied). These time-temperature characteristics suggested that no break occurred in the notched specimen rupture curve for the 0.050-inch thick material at times longer than those tested at 1000°F.

2. For the material aged at 1700°F (see figs. 30 and 31), no notch sensitivity (e.g., notch to smooth strength ratio = 1) was exhibited for the 0.050-inch thick material. The 0.026-inch thick material exhibited a slight increase in notch sensitivity with increasing rupture time.

Consistent with slightly higher rupture strengths for the thicker material, the creep resistance of these materials was also generally slightly higher (see table 8 and fig. 32).

The elongation at rupture (see tables 8 and 9) for a given stress was significantly higher for the 0.050-inch thick material than for the 0.026-inch thick material. Thus, the higher elongation for thicker material corresponded to longer rupture times when compared with the 0.026 inch thick material. When the variations in elongations were represented as functions of the time-temperature parameter (see figs. 33 and 34), the following factors were evident:

1. The 0.050-inch thick material exhibited greater rupture elongation than the thinner material for a P value as well as for a given stress level.

2. The greater elongation for the thicker material in tests at 1000°F (low values of P) resulted almost totally from a greater amount of deformation on loading. This difference would be expected because of the lower yield strength for the thicker material.

3. At 1200°F (high values of P), the greater elongation for the thicker material was due primarily to larger amounts of third stage deformation than for the 0.026-inch thick material.

4. The total elongation for the 0.050-inch thick material aged at 1700°F increased with time for the tests at 1200°F. This increased an apparent ductility trough to form in the curve for the parametric representation (see fig. 34). This result is in contrast to that for the 0.026-inch thick material where no ductility trough was delineated.

ORIGINAL MICROSTRUCTURES

The objective of the heat treatment variations was to alter properties by the consequent variations in microstructure and, in turn, to relate both of these to notch sensitivity. For this reason and because specific microstructural features such as the form of the grain boundary precipitate or the nature of the γ' dispersion could influence the notch sensitivity

apart from properties, the microstructures were investigated in detail. Only the microstructural study of the 0.026-inch thick sheet was completed at the time of this report.

Typical Structures

Typical microstructures after the various heat treatments are shown by optical micrographs in figures 35 through 42, and by electron micrographs in figures 43 through 50. Solution treatment at 2150°F resulted in almost a ten-fold increase in grain size (see table 1) compared to the treatments at lower temperatures. Presumably, the marked increase in grain size from the 2150°F treatment reflects not only the removal of grain growth restraining effects of both γ' and carbides by solution, but also relatively easy grain boundary migration at this temperature.

Aging 16 hours at 1400°F generally resulted in a dispersion of the γ' particles which were too small to be readily resolvable in the electron microscope using replica techniques (see figs. 45, 47 and 49). Aging for 10 hours at 1700°F produced significantly larger γ' particles (approximately 700A in diameter (see figs. 14, 48 and 50). Since 1825°F is below the temperature required for complete solution of the γ', relatively large γ' particles were formed during the 1/2-hour solution treatment at this temperature. Subsequent aging at 1400°F produced a second, finer dispersion of γ', thus resulting in a bimodal distribution of sizes. After this aging treatment, the finer dispersion of γ' was again not readily resolvable, although the larger γ' particles which developed during the 1825°F treatment were readily observed (see fig. 43). Aging 10 hours at 1700°F tended to merge the two individual size distributions because of the more rapid growth rate of fine particles compared with the larger ones. The resulting γ' size distribution is thus similar to those obtained after higher solution temperature treatments, but with a slightly higher average particle size (see fig. 44).

Those materials with the larger γ' particles present (all aged at 1700°F and the 1825°F treatment and aged at 1400°F) exhibited a mottled

effect within the grains under the optical microscope. The degree to which this occurred was related to the severity of etching.

Grain Boundary Structures

All of the micrographs previously discussed showed the presence of precipitate in the grain boundaries. The amount present in the aged materials tended to increase with solution temperature. In addition, the material solution treated at 1825°F and aged also showed evidence of precipitation in twin boundaries (see figs. 35, 36 and 43). The following features of the solution treated and aged materials were noted:

1. When solution treated at 1825°F, the grain boundaries were only partially filled with particles.

2. When heat treated at 2150°F, the boundary phases were continuous.

3. The boundaries were filled to an intermediate degree after solution treatment at 1900°F or 1975°F, with little difference between the two.

4. Quantitative comparisons were difficult because the amount of material in the brain boundaries appears to vary considerably from grain to grain. Apparently, this was due at least in part to the angle at which the polished plane intercepted the grain boundary.

In a few cases, two separate phases were present in the grain boundaries (see figs. 51 and 52). This was evident in the material solution treated at 1975°F or 2150°F (particularly the latter) and aged at 1700°F. The grain boundary precipitate in these cases consisted of carbides surrounded by massive γ'. The continuous nature of the boundary phases in the material solution treated at 2150°F and aged at 1700°F was due to the extensive precipitation of γ' in the grain boundaries.

Because of the presence of γ' in grain boundaries, it was very

difficult to estimate whether the amount of carbide in the grain boundaries varied with heat treatment. General examination by electron microscopy did indicate, however, that the amount of grain boundary carbide increased with solution temperature. No marked effect of aging on the amount of grain boundary carbide was observed.

Carbide Phase Identification by X-Ray Diffraction

X-ray diffraction patterns were obtained from bromine-extracted residues from each of the heat treated materials. The "d" values determined from these patterns are presented in table 10. By analysis of these values, two compounds: Ti(CN) and $M_{23}C_6$, were shown to be present after all of the eight different heat treatments. The Ti(CN) phase is a cubic phase with a lattice parameter of 4.32Å, while the $M_{23}C_6$ phase has a face centered, cubic structure and a lattice parameter of 10.7Å. No significant differences were found between the relative intensities of corresponding lines as a result of varying the heat treatment.

Orientation Relationships of Grain Boundary Phases

The study of the materials by transmission electron microscopy was used not only to confirm the results established by the replica methods, but more important, to establish the orientation relationships and the identification of the phases present. An example of a selected area diffraction pattern of a grain boundary, which was used to establish these factors for the grain boundary carbide phase, is presented in figure 53. The diffraction patterns, utilizing the matrix as a basis for comparison (established by X-ray diffraction), showed that the grain boundary carbide was $M_{23}C_6$, as the results of the X-ray diffraction study had indicated. The diffraction patterns also showed that $M_{23}C_6$ has the same orientation as one of the adjacent grains. These results were confirmed using dark field techniques. This orientation is possible since the carbide phase is face-centered cubic with a lattice parameter which is almost exactly

three times that of the matrix. This situation is identical to that reported by Wolff (ref. 7) in an extensive study or the orientation and morphology of $M_{23}C_6$ precipitated in an iron base alloy (with 33% Ni, 21% Cr, and 0.05% C).

In the case of the material exhibiting precipitation of the γ' phase in the grain boundary, the above situation can be expected to be somewhat complicated. The selected area diffraction patterns of the grain boundaries were similar to those when no γ' was present, thus showing that the orientation and registry conditions, as discussed previously, apply. In no case did selected area diffraction patterns of grain boundary areas show a series of spots in addition to those due to the adjacent matrices, which could be attributed only to the γ' in the grain boundaries. The carbide phase could be completely enveloped in the γ' phase, as was evident in several electron micrographs of replicas. Several orientation relationships between the grain boundary phases are possible. To date, the results obtained are inadequate to determine which of the following relationships occur.

1. The γ' precipitates in the grain boundary in such a way that it is oriented (perhaps even coherent) with the matrix. The $M_{23}C_6$ carbide phase is oriented relative to the matrix, as indicated by the diffraction patterns. Due to the similarity of the structures of the γ and γ' phases, this would also mean that $M_{23}C_6$ was oriented with respect to the γ' phase. In this situation, only γ' superlattice spots would distinguish the γ and γ' phases, and these spots were too weak to be observed in the orientations studied; the normal fcc. spots would lie in exactly the same position as the matrix spots (γ and γ' have almost the same lattic parameter in this alloy).

2. The γ' precipitates in random orientations in the grain boundary. This precipitation would have to occur, however, without destroying the already fixed orientation relation of the $M_{23}C_6$ to the matrix. If this were the case, diffraction spots due to the γ' should appear in the patterns obtained from grain boundary regions.

Occurrence of Twin Boundaries

Optical micrographs of the materials solution treated at 1825°F and aged showed the presence of a large number of twin boundaries, whereas the materials solution treated at higher temperatures showed little or no twin occurrence. Subsequent study by transmission electron microscopy showed that twins also occurred in the materials solution treated at higher temperatures. These boundaries were not readily visible during optical examination (except in the case of material solution treated at 2150°F and aged 16 hours at 1400°F), since no twin boundary precipitation of carbide had occurred. Increasing the time or temperature of the aging treatment in Waspaloy increased the tendency for carbide precipitation to occur in twin boundaries. Precipitation occurred initially in twin ends and subsequently in twin edges. The 1825°F solution treatment therefore acted as a high-temperature aging treatment: not only did a proportion of the γ' particles precipitate and grow during this treatment, but, apparently, carbide reactions such as precipitation in twins occurred.

The boundaries of the twins present in the materials solution treated at 1825°F showed the presence of considerable amounts of carbide precipitation. This carbide was present in both the twin sides and ends. This precipitation of carbide in the twins could be expected to reduce the amount of carbide present in the grain boundaries.

Transmission electron microscopy showed that the twin boundary precipitate was $M_{23}C_6$, and, like the carbide in the grain boundaries, it had the same orientation as the adjacent matrix; unlike the grain boundaries, however, no γ' phase was observed precipitated in the twin boundaries.

The existence of one further microstructural feature was detected by optical and replica methods. In the material solution treated at 2150°F and aged 10 hours at 1700°F, a phase was observed which could not be identified by its morphology. The phase appeared in the form of a "Chinese Script" throughout the material (see fig. 54). In many cases, the structure appeared to be associated with twin boundaries, particularly twin ends. In addition to the apparent precipitation in twin boundaries, the phase also

occurred in parallel planes in areas adjacent to twins. During the electron microscopic examination of thin films prepared from this material, selected area electron diffraction patterns (see fig. 55) indicated that the structure was formed by $M_{23}C_6$, whose orientation, again, coincided with that of the matrix.

Gamma Prime Depletion

A number of the grain boundaries in the optical micrographs of material solution treated at 2150°F and aged 10 hours at 1700°F had a whitish appearance (see fig. 42). Although the occurrence of this effect depended upon the etching time employed, it probably arose from depletion of γ' particles and/or other elements from areas adjacent to the grain boundaries.

Depletion of the areas adjacent to the grain boundaries of γ' particles was most evident in the electron micrographs of replicas taken from the material solution treated at 2150°F and aged 10 hours at 1700°F (see figs. 50 and 51). The material solution treated at 1975°F and aged 10 hours at 1700°F also showed the presence of a small depleted region, while the other heat treated materials showed little or no γ' depletion. The amount of depletion correlated directly with the extent of γ' precipitation in the grain boundaries. Therefore, the depleted region resulted from the removal of the γ'-forming elements from this area and their transfer into the grain boundaries.

The occurrence of γ' depletion in these two materials raised an interesting question. In many cases, gamma prime depletion is considered to be due to the removal of chromium from the area adjacent to the grain boundaries by carbide formation, causing an increase in the γ' solubility. The greatest amount of grain boundary carbide precipitate was formed in the materials solution treated at the higher temperatures, which also exhibited the greatest amount of γ' depletion. This behavior precludes the depletion from being due to the influence of chromium on γ' solubility.

RUPTURED-SPECIMEN CHARACTERISTICS

Perhaps the most significant observation from examination of the failed notched and smooth specimens was related to the fracture characteristics. For all but a few of the short-time tests, the fracture of the specimens consisted of two distinct parts (see fig. 56). One section was roughly perpendicular to the loading axis and was dark in color from being oxidized. The remainder of the fracture was not colored from oxidation, and was a typical shear fracture. This situation existed for both notched and smooth specimens. In each case, the length of each type of fracture varied significantly with testing conditions. Detailed examination of the relationships of these fractures to the microstructures was carried out by optical and electron microscopy.

Fracture Sequence

Optical examination showed that the oxidized part of the fracture was intergranular, while the unoxidized shear failure was transgranular. A series of micrographs taken at regular intervals along the fracture of a notched creep-rupture specimen is presented in figure 57 (because of its large grain size, the material solution treated at 2150°F and aged at 1400°F provided the clearest illustration at low magnification of the fracture type which occurred in a similar manner for all of the heat treated materials). These micrographs show clearly the presence of the intergranular and transgranular fracture. Intergranular cracks were also found in several of the specimens that were discontinued before rupture, particularly those which had nearly attained the expected rupture time (see fig. 58). Some of the specimens which broke in the pin holes also had intergranular cracks at the notches. In no case, however, was a specimen found before rupture which exhibited transgranular cracking. The above results indicated that failure of the specimens occurred by initiation and relatively slow growth of the intergranular crack, followed by the shear failure, in a time period short enough to avoid discoloration by oxidation. The shear failure

occurred when the intergranular cracking raised the stress high enough for the crack to initiate transgranular failure. This is in agreement with the concept that with increasing stress levels and strain rates, a failure will tend to shift from an intergranular to a transgranular mode of fracture.

Measurements across the fracture of both smooth and notched specimens showed that, although some reduction in thickness occurred in the regions of the intergranular fracture, a much larger reduction occurred at the transgranular failure (values for the reduction of area as reported in tables 1 and 2 are average values). The microstructures also showed evidence of deformation associated with the transgranular fracture. These observations indicated that the transgranular failure was ductile.

Subsidiary Intergranular Cracking

In addition to the main intergranular and shear cracks, the majority of both smooth and notched fractured specimens showed the presence of subsidiary intergranular cracks. Examples of this cracking, which were observed in sections parallel to the plane of the sheet specimens, are presented in figures 57-60. Similar to the major intergranular crack, the subsidiary cracks occurred predominantly in boundaries perpendicular to the loading axis.

It was evident from metallographic examinations that at least the majority of these subsidiary cracks terminated on the surfaces of the specimens. The extent of the cracking observed (in the sections parallel to the plane of the sheet specimens) decreased as the depth of the section below the surface increased. The edge cracks observed generally extended through the thickness of the specimen so that the amount of edge cracking was, in this case, much less dependent on the sample section.

The amount of intergranular cracking which occurred is of importance for two reasons:

1. Presumably, extensive subsidiary cracking indicates that,

although cracks initiate readily, their growth rate must be restricted by other factors. The extent of subsidiary cracking will therefore reflect the resistance of the material to intergranular crack initiation relative to the resistance to crack growth.

2. The shear failure occurred when the intergranular cracking raised the stress high enough for the crack to initiate the transgranular crack. The stage at which this occurred must be dependent not only on the length of the major intergranular crack, but also on the mechanical properties of the load-bearing section. The mechanical characteristics of this section will be affected by the degree of subsidiary cracking present as well as by other creep damaging (or strengthening) processes occurring.

Within the context of the difficulties involved in estimating the degree of subsidiary cracking in the rupture specimens, the following observations were made.

1. The fracture surface of the tensile-tested notched specimens was entirely transgranular. In addition, no subsidiary intergranular cracking was detected. On the other hand, in some cases a limited number of subsidiary intergranular cracks were observed in the notched, creep-rupture specimens, which had occurred in addition to the major intergranular crack. The subsidiary cracks (see figs. 58-59) occurred in regions immediately adjacent to the major intergranular cracks and also slightly in front of these cracks (observed in cases where tests were discontinued before rupture, but after cracking had started).

2. The smooth specimens showed the presence of far more subsidiary cracks than did the notched ones. Although the major fracture path in the tensile specimens was a transgranular shear failure, a limited number of intergranular subsidiary cracks were observed in several of the specimens studied. This intergranular cracking associated with the

transgranular fracture was assumed to be evidence that there was little difference in the tendency for intergranular- versus transgranular-crack initiation to occur. Extensive subsidiary cracking occurred in the rupture specimens, with a distinct tendency for the extent of cracking to increase with rupture time. Unlike the notched specimens, although the majority of the subsidiary cracks in smooth specimens occurred in the regions of major crack path, some additional subsidiary cracks occurred throughout the gage section (see figs. 60-61). In addition to the increase in cracking with rupture time, increasing the test temperature from 1000° to 1400°F resulted in a pronounced increase in the amount of subsidiary cracking.

3. The behavior of the smooth specimens of the materials solution treated at 1975°F and 2150°F, and aged 10 hours at 1700°F, appeared to differ from the other heat treated materials when tested at 1200°F since they exhibited significantly more subsidiary cracking. For notched specimens tested at 1000° and 1200°F and for smooth specimens tested at 1000°F, the above two materials did, however, exhibit a degree of subsidiary cracking similar to the other heat treated materials.

With reference to the above results, a number of observations can be made.

1. The formation of a crack in one particular area of a smooth specimen does not reduce the stress level seen by other areas in the specimen gage length. Cracks can therefore be initiated throughout the specimen subsequent to the initiation of the first crack. The formation of a crack will, however, set up a complex stress system in the region of the crack which can be considered to be somewhat similar to that in a notched specimen.

2. a) The amount of subsidiary cracking in the smooth specimens increases with increasing rupture time (decreasing stress) and with increasing test temperature. This indicates that reducing the stress or

increasing the temperature reduces the ratio of time for crack initiation to time for crack propagation.

b) Similarly, the extensive subsidiary cracking observed after testing at 1200°F in the smooth specimens of the two materials solution treated at the highest temperatures (solution treated at 1975° and 2150°F and aged 10 hours at 1700°F) must reflect a shorter time period for crack initiation relative to the time period for crack propagation in comparison to the materials in the other heat treated conditions.

3. The limited subsidiary cracking observed in the notched specimens was presumably due to the complex stress and strain distribution introduced by the notch. Deformation at the root of the notch is much greater than in the remainder of the specimens and, hence, cracking will be initiated only in this region. Once a crack has formed, then deformation will be concentrated in the area adjacent to the crack tip where the stress level is high. Subsidiary cracking in notched specimens will thus be limited to areas immediately adjacent to, and in front of the major crack path, where the stress and the deformation are the highest.

Intergranular Crack Lengths

The lengths of the intergranular cracks as determined from the fracture surfaces of the smooth and notched, 0.026-inch thick specimens tested at 1000°, 1200° and 1400°F are presented in figures 62-65. From these results, the following observations can be made.

1. Generally, the lengths of the intergranular cracks measured increase with decreasing applied loads and, thus, with increasing rupture times. This result was to be expected (if it is assumed that the transgranular strength did not change markedly with time), since, with lower applied loads, the intergranular cracks have to grow more before the stress becomes high enough to initiate the transgranular fracture.

2. It is apparent that the intergranular crack length for a given stress is determined, to a great extent, by the tensile strength levels.

Increasing the tensile strength of the materials (lower solution treatment temperatures) generally resulted in an increase in the intergranular crack length exhibited for a given loading stress. The effect of test temperature on the intergranular crack length of a material tested at a given stress level is much more difficult to establish from the results. In a number of cases, however, tests at 1000°, 1200° and 1400°F resulted in similar crack lengths, presumably reflecting the similarity of the tensile-strength levels of the materials tested in this temperature range.

3. At 1000°F, the smooth specimens generally fail at significantly higher loading stresses for the same degree of intergranular cracking than the notched specimens. However, at 1200°F and 1400°F, the amount of intergranular cracking (expressed as a percentage of the total fracture width) was apparently much less dependent upon specimen type.

a. The relative behavior of the smooth and notched specimens can be explained, at least to some extent, by the stress states existing in the specimens. Once a crack has developed in a smooth specimen, its behavior will be somewhat similar to that of a notched specimen with an equivalent length of crack present. The presence of the machined notches in the notched specimens can be expected to change the relative nature of the behavior of the two specimens, especailly for short and long intergranular crack lengths. In addition, the degree of creep damage or strengthening occurring in the load-bearing section can be expected to differ between the specimen types.

b. From the graph of percentage intergranular crack length versus the load for the specimens tested at 1000°F (see figs. 62-65), it can be seen that the curves for the smooth specimens approach those for the notched specimens as the loads are decreased. In order for 5 to 10 per cent intergranular cracking to occur, the required loading stresses for the notched and smooth specimens must be approximately the same. It is not

clear from these results whether this similarity continues for greater amounts of intergranular cracking for tests conducted at 1000°F. For the rupture tests at a given load at 1200°F, the intergranular cracking, expressed as a percentage, is generally of the same order of magnitude in both specimen types.

c. Measurements of the intergranular crack lengths of Inconel 718 specimens rupture tested in a previous study (ref. 3) showed tendencies similar to those described above. An example of these results is presented in fig. 66 since the number of test points were in this case sufficient to establish the shape of the curves with great certainty.

1) In order for from 5 to 10 per cent intergranular cracking to occur in notched and smooth specimens, they must be rupture-tested under similar, and relatively high loading stresses.

2) At intermediate loading-stress levels, approximately the same amount of intergranular cracking occurs in the notched and smooth specimens.

3) At "relatively" low loading-stress levels, where the amount of intergranular cracking is high, smooth specimens tend to exhibit greater amounts of cracking than notched ones.

d. Within the range of testing at 1200°F, only the Waspaloy material solution treated at 2150°F and aged at 1700°F exhibited a substantial difference inthe behavior of the smooth and notched specimens at low loading-stress levels. The smooth specimens showed no evidence of a transgranular fracture surface, while the notched ones did to a significant degree. This dissimilarity in behavior could possibly be due in this case to a combination of two factors:

1) The material which showed large differences in

behavior (solution treated at 2150°F and aged 10 hours at 1700°F) also exhibited very extensive subsidiary cracking in the smooth specimens. Therefore, this suggests that a greater amount of creep damage (for a given loading stress) occurs in the smooth specimens, thus severely weakening the grain boundaries relative to the grains. In this case, weakening occurred to such an extent that it was energetically more feasible for the total fracture to occur in the smooth specimens by intergranular cracking without the initiation of a transgranular fracture.

2) In general, the intergranular crack develops from only one side of the specimen. In the notched specimens, for large intergranular crack lengths, the presence of the second notch (without an intergranular crack) could produce stress and strain states which result in the specimen failing with less intergranular cracking than for the smooth specimen tested at the same loading stress.

Net Section Stress at Transgranular Crack Initiation

As the intergranular crack develops for a fixed loading stress, the stress level in the load-bearing section increases. It is possible to calculate the values of the net section stress of the load-bearing area at the point of transgranular crack initiation from the load and the length of the intergranular crack. To determine the stress level at the intergranular crack tip at this stage, the net section must be modified by a number of factors:

1. A stress concentration factor, "K_t", of the crack, which tends to increase the stress level at the crack tip. This factor will vary with the degree of biaxiality, which, in turn, is dependent on the crack depth.

2. Relaxation, both time-independent yielding (deformation on loading) and the time-dependent deformation occurring due to creep, which tends to reduce the stress level at the crack tip.

Since these factors cannot be evaluated at the present time, only the net section at transgranular crack initiation has been calculated from the intergranular crack lengths for both specimen types (see tables 2 and 3). Any tendencies in these results, therefore, only reflect the load versus intergranular crack length curves. However, from these tabulations, the following factors were evident:

1. For the smooth specimens, variations in the net section stress (i.e., on the load-bearing section), the time of transgranular crack initiation could be correlated with the variation in ductility. For the tests at 1000°F, the values for the net section stress decreased with increasing rupture time, i.e., decreasing loads. At higher temperatures, the values for the net section stresses tended to reverse from a decreasing trend to an increasing trend with rupture time. This behavior followed the same pattern described earlier (as a function of the time-temperature parameter T(20+Log t)) for the ductility, particularly the values of reduction in area.

2. Although the smooth rupture specimens tested at 1000°F contained intergranular cracks in the majority of cases, transgranular failure occurred when the net section stresses were higher than the notched specimen tensile strengths.

3. The net section stresses at the point of transgranular crack initiation for the notched specimens followed a pattern similar to that of the smooth specimens. In this case however, the decrease and subsequent increase in the values (i.e., with increasing values of the time-temperature parameter) was much less marked than for the smooth specimens.

The Effect of Specimen Thickness on Fracture Appearance

The lengths of the intergranular cracks in the ruptured 0.050-inch thick specimens were measured using the procedure previously described for the 0.026-inch thick specimens. These values (see table 8) were then compared with those of the thinner specimens. As was the case for the 0.026-inch thick material, the fractures of the tensile-tested 0.050-inch thick material did not exhibit any intergranular cracking. For a given loading stress, the intergranular crack was longer in the 0.050-inch thick creep-ruptured specimens than for the thinner material for both specimen types.

The longer intergranular cracks in the thicker specimens cannot, alone, be used to explain the higher rupture strengths and little or no notch sensitivity of this material when compared with the results for the 0.026 inch thick material. It is indeed conceivable that the slightly higher rupture strength levels for the smooth specimens resulted, at least in part, from the larger intergranular crack length and, hence, from a longer period of crack growth. However, the following should be noted:

1. On the basis of prior discussion (in particular, regarding the similarity in behavior of notched and smooth specimens after a small amount of intergranular crack growth), the increase in notched specimen rupture time due to the increase in crack length could be expected to be similar to the increase in smooth specimen rupture time due to this effect. The notch sensitivity would not, therefore, be greatly influenced.

2. Due to the increasing stress level on the load-bearing section as the crack develops, the crack growth rate is expected to increase. Only a small proportion of the rupture time is therefore accounted for by the additional distance of crack growth in the 0.050-inch thick specimens when compared to the total length of cracking in the 0.026-inch specimens.

These results suggest that differences in strength levels with thickness variation are due to variations in the time period for crack initiation and/or propagation rates of the intergranular cracks. Variations

in the intergranular crack lengths may therefore be reflective of associated changes in the earlier stages of cracking.

DISCUSSION

As a means of establishing the scope and causes of the notch sensitivity in Ni-base superalloys, variations in the heat treatment of Waspaloy were used to allow assessment of the influence of microstructural features and mechanical properties on the sensitivity to notches.

Examination of the creep-rupture tested specimens showed that the failures occurred by intergranular crack growth followed by transgranular fracture. Since the material variations introduced by the heat treatments can be expected to influence each of the stages of the fracture process differently, they must be considered within the context of the proper balance (or influence) of the fracture processes occurring.

The relationships between microstructural features and mechanical characteristics and notch sensitivity were investigated at testing temperatures of 1000°, 1200°, and 1400°F. Although the majority of the testing utilized sheet specimens 0.026-inch in thickness, limited testing was also carried out using 0.050-inch thick material.

Relationships to the "Material Fracture Toughness"

The rupture life of the material at a given stress was governed by the rate of formation and growth of the intergranular and transgranular cracks. After initiation of the transgranular crack, the rate of crack growth can be considered in terms of the fracture toughness of the remaining cross sectional area. The fracture toughness, or K_C value of a material is determined by measuring the loading stress at which a crack initiated by a notch or fatigue crack becomes unstable, thus resulting in rapid crack propagation. In a determination of this type, the externally-applied load is increased during the test, thereby increasing the stress. In the

case under study, the stress was increased by the decreasing load-bearing section by slow intergranular crack propagation and then by transgranular cracking.

From the fractured specimens it was possible to determine the stage at which the shear fracture initiated. It was not possible, however, to determine if and when rapid transgranular crack propagation, or "pop in" occurred.

The Significance of Transgranular Crack Initiation

The nominal stress levels existing at the point of transgranular crack initiation were high (see tables 2 and 3). In addition, the transgranular cracks showed very little evidence of oxidation. It may therefore be concluded that the time taken for fracture after transgranular crack initiation was short. Therefore, the time for transgranular fracture was sufficiently short to be of no significant part of the rupture time (except for tensile tests and, possibly, extremely short-time rupture tests).

For the hypothetical case of a material with a given resistance to intergranular crack initiation and growth, the transgranular strength controls the rupture time on the basis that it determines the end of the intergranular crack growth. The rupture time is essentially made up of the times for intergranular crack initiation and growth, the latter being dependent on the length of the intergranular crack. It should be noted that the intergranular crack propagation rate could well increase as the crack develops due to the increase in stress on the load-bearing section. If this is indeed the case, a relatively small time period is taken for a considerable proportion of the total crack growth just prior to transgranular crack initiation. For materials or test conditions which result in comparatively long cracks to initiate transgranular fracture, the time involved in propagating the crack just prior to transgranular fracture would therefore not be influenced very much by the variations in transgranular strength. Experimental evaluation of the effect of variations in the transgranular

strength on the rupture time would be extremely difficult, however, since it is impossible to vary the transgranular strength level without also varying the factors that control the intergranular cracking process.

The Dependence of Notch Sensitivity on the Initial Stages of Intergranular Cracking

The notch sensitivity of a given material can be considered to be the difference in rupture times between notched and smooth specimens tested at the same initial net section stresses. This difference will be dependent on the relative values of the time periods for the various stages of fracture (initiation and growth of the intergranular and shear cracks) of the specimens. Once a crack has developed in a smooth specimen, its behavior and ultimate failure is somewhat related to the failure of a cracked, notched specimen tested at the same temperature and stress level. On this basis, the difference in rupture times and, hence, the notch sensitivity could be considered essentially as the difference in the intergranular crack initiation time of the smooth and notched specimens. This analysis must be qualified by the influence of the following two factors, which could affect the fracture behavior subsequent to crack initiation.

1. During the intergranular crack initiation period, the changes due to stresses exposure occurring throughout the specimen cross section will differ for smooth and notched specimens. These changes, whether they are strengthening or damaging in nature, will influence the subsequent intergranular crack propagation rate and the transgranular strength of the remaining section, which must be exceeded for final failure. In a previous investigation (ref. 2), it was shown that long-time exposure of Waspaloy at 1000°F and at relatvely low stresses did not influence the tensile strength of the material to any extent. At this temperature, it may therefore be concluded that no significant creep damage will occur in specimens during the initial stages of rupture life. However, the amount of damage occurring will increase with temperature, and thus may

become a significant factor in the behavior of the materials subsequent to crack initiation.

2. The major crack in both the smooth and notched specimens develops almost always from one of the specimen edges. Physically, then, the specimens are similar after crack initiation, except for the presence of the notches in the case of the notched specimens. These notches will modify the stress and strain distribution, thus resulting in a difference in behavior, as was discussed previously.

a. The propagation of the intergranular crack, especially in the early stages of growth, will be affected by the geometry of the specimen surrounding the crack. It is impossible to evaluate this effect for notched and smooth specimens without experimentation, however, the amounts of intergranular cracking observed in this investigation can be used to clarify the extent of this effect somewhat. Consideration should be centered, where possible, on the 1000°F tests where the amount of creep damage occurring in the specimens ahead of cracks can be expected to be limited. Comparison of the results at this temperature showed that for a given stress on the load-supporting section, the two specimens failed with similar intergranular crack lengths when the amount of intergranular cracking reached 5 to 10 per cent. For lower loads (from the results at 1200°F and 1400°F), the two specimens failed with similar intergranular crack lengths at least until these lengths have increased to approximately 50 per cent. This would suggest that the stress and strain distributions at the crack tips of both specimen types was similar for crack lengths of 5 to 10 per cent to 50 per cent. On the basis that the intergranular crack growth rates are primarily dependent on the stress and strain states at the crack tips and that they also govern the transgranular crack initiation, the crack growth rates for notched and smooth specimens can be assumed to be approximately equal for intermediate crack lengths. Therefore, the notch sensitivity for a given

material is dependent not only on the crack initiation time, but also on the difference in time for cracks to grow to 5 to 10 per cent of the width in notched and smooth specimens.

b. It was apparent from the measured intergranular crack lengths that the notched and smooth specimens did not behave similarly in cases where very large intergranular crack lengths developed, i.e., for a given load, smooth specimens had larger crack lengths. However, due to the probable occurrence of increases in crack growth rates as the intergranular crack developed (because of increasing stress levels on the load-bearing section), the time period for the final stages of crack growth will be small relative to the rupture time, thus minimizing the effect of any differences between the specimens.

Examination of the rupture curves determined at 1000° and 1200°F for the materials aged at 1400°F showed that, for a given stress level, the notches reduced the rupture time to less than 10 per cent of that for the smooth ones. This result therefore indicates that the crack initiation in smooth specimens could take place after as much as 90 per cent of the rupture life has been used up. Even when modified by the additional effects discussed above, this result indicates that a high proportion of the rupture life of smooth specimens is made up of the time period for intergranular crack initiation and growth to a depth of 5 to 10 per cent of the specimen width.

This conclusion is in agreement with the results obtained in the previous investigation (ref. 2). Exposure of Waspaloy (in both the cold-worked and aged, and annealed and aged conditions) at 1000°F under a stress of 40 ksi resulted in only a slight increase in the room-temperature tensile strength. This can only be explained if no cracking occurred during exposure. A similar set of experiments utilizing notched specimens resulted in a number of unexpected failures. However, the specimen which did not rupture during exposure showed a slight increase in tensile strengths on subsequent testing. Thus, the results indicate that intergranular crack initiation

in smooth and possibly notched specimens occurs after a substantial proportion of the rupture life has been used up.

It is more difficult to delineate the significance of the individual stages of the fracture sequence to the rupture lives of those specimens which exhibited little or no notch sensitivity and, particularly, to the materials in the standard condition of heat treatment and tested at 1400°F. For a given nominal stress level, the rupture times for both specimen types were of the same order of magnitude. These results could be explained in terms of a rupture life composed primarily of the period in which intergranular crack propagation occurred. If this were the case, the rate of crack propagation would have to be low, resulting in similar rupture times for both kinds of specimen. On the other hand, if the time for crack initiation occupied a significant proportion of the rupture time, this period must have been similar for both specimens. This would suggest that the stress and strain states developed at the notches result in notch strengthening at this temperature.

It should be noted that the amount of subsidiary cracking observed for a given rupture time increased with test temperature. As discussed previously, this result supports the contention that with increasing temperature there is an increasing dependence of rupture time upon the time period for intergranular crack propagation.

The Relationship of Microstructure to Notch Sensitivity

Variations in both solution and aging treatments were used in an attempt to control microstructural features, in particular, the γ' distribution and the amount of grain boundary carbide. Aging at 1700°F, when compared with the aging treatment at 1400°F, did result in a marked difference in the size of the γ' particles (approximately a ten-fold increase), but little variation in other microstructural features. The solution treatments were designed to vary the amount of grain boundary carbide. Although a variation was achieved, the treatments also resulted in variations in other microstructural features, e.g., γ' precipitation in grain boundaries and grain growth. In addition, the variations in solution treatment resulted in

large variations in the tensile and creep-rupture strength levels, which probably do not reflect variations in the grain boundary characteristics, but rather the intragranular characteristics. Because of these factors, no way has been found to correlate the variations in grain boundary characteristics with notch sensitivity. However, it should be noted that the changes in solution treatment did not result in any great variation in the range of N/S ratios occurring in either tensile or rupture tests. In addition, the ductility changes which occurred with increasing time-temperature parameter followed similar trends for the different solution treatments.

The aging treatments of the type of alloys studied in this investigation are used to control the γ' particle size and distribution, which in turn has a very marked influence on the creep resistance. The two aging treatments studied in this investigation, however, resulted only in a small variation in the creep resistance (and tensile strengths). This variation was, in fact, much smaller than that produced by the variations in the solution treatments. For these alloys, also, the creep resistance increases and subsequently decreases with increasing time and temperature of aging. The aging treatments in this program could be, therefore, on either side of this maximum, thus resulting in similar levels of creep resistance observed. Aging at the higher temperature also resulted in slightly lower tensile strength levels and slightly lower N/S tensile strength ratios. More significant, however, the aging treatment had very marked influence on the N/S ratio in rupture tests and on the rupture ductility. Aging at 1700°F resulted in much higher N/S ratios and higher rupture ductilities than aging at 1400°F. Further discussion of these features will be presented in the following section, since it is evident that the notch sensitivity can be related most readily to specific mechanical characteristics rather than to microstructural features.

The Relationship of Mechanical Characteristics to Notch Sensitivity

Notch Sensitivity of 0.026-inch Thick Material

For the 0.026-inch thick material there is an apparent correlation

between the rupture ductility of the smooth specimens and the time-dependent notch sensitivity. For loading-stress levels below the 0.2 per cent yield strength, the notch sensitivity of the material increased with decreasing ductility. At higher temperatures and longer rupture times, the rupture ductility increased, which correlates with a decrease in the notch sensitivity. However, it is apparent that the ductility level, itself, was not an important factor, but rather it was the factors contributing to the ductility that influenced the notch sensitivity. (There is not a 1:1 correspondence between absolute ductility level and the N/S ratio.)

For the tests at 1000°F, the majority of the deformation occurred on loading. As the deformation on loading decreased, so did the N/S strength ratio. This decrease in N/S ratio was apparent for notched specimen loads below the 0.2 per cent yield strength, where the deformation on loading was limited to the areas of stress concentration at the notches. At loads above the yield strength, the N/S ratios observed were at or above the ratios determined in tensile tests. These results suggest that at the higher loads, sufficient (time-independent) deformation occurred for complete relaxation of the stresses to occur at the root of the notches. This relaxation of the stresses acted to slow the initiation and growth of the intergranular crack, thus resulting in high N/S ratios. At the lower loads, sufficient relaxation of the stresses at the notches apparently did not occur so that creep deformation rapidly resulted in intergranular cracking and, hence, in fracture.

At longer rupture times and higher temperatures, i.e., at lower load levels, appareciable amounts of deformation occurred during third stage creep. Corresponding to this introduction of third stage creep deformation, the materials became less notch sensitive. In the tests at 1000°F, intergranular crack initiation and growth presumably must have occurred during second stage creep (there was no third stage creep and discontinued specimens exhibited no cracks at shorter times). Relaxation of the stress at the notches, due to the deformation occurring on loading in these cases, would therefore be effective in slowing crack initiation by creep processes.

In considering the tests which exhibited third stage creep, that is, at the lower stress levels, two principal factors must be taken into account:

a. relaxation of the stresses at crack tips and notches by deformation on loading and due to creep; and,

b. the creep deformation required to initiate and propagate the intergranular cracks.

If crack initiation in these tests occurred during the second or third stages of creep prior to the time when large amounts of creep deformation occurred, then it is possible that the stress concentration at the notches was not completely relaxed prior to crack initiation. Crack growth for both kinds of specimen should be slowed due to relaxation of stresses at the crack tips due to creep deformation. It is also possible that creep deformation caused relatively easy crack initiation and growth in the smooth specimens. In the notched specimens, on the other hand, creep deformation was constrained by the notches, although the stress levels at the notches may have been higher. And, the combination of these effects could result in crack initiation times which are similar to those of the smooth specimens. Thus, the introduction of third stage creep deformation, itself, may not affect the notch sensitivity, but it apparently reflects processes occurring in the earlier stages of creep and/or intergranular cracking that result in elimination of the notch sensitivity.

The above factors were especially evident for the materials aged at 1400°F. The N/S ratio decreased with decreasing elongation on loading, and, subsequently, increased as the amount of third stage creep increased at the higher temperatures and longer rupture times. For the material aged at 1700°F, some increased in notch sensitivity occurred with decreasing loads (decreasing elongation on loading). Significant amounts of third stage creep occurred at high enough loads, apparently, to prevent notch sensitive behavior as the loads were reduced below the levels of the yield strength.

It is of interest to comment on the influence of creep resistance on the notch sensitivity. The creep resistance of a material can be expected

to influence the degree of notch sensitivity because of the two main opposing effects: creep relaxation of the stresses, and the crack initiation and growth due to creep strain.

For the tests at 1000°F, the minimum creep rate curves, as a function of stress, had similar slopes and the creep resistance levels followed a pattern with heat treatment similar to the tensile strengths. The degree of notch sensitivity was shown to be related to the load to yield strength ratio and, hence, somewhat related to the load to tensile strength ratio. It should be noted that comparsion of the individual heat treated materials for loads established from a given percentage, e.g., 90 per cent of the individual tensile strengths, resulted in a minimum creep rate value which is roughly independent of heat treatment. In addition, it was evident from the slopes of the curves for the various materials that, for a given amount of stress relaxation, all materials will undergo approximately the same strain. The marked degree of change in notch sensitivity due to aging at 1700°F as compared to 1400°F, probably resulted from changes in the amount of relaxation occurring on loading and not on the small variation in creep resistance. The above explanation also conforms to the fact that varying the solution treatment had a marked influence of the creep resistance, yet very little influence on the degree of notch sensitivity.

For the tests at the higher temperatures, the creep resistance could be expected to have a greater influence on the notch sensitivity since less relaxation of stress can occur, due to the smaller amounts of deformation occurring on loading. However, because of the nature of the dual influence of the creep resistance, and since little deformation, or time occurred in second stage, it is not possible to arrive at any appropriate conclusions at the present time.

Effect of Sheet Thickness on the Notch Sensitivity

The relationships between ductility and notch sensitivity, which were discussed earlier, appear to be the basis of a satisfactory explanation of the behavior of the 0.026-inch thick material. The results for the

0.050-inch thick material either contradict this explanation, or require the inclusion of added major effects. Ductility troughs also occurred for this material (in some cases, with very low elongations on loading and during creep), and yet no marked time-dependent notch sensitivity was observed. Two factors which may possibly contribute to this discrepancy immediately present themselves:

1. Stress and/or strain states in the 0.050-inch thick, notched specimens were sufficiently different from those in the 0.026-inch thick specimens that the deformation on loading or during creep was sufficient in all cases to relax the stresses and/or slow crack initiation and growth in the notched specimens, and so prevented notch sensitive behavior.

2. Crack initiation and growth characteristics cound have varied with specimen thickness due to factors such as metallurgical surface effects.

The results from the investigations reported previously which involved the effect of K_t on the notch sensitivity of 0.025-inch thick sheet material, are relevant to an explanation of the effect of changes in stress or strain states, such as those which could occur because of thickness variation. For Waspaloy tested at 1200°F (see table 11), a K_t of 3.0 was found to be nearly as detrimental to the rupture strength as a K_t of 20 (the material was in the cold-worked and aged condition). Similar results were obtained for Inconel 718 tested at 1000°F and 1200°F, in both the cold-worked and aged condition, and after a 1950°F annealing plus aging treatment. For one heat treatment (1750°F anneal plus age), Inconel 718 was extremely notch sensitive at 1000°F and much less so at 1200°F for a K_t of 20 (see fig. 67). For K_t's of 2.3 and 6.0, however, very little notch sensitivity was observed at either temperature. These results suggest that for a given material, a critical K_t, or stress concentration level exists below which the material exhibits little or not notch sensitivity, whereas

above it, the material becomes rapidly more notch sensitive. Similarly, it is possible that a critical thickness exists (corresponding to a critical stress or strain state), above which little or no notch sensitivity is exhibited, and, for thicknesses below this level, the notch sensitivity can be expected to increase. Unpublished results for René 41 (see fig. 2) also show a significant influence of stress and strain states on the time-dependent notch sensitivity. Although each series of tests was carried out with material from different heats, the similarity of the smooth specimen strengths allow some confidence to be placed in the differences in behavior observed. As was true with Waspaloy, sheet thickness had an effect on the notch sensitivity. The 0.04-inch thick sheet showed markedly less notch sensitivity at 1000°F than did the 0.026-inch thick material. In addition, testing round bars at 1200°F resulted in a slight degree of notch strengthening, whereas the 0.026-inch thick sheet showed very marked notch sensitivity.

It is apparent from the results that the notch sensitivity was influenced by the relative rates at which the initial period of intergranular cracking occurred in the notched and smooth specimens. Observation of the failed specimens indicated that the subsidiary cracks (and, hence, the major intergranular crack) formed at or close to the surfaces or edges of the specimens. Surface characteristics of the materials, therefore, could have had a marked influence on the crack initiation and, hence, on the notch sensitivity. It is well known that element losses, e.g., B and Al, and other environmental effects can occur on the surface of superalloys during manufacture, high temperature testing, or heat treatment. These effects may or may not be visible as microstructural changes, although they can influence the mechanical properties of the surface material. In the present study, the specimens tested at the higher temperatures and longer times showed the presence of an oxidized layer, and a depletion of γ' in the surface layers (see figs. 61 and 68) which is probably associated with Al surface losses. At the lower temperatures of testing, no marked surface effects were noted; losses in elements, however, could also have

have occurred prior to, or during testing. Surface effects could be expected to have an increasing influence on properties of sheet material, the thinner the sheet; and, the behavior of notch sensitivity with varying thickness is not inconsistent with this effect. It should be noted that if, in fact, surface effects do have a marked influence on rupture strengths, it would be necessary to explain why the smooth specimen strengths were apparently independent of sheet thickness.

CONCLUSIONS

As part of a study of the scope and causes of the time-dependent notch sensitivity, which is exhibited by Ni-base sheet superalloys at temperatures of 1000° and 1200°F, the influence of heat treatment variations, test temperature, and sheet thickness on the notch sensitivity of Waspaloy was investigated. The heat treatments were designed to enable the establishment of the influence of microstructural features and mechanical characteristics on the notch sensitivity. Consequently, in addition to those pertaining to these correlations, several observations were made which were related to the effect of heat treatment on the microstructure and mechanical behavior of the alloy.

Effect of Heat Treatment on the Mechanical Properties of 0.026-inch Thick Sheet

1. For aging at both 1400° and 1700°F, increasing the solution temperature from 1825° to 2150°F (1/2 hour) resulted in a very marked decrease in the ultimate tensile strength, the 0.2 per cent offset yield strength, and the notch tensile strength at 1000°F. For a given solution treatment, the tensile and yield strengths were slightly lower at 1000°F after aging at 1700°F than after aging at 1400°F.

2. For aging at 1400°F and 1700°F, increasing the solution temperature from 1825° to 2150°F resulted in a marked decrease in the smooth

specimen rupture strengths at 1000°F and, to a lesser extent, at 1200°F, and in a decrease in creep resistance at 1000°F.

3. For materials aged at 1400°F, the notched specimen rupture curves at 1000°F underwent a drastic increase in slope when the load was reduced below the 0.2 per cent yield strength. These "breaks" in the rupture curves occurred at longer times, the higher the solution temperature (i.e., 110 hours for 1825°F and 2150 hours for 2150°F). There was also some evidence that the curves decreased in slope again at low stress levels.

4. Rupture ductility decreased with time at 1000°F, and both increased and decreased with time at 1200°F. Ductilities were higher for materials aged at 1700°F than for those aged at 1400°F. The elongation was made up, principally, of the large contributions of the elongation on loading (at higher stress levels) and the elongation in third stage creep (at lower stress levels). The time to rupture, on the other hand, was determined prinicipally by the time periods for second and third stage creep.

Effect of Heat Treatment on Microstructural Features

1. In addition to the major dispersion-strengthening phase γ' $Ni_3(Al, Ti)$ two carbides, Ti(C, N) and $M_{23}C_6$, were present as intragranular and intergranular phases, respectively.

2. After heat treatment for 1/2-hour at 1825°F, the γ' was not completely dissolved, whereas complete solution occurred after heat treatment for 1/2-hour at 1900°F. Substantial grain growth occurred after heat treatment at 2150°F, but not after the lower-temperature heat treatments. Aging at 1400°F resulted in a γ' precipitate which was too fine to be resolved easily by replica methods, whereas aging at 1700°F produced γ' particles approximately 700A in diameter.

3. Grain boundary and twin boundary carbide ($M_{23}C_6$) precipitated with an orientation identical to that of the neighboring grain on one side of

the boundary.

4. Solution treatment at 1975°F and particularly 2150°F, and aging at 1700°F resulted in minor amounts of γ' depletion adjacent to the grain boundaries and precipitation of γ' in the grain boundaries. These effects were not observed to any extent after the lower-temperature heat treatments.

5. The materials solution treated at 1825°F and aged exhibited relatively heavy precipitation of $M_{23}C_6$ carbide in twin boundaries. The material solution treated at 2150°F and aged at 1700°F exhibited precipitates of $M_{23}C_6$ in twin boundaries and in areas adjacent to twins. The other heat treatment did not exhibit twin boundary precipitation.

The Fracture Process

1. Rupture of both smooth and notched specimens occurred by slow intergranular cracking followed by abrupt transgranular fracture. The intergranular cracking appeared to occur by creep-induced initiation and growth. The occurrence of the shear failure was dependent upon the intergranular crack growth for raising the stress level in the load-bearing section high enough to initiate transgranular cracking. In both specimen types, the time to rupture was determined by all of these fracture processes.

2. It was evident that the initiation and growth of the intergranular crack assumed most of the time leading to rupture. In addition, for a given stress and temperature, the difference in rupture times for smooth and notched specimens (i.e., the notch sensitivity), was primarily determined by the first stages of intergranular cracking. This was mainly a consequence of the developing similarity of the stress-strain states of the notched and smooth specimens as the crack advanced.

Time-Dependent Notch Sensitivity

1. No direct correlation between microstructural features, such as carbide in grain boundaries and grain size, and notch sensitivity was established from the results of this investigation. Although the aging treatment (i.e., γ' size) had a marked influence on the notch sensitivity, microstructural variations appeared to influence the plastic deformation characteristics which, in turn, seemed, at least for the 0.026-inch thick material, to control the notch sensitivity most directly. For this sheet thickness, the notch sensitivity fell in the general range where plastic flow (i.e., ductility) was limited by low yielding on application of the stress and/or low creep deformation.

2. The correlations which were established between the notch sensitivity and the ductility for the 0.026-inch thick material were not the complete explanation, as evidenced by the effect of sheet thickness on the notch sensitivity (in the presence of the described changes in properties).

No time-dependent notch sensitivity was observed for the 0.050-inch thick material solution treated at 1975°F and aged at either 1400°F or 1700°F within the testing times studied, at 1000° or 1200°F. Because the ductility levels were similar to those exhibited by the 0.026-inch thick material (exhibited time-dependent notch sensitivity), it was evident that the notch sensitivity was dependent on major factors, in addition to the deformation behavior, which influenced strength levels in the presence of sharp-edged notches. Possible effects which could have contributed to the observed behavior were stress or strain state variations and surface effects.

Time-Dependent Notch Sensitivity and Ductility for the 0.026-inch Thick Sheet

1. The notch sensitivity increased markedly as the loads were reduced below the 0.2 per cent yield strengths. This increase was especially

evident for the materials aged at 1400°F and tested at 1000°F. For loads above the yield strength, the notch to smooth rupture strength ratio was greater than in tensile tests.

2. Presentation of the creep-rupture strengths in terms of a time-temperature parameter P ((in this case, T(Constant + Log t) was chosen)) led to the following:

   a. For materials aged at 1400°F, the notch sensitivity increased and subsequently decreased with increasing values of the parameter P. The minimum values of N/S (0.55-0.65) occurred at larger values of P, the higher the solution temperature. The smooth specimen rupture strengths exhibited gradually decreasing levels with increasing values of P. The changes in notch sensitivity observed were therefore primarily reflective of marked variations in the notched specimen rupture strengths.

   b. Aging at 1700°F produced comparable trends, although it appeared that the N/S ratios may never have falled below about 0.7.

   c. The changes in notch sensitivity could be correlated with the variations in ductility of the smooth specimens. Rupture ductility values also exhibited troughs (these were especially evident when considered in terms of the time-temperature parameter). The troughs were formed due to the large contributions of the elongation on loading at low parameter values (i.e., high loads) and the elongation in third stage creep at higher parameter values (i.e., lower loads). The evidence indicated that relaxation of stresses around notches was a critical factor affecting the intergranular fracture process and, thus, the notch sensitivity. This relaxation resulted from deformation by yielding and by subsequent creep. On the other hand, excessive creep deformation could promote intergranular cracking. The interaction of these two effects apparently resulted in the notch sensitivity being more dependent on the processes contributing to the ductility of the material than on the actual level of ductility.

LIMITATIONS OF RESULTS

In most cases, only limited test results were available for developing the explanation of the notch sensitivity. More data are needed to verify the indication that deformation in the various stages of creep controls the fracture processes in both smooth and notched specimens. Data are also needed on the nature of the contribution of the deformation on loading to the relaxation of stress and to the introduction of creep-induced intergranular cracks. In particular, detailed data are needed to establish the time periods for initiation and growth of the intergranular cracks.

The recourse to parameter-type presentation of the results was used entirely as a convenient way of showing the probable inter-relationship of mechanical properties and notch sensitivity. The ability to combine time-temperature effects on properties with notch sensitivity seemed to justify this procedure. However, the data were incomplete. Furthermore, this method of presentation should be checked further to demonstrate definitely whether or not it has any validity for use in predicting notch sensitivity characteristics.

Results obtained previously did not show notch sensitivity at 800°F. However, it was severe at 1000°F. Further work seems necessary to determine the lowest temperature at which notch sensitivity becomes a problem. This would also necessitate consideration of longer times than have yet been used for testing.

The effect of thickness and K_t on the notch sensitivity should be clarified. Consideration should be given to stress and strain state effects. In addition, further work should be done to determine if environmental or surface composition effects contribute to the cause of notch sensitivity.

REFERENCES

1. Raring, R. H.; Freeman, J. W.; Schultz, J. W.; and Voorhees, H. R.: Progress Report of the NASA Special Committee on Materials Research for Supersonic Transports. NASA TN D-1798, May 1963.

2. Cullen, T. M.; and Freeman, J. W.: The Mechanical Properties at 800°, 1000°, and 1200°F of Two Superalloys under Consideration for Use in the Supersonic Transport. Prepared under Grant. No. NsG-124-61 (NASA CR-92) for NASA by The University of Michigan, September 1964.

3. Cullen, T. M.; and Freeman, J. W.: The Mechanical Properties of Inconel 718 Sheet Alloy at 800°, 1000°, and 1200°F. Prepared under Grant No. NsG-124-61 (NASA CR-268) for NASA by The University of Michigan, July 1965.

4. Bigelow, W. C.; Amy, J. A.; and Brockway, L. O.: Electron Microscope Identification of the Gamma Prime Phase of Nickel-Base Alloys. Proc. ASTM, 56, p 945 (1956).

5. Wilson, D. J.; Cullen, T. M.; and Freeman, J. W.: Strain-Induced Precipitation of $Ni_3(Al, Ti)$ Phase in a Nickel-Base Superalloy. Rep. No. 04368-12-T, prepared for NASA under Grant No. NsG-124-61 by The University of Michigan, August 1966, p 4.

6. Larson, F. R.; and Miller, J.: A Time-Temperature Relationship for Rupture and Creep Stresses. Trans. Amer. Soc. Mech. Engrs., 74, p 765 (1952).

7. Wolff, Ursula R.: Orientation and Morphology of $M_{23}C_6$ Precipitated in High-Nickel Austenite. Trans. AIME, 236, p 19 (1966).

Table 1

HIGH-TEMPERATURE TENSILE PROPERTIES OF 0.026-INCH THICK WASPALOY SHEET

Heat Treatment	Test Temp. (°F)	Smooth Specimen Properties: Tensile Strength (ksi)	2% Offset Yield Strength (ksi)	Y.S./T.S.	Elong. (%)	R.A. (%)	Notch Tensile Strength (ksi)	N/S Tensile Strength Ratio	Grain Size (mm)
1/2 hr 1825°F									
+ 16 hrs 1400°F	1000	187.2	155.8	.83	12.5	21	162.0	0.86	0.025
+ 10 hrs 1700°F	1000	161.0	113.0	.70	19.5	21			0.026
1/2 hr 1900°F									
+ 16 hrs 1400°F	1000	163.8	113.0	.69	31.4	30	134.7	0.82	0.019
+ 10 hrs 1700°F	1000	149.2	91.5	.61	26.2	24	109.0	0.73	0.018
1/2 hr 1975°F									
+ 16 hrs 1400°F	1000	161.0	115.0	.71	33.4	32	132.5	0.82	0.020
+ 10 hrs 1700°F	1000	148.5	94.9	.64	36.0	28			0.021
1/2 hr 2150°F									
+ 16 hrs 1400°F	1000	134.0	91.0	.68	29.5	26	112.0	0.84	0.13
+ 10 hrs 1700°F	1000	130.0	74.0	.57	28.5	23	95.8	0.74	0.14
1/2 hr 1825°F									
+ 10 hrs 1700°F	1200	166.3	121.5	.73	20.5	19			
1/2 hr 1975°F									
+ 10 hrs 1700°F	1200	145.0	91.0	.63	31.0	25			
1/2 hr 1975°F									
+ 16 hrs 1400°F	1200	167.7	111.3	.67	21.7	20			
1/2 hr 1975°F									
+ 16 hrs 1400°F	1400	125.0	102.0	.82	6.5	16	117.5	0.94	

Table 2

SMOOTH SPECIMEN TENSILE AND CREEP-RUPTURE PROPERTIES OF 0.026-INCH THICK WASPALOY

Heat Treatment	Test Temp. (°F)	Stress (ksi)	Rupture Time (hrs)	Elong. (%)	R.A. (%)	Min. Creep Rate (%/hour)	Intergranular Crack Length (%)	Net Section Stress (ksi)
1/2 hr at 1825°F								
+ 16 hrs at 1400°F	1000	187.2	Tens.	12.5	21		0	187.2
		175	106.7	10.0	14	0.038	1	176
		165	479.8	4.29	10	0.0051	5	174
		155	2540.6	2.44	5	0.00051	6	165
	1200	120	57.7	5.12	6	0.064	5	126
		85	2560.3	3.40	6.5	0.00050	38	137
+ 10 hrs at 1700°F	1000	161	Tens.	19.5	21		0	161
	1200	166.3	Tens.	20.5	19		0	166.3
		95	322.9	5.10	6	0.0105	25	127
		85	894.5	5.50	8	0.00345	35	131
1/2 hr at 1900°F								
+ 16 hrs at 1400°F	1000	163.8	Tens.	31.4	30		0	163.8
		150	113.0	10.30	17	0.00255	3	155
		140	1060.8	6.68	11	0.00034	6	149
	1200	95	374.5	0.86	8	0.000355	23	123
		85	1046.9	2.20	8	0.00016	32	125
+ 10 hrs at 1700°F	1000	149.2	Tens.	26.2	24		0	149.2
		140	86.9	19.6	19	0.0305	3	144
		130	350.5	13.5	14	0.00175	7	144
	1200	90	570.6	5.60	12	0.0016	23	103
		75	2363.7	4.00		0.000245	43	132
1/2 hr at 1975°F								
+ 16 hrs at 1400°F	1000	161	Tens.	33.4	32		0	161
		150	131.9	14.6	24	0.017	3	155
		145	207.6		19	0.00525	7	156
		135	517.0	6.15	14	0.00050	8	147
	1200	167.7	Tens.	21.7	20		0	167.7
		120	3.6	3.63	13		8	131
		90	376.5	0.74	9	0.00045	23	117
		80	1240.8	1.40	9	0.000096	34	121
	1400	125	Tens.	6.5	16		0	125
		65	18.8	3.3	8		36	102
		45	406.1	6.5	11	0.0025	70	150
		38	1006.9	8.1	15	0.00053		
+ 10 hrs at 1700°F	1000	148.5	Tens.	36.0	28		0	148.5
	1200	145	Tens.	31.0	25		0	145
		100	38.7	5.96	12	0.062	20	125
		80	1870.1	3.88	11	0.00018	32	118
1/2 hr at 2150°F								
+ 16 hrs at 1400°F	1000	134	Tens.	29.5	26		0	134
		120	93.0	14.90	20	0.00090	1	121
		110	370.5	6.16	15	0.00013	5	116
		100	985.3	3.18	12	0.000017	6	106
	1200	70	90.2ph	0.35		0.004	34	106
		50	199.5ph	0.15		0.00003	51	102
+ 10 hrs at 1700°F	1000	130	Tens.	28.5	23		0	130
		120	146.3	21.1	20	0.0039	0	120
		110	483.0	11.37	15	0.00050	3	114
		100	6862 Discontinued			0.00003		
	1200	90	64.4	10.5		0.011	100	∞
		70	4419.4	1.36	2	0.00058	100	∞

ph = pin hole.

Table 3

NOTCH SPECIMEN (K_t>20) TENSILE AND CREEP-RUPTURE PROPERTIES OF 0.026-INCH THICK WASPALOY

Heat Treatment	Test Temp. (°F)	Stress (ksi)	Rupture Time (hrs)	Intergranular Crack Length (%)	Net Section Stress (ksi)
1/2 hr at 1825°F					
+ 16 hrs at 1400°F	1000	162	Tens.	0	162
		135	227.7	13	155
		100	831.7	22	128
	1200	80	253.2	36	125
		65	4064.0	50	130
+ 10 hrs at 1700°F	1200	90	77.2	37	143
		75	379.1	44	134
		55	5000 Discontinued		
1/2 hr at 1900°F					
+ 16 hrs at 1400°F	1000	134.7	Tens.	0	134.7
		110	386.6	18	134
		85	2153.6	31	123
	1200	75	82.2	39	123
		65	174.2	44	116
		50	10,000 Discontinued		
+ 10 hrs at 1700°F	1000	109	Tens.	0	109
		95	7487 Discontinued		
		85	6144.7 Discontinued		
	1200	75	198.5	37	119
		62	4238	51	126
		45	4991 Discontinued		
1/2 hr at 1975°F					
+ 16 hrs at 1400°F	1000	132.5	Tens.	0	132.5
		110	728.0	12	125
		90	706.2	15	106
		70	4648.1	42	120
	1200	70	42.5	28	97
		50	290.3	50	100
	1400	117.5	Tens.	0	117.5
		95	0.1	10	105
		45	260.7ph		
		38	1066.8	74	105
+ 10 hrs at 1700°F	1200	85	164.9	26	115
		70	928.1	34	106
		45	4182.7 Discontinued		
1/2 hr at 2150°F					
+ 16 hrs at 1400°F	1000	112	Tens.	0	112
		90	2572.5	19	111
		75	5038.9	24	99
	1200	65	59.1	47	123
		50	76.7ph	69ph	161
+ 10 hrs at 1700°F	1000	95.8	Tens.	0	95.8
		85	8112 Discontinued		
		75	6144.7 Discontinued		
	1200	85	42.6	13	98
		70	358.8ph		

ph = pin hole

Table 4A

NOTCH AND SMOOTH SPECIMEN TENSILE AND CREEP-RUPTURE STRENGTHS OF 0.026-INCH THICK WASPALOY SHEET AT 1000°F

Heat Treatment	Smooth Specimen Tests: Tensile Properties: Yield Strength (ksi)	Elong. (%)	R.A. (%)	Tensile Strength (ksi)	Rupture Strengths: 1000-hr Strength (ksi)	10,000-hr Strength (ksi)	Notched Specimen Tests: Tensile and Rupture Strengths: Tensile Strength (ksi)	1000-hr Strength (ksi)	10,000-hr Strength (ksi)	$\frac{N}{S}$ Strength Ratios: Tensile Strength (ksi)	1000-hr Strength (ksi)	10,000-hr Strength (ksi)
1/2 hr at 1825°F												
+ 16 hrs at 1400°F	155.8	12.5	21	187.2	159	144	162.0	96	58	0.86	0.60	0.40
+ 10 hrs at 1700°F	113.0	19.5	21	161.0								
1/2 hr at 1900°F												
+ 16 hrs at 1400°F	113.0	31.4	30	163.8	139	129	134.7	94	66	0.82	0.68	0.51
+ 10 hrs at 1700°F	91.5	26.2	24	149.2	123	108	109.0	>103	>90	0.73	>0.84	>0.83
1/2 hr at 1975°F												
+ 16 hrs at 1400°F	115.0	33.4	32	161.0	128	108	132.5	94	58	0.82	0.73	0.54
+ 10 hrs at 1700°F	94.9	36.0	28	148.5								
1/2 hr at 2150°F												
+ 16 hrs at 1400°F	91.0	29.5	26	134.0	99	83	112.0	97	62	0.84	0.98	0.75
+ 10 hrs at 1700°F	74.0	28.5	23	130.0	110	100	95.8	> 90	>82	0.74	>0.82	>0.82

Table 4 B

NOTCH AND SMOOTH SPECIMEN TENSILE AND CREEP-RUPTURE STRENGTHS OF 0.026-INCH THICK WASPALOY SHEET AT 1200°F

Heat Treatment	Smooth Specimen Tests						Notched Specimen Tests		$\frac{N}{S}$ Strength Ratios	
	Tensile Properties				Rupture Strengths		Rupture Strengths			
	Yield Strength (ksi)	Elong. (%)	R.A. (%)	Tensile Strength (ksi)	1000-hr Strength (ksi)	10,000-hr Strength (ksi)	1000-hr Strength (ksi)	10,000-hr Strength (ksi)	1000-hr Strength (ksi)	10,000-hr Strength (ksi)
1/2 hr at 1825°F										
+ 16 hrs at 1400°F					92	74	72	60	0.78	0.81
+ 10 hrs at 1700°F	121.5	20.5	19	166.3	74	65	68	51	0.92	0.78
1/2 hr at 1900°F										
+ 16 hrs at 1400°F					84	66	58	>50	0.69	>0.76
+ 10 hrs at 1700°F					74	61	68	>59	0.92	>0.97
1/2 hr at 1975°F										
+ 16 hrs at 1400°F	111.3	21.7	20	167.7	84	71	40	27	0.48	0.38
+ 10 hrs at 1700°F	91.0	31.0	25	145.0	84	73	70	55	0.83	0.75
1/2 hr at 2150°F										
+ 16 hrs at 1400°F					Low strength levels					
+ 10 hrs at 1700°F					76	66	64	54	0.84	0.82

Table 5

ELONGATIONS AND TIME PERIODS OF CREEP AT 1000°F

FOR 0.026-INCH THICK WASPALOY SHEET

Heat Treatment	Stress (ksi)	Total Elong. (%)	Elong. on Loading (%)	Creep Elongation 1st Stage (%)	Creep Elongation 2nd Stage (%)	Creep Elongation 3rd Stage (%)	Creep Elongation Total (%)	Rupture Time (hrs)	Time Periods for Creep 1st Stage (hrs)	Time Periods for Creep 2nd Stage (hrs)	Time Periods for Creep 3rd Stage (hrs)
1/2 hr at 1825°F											
+ 16 hrs at 1400°F	187.2	12.5						Tens.			
	175	10.0	4.87	0.78	4.35	0.00	5.13	106.7	7	100	0
	165	4.29	1.12	0.28	2.89	0.00	3.17	479.8	16	464	0
	155	2.44	0.63	0.28	1.53	0.00	1.81	2540.6	100	2441	0
+ 10 hrs at 1700°F	161	19.5						Tens.			
1/2 hr at 1900°F											
+ 16 hrs at 1400°F	163.8	31.4						Tens.			
	150	10.3	8.77	1.08	0.45	0.00	1.53	113	40	73	0
	140	6.78	5.80	0.53	0.45	0.00	0.98	1060.8	200	861	0
+ 10 hrs at 1700°F	149.2	26.2						Tens.			
	140	19.6	14.24	3.46	1.9	0.00	5.36	86.9	33	54	0
	130	13.5	10.27	2.13	1.1	0.00	3.23	350.5	65	285	0
1/2 hr at 1975°F											
+ 16 hrs at 1400°F	161	33.4						Tens.			
	150	14.6	12.61	0.84	1.15	0.00	1.99	131.9	12	120	0
	145			0.79	1.00	0.00	1.79	207.6	34	170	0
	135	6.15	5.72	0.23	0.20	0.00	0.43	517	26	491	0
+ 10 hrs at 1700°F	148.5	36.0									
1/2 hr at 2150°F											
+ 16 hrs at 1400°F	134	29.5						Tens.			
	120	14.9	14.60	0.02	0.28	0.00	0.30	93	1	92	0
	110	6.16	6.00	0.07	0.09	0.00	0.16	370.5	20	350	0
	100	3.18	2.36	0.10	0.055	0.66	0.815	985.3	5	850	85
+ 10 hrs at 1700°F	130	28.5						Tens.			
	120	21.1	19.20	0.90	1.00	0.00	1.90	146.3	20	126	0
	110	11.37	10.22	0.78	0.37	0.00	1.15	483	30	453	0
	100		5.34	0.20				6862 Discontinued			

Table 6

ELONGATIONS AND TIME PERIODS OF CREEP AT 1200°F

FOR 0.026-INCH THICK WASPALOY SHEET

Heat Treatment	Stress (ksi)	Total Elong. (%)	Elong. on Loading (%)	Creep Elongation 1st Stage (%)	Creep Elongation 2nd Stage (%)	Creep Elongation 3rd Stage (%)	Creep Elongation Total (%)	Rupture Time (hrs)	Time Periods for Creep 1st Stage (hrs)	Time Periods for Creep 2nd Stage (hrs)	Time Periods for Creep 3rd Stage (hrs)
1/2 hr at 1825°F											
+ 16 hrs at 1400°F	120	5.12	0.45	0.45	4.22	0.00	4.67	57.2	4	53	0
	85	3.40	0.30	0.06	1.14	1.90	3.10	2560.3	30	1670	860
+ 10 hrs at 1700°F	95	5.10	0.41	1.14	3.45	0.00	4.69	322.9	45	278	0
	85	5.50	0.31	0.86	3.43	0.90	5.19	894.5	90	660	145
1/2 hr at 1900°F											
+ 16 hrs at 1400°F	95	0.86	0.34	0.07	0.13	0.32	0.52	374.5	20	220	135
	85	2.20	0.27	0.06	0.23	1.64	1.93	1046.9	10	610	427
+ 10 hrs at 1700°F	90	5.60	0.49	0.05	0.86	4.50	4.96	570.6	5	145	421
	75	4.00	0.31	0.07	0.42	3.20	3.29	2363.7	3	147	1514
1/2 hr at 1975°F											
+ 16 hrs at 1400°F	167.7	21.7						Tens.			
	120	3.63	2.55				1.08	3.6			
	90	0.74	0.30	0.04	0.16	0.24	0.44	376.5	2	278	96
	80	1.40	0.30	0.04	0.09	0.97	1.10	1240.8	70	530	641
+ 10 hrs at 1700°F	100	5.96	2.83	0.60	2.43	0.00	3.03	38.7	3	36	0
	80	3.88	0.35	0.10	0.37	3.06	3.53	1870.1	20	>80	1070
1/2 hr at 2150°F											
+ 16 hrs at 1400°F	70	0.35	0.23	0.07	0.05	0.00	0.12	90.2ph	4	86	0
	50	0.19	0.17	0.01	0.01	0.00	0.20	199.5ph	2	198	0
+ 10 hrs at 1700°F	90	10.5	6.85	0.65	0.50	2.50	3.60	64.4	8	27	29
	70	1.36	0.66	0.01	0.31	0.38	0.70	4419.4	20	3100	1299

ph = pin hole

Table 7

ELONGATIONS AND TIME PERIODS OF CREEP AT 1000°, 1200° AND 1400°F
FOR 0.026-INCH THICK WASPALOY SHEET
SOLUTION TREATED AT 1975°F AND AGED AT 1400°F

Test Temp. (°F)	Stress (ksi)	Total Elong. (%)	Elong. on Loading (%)	Creep Elongation 1st Stage (%)	Creep Elongation 2nd Stage (%)	Creep Elongation 3rd Stage (%)	Creep Elongation Total (%)	Rupture Time (hrs)	Time Periods for Creep 1st Stage (hrs)	Time Periods for Creep 2nd Stage (hrs)	Time Periods for Creep 3rd Stage (hrs)
1000	161	33.4						Tens.			
	150	14.6	12.61	0.84	1.15	0.00	1.99	1319	12	120	0
	145			0.79	1.00	0.00	1.79	207.6	34	170	0
	135	6.15	5.72	0.23	0.20	0.00	0.43	517	29	491	0
1200	167.7	21.7						Tens.			
	120	3.63	2.55				1.08	3.6			
	90	0.74	0.30	0.04	0.16	0.24	0.44	376.5	2	278	96
	80	1.40	0.30	0.04	0.09	0.97	1.10	1240.8	70	530	641
1400	125	6.5						Tens.			
	65	3.3	0.28				3.02	18.8			
	45	6.5	0.19	0.21	0.90	5.20	6.31	406.1	25	225	181
	38	8.1	0.14	0.06	0.90	7.00	7.96	1006.9	25	575	432

Table 8

CREEP-RUPTURE PROPERTIES OF 0.026-INCH AND 0.050-INCH THICK WASPALOY

Sheet Thickness (inches)	Specimen Type	Test Temp. (°F)	Stress (ksi)	Rupture Time (hrs)	Elong. (%)	R.A. (%)	Min. Creep Rate (%/hour)	Intergranular Crack Length (%)	Net Section Stress (ksi)
Aged 16 hours at 1400°F									
0.026	Smooth	1000	161	Tens.	33.4	32		0	161
			150	131.9	14.6	24	0.017	3	155
			145	207.6		19	0.00525	7	156
			135	517.0	6.15	14	0.00050	8	147
0.050	Smooth	1000	158.5	Tens.	38.0			0	158.5
			150	145.1	16.2	24	0.018	3	155
			145	323.5		22	0.0039	7	156
			140	475.5	11.5	19	0.0012	4	149
0.026	Notch	1000	132.5	Tens.				0	132.5
			110	728.0				12	125
			90	706.2				15	106
			70	4648.1				42	120
0.050	Notch	1000	115	896.5				13	132
0.026	Smooth	1200	167.7	Tens.	21.7	20		0	167.7
			120	3.6	3.63	13		8	131
			90	376.5	0.74	9	0.00045	23	117
			80	1240.8	1.40	9	0.000096	34	121
0.050	Smooth	1200	90	513.1	1.45	9	0.00013	35	139
0.026	Notch	1200	70	42.5				28	97
			50	290.3				50	100
0.050	Notch	1200	85	32.6				30	121
			60	9960 Discontinued					
Aged 10 hours at 1700°F									
0.026	Smooth	1000	148.5	Tens.	36.0	28		0	148.5
0.050	Smooth	1000	139.8	Tens.	34.0	36		0	139.8
			125	1109.1	17.0	19	0.00148	7	134
0.026	Smooth	1200	145	Tens.	31.0	25		0	145
			100	38.7	5.96	12	0.062	20	125
			80	1870.1	3.58	11	0.00018	32	118
0.050	Smooth	1200	90	331.6	6.0	14	0.0047	26	122
			80	2937.2	8.9	13	0.0001	34	121
0.026	Notch	1200	85	164.9				26	115
			70	928.1				34	106
			45	4182.7 Discontinued					
0.050	Notch	1200	85	1332.8				37	135
			60	5349.0 Discontinued					

Table 9

ELONGATIONS AND TIME PERIODS OF CREEP FOR 0.026-INCH AND 0.050-INCH THICK WASPALOY

Sheet Thickness (inches)	Aging Treatment	Test Temp. (°F)	Stress (ksi)	Total Elong. (%)	Elong. on Loading (%)	Creep Elongation 1st Stage (ksi)	Creep Elongation 2nd Stage (ksi)	Creep Elongation 3rd Stage (ksi)	Creep Elongation Total (ksi)	Rupture Time (hrs)	Time Periods for Creep 1st Stage (hrs)	Time Periods for Creep 2nd Stage (hrs)	Time Periods for Creep 3rd Stage (hrs)
0.026	16 hrs at 1400°F	1000	161	33.4						Tens.			
			150	14.6	12.61	0.84	1.15	0.00	1.99	131.9	12	120	0
			145			0.79	1.00	0.00	1.79	207.6	34	170	0
			135	6.15	5.72	0.23	0.20	0.00	0.43	517	29	491	0
0.050	16 hrs at 1400°F	1000	158.5	38.0						Tens.			
			150	16.2	13.8	0.40	2.00	0.00	2.4	145.1	3	142	0
			145			0.70	2.00	0.00	2.6	323.5	15	308	0
			140	11.5	10.2	0.40	0.90	0.00	1.3	475.5	22	453	0
0.026	16 hrs at 1400°F	1200	167.7	21.7						Tens.			
			120	3.63	2.55				1.08	3.6			
			90	0.74	0.30	0.04	0.16	0.24	0.44	376.5	2	278	96
			80	1.40	0.30	0.04	0.09	0.97	1.10	1240.8	70	530	641
0.050	16 hrs at 1400°F	1200	90	1.45	0.31	0.03	0.11	1.00	1.14	513.1	1	300	212
0.026	10 hrs at 1700°F	1000	148.5	36.0						Tens.			
0.050	10 hrs at 1700°F	1000	139.8	34.0						Tens.			
			125	17.0	12.52	2.00	2.48	0.00	4.48	1109.1	150	959	0
0.026	10 hrs at 1700°F	1200	100	5.96	2.83	0.60	2.43	0.00	3.03	38.7	3	36	0
			80	3.88	0.35	0.10	0.37	3.06	3.53	1870.1	20	780	1070
0.050	10 hrs at 1700°F	1200	90	6.0	1.70	0.15	1.25	2.90	4.30	331.6	10	160	162
			80	8.9	0.36	0.04	0.40	8.10	8.54	2937.2	10	990	1937

Table 10

X-RAY DIFFRACTION DATA OF EXTRACTED RESIDUES OF WASPALOY IN THE HEAT TREATED CONDITIONS

Solution Treatment	½ hr at 1825°F	½ hr at 1825°F	½ hr at 1900°F	½ hr at 1900°F	½ hr at 1975°F	½ hr at 1975°F	½ hr at 2150°F	½ hr at 2150°F	Standard Patterns for Indicated Phases			
Aging Treatment	16 hrs at 1400°F	10 hrs at 1700°F	16 hrs at 1400°F	10 hrs at 1700°F	16 hrs at 1400°F	10 hrs at 1700°F	16 hrs at 1400°F	10 hrs at 1700°F	TiC a = 4.32		$M_{23}C_6$ a = 10.7	
Intensity	"d"	"d"	"d"	"d"	"d"	"d"	"d"	"d"	"d"	Intensity	"d"	Intensity
s	2.49	2.49	2.49	2.50	2.50	2.49	2.49	2.49	2.49	m		
s	2.38	2.39	2.39	2.40	2.39	2.39	2.39	2.39			2.39	s
s*		2.18		2.19		2.18		2.18			2.18	s
s*	2.16	2.16	2.15	2.16	2.16	2.14	2.16		2.16	vs		
vs	2.054	2.058	2.051	2.065	2.056	2.058	2.054	2.052			2.055	s
w	1.888	1.891	1.888	1.900	1.888	1.889	1.887	1.886			1.888	m
w	1.803	1.805	1.802	1.813	1.806	1.81	1.808	1.806			1.805	s
vvw		1.786				1.781	1.784				1.78	mw
vw	1.605	1.614		1.616	1.611	1.629	1.611				1.61	vw
w	1.524	1.529	1.525	1.533	1.529	1.518	1.527		1.525	s		
vvw		1.338			1.337	1.339		1.336			1.335	w
s	1.298	1.301	1.31	1.303	1.305	1.301	1.304	1.297	1.305	m	1.30	s
s	1.260	1.264	1.261	1.264	1.261	1.261	1.253	1.259			1.258	ms
m		1.237	1.248	1.240	1.249		1.248		1.25	m		

* Two lines which were difficult to separate in the patterns.

Table 11

INFLUENCE OF NOTCH ACUITY ON THE RUPTURE PROPERTIES OF WASPALOY IN THE COLD WORKED AND AGED CONDITION TESTED AT 1200°F AND 100,000 PSI

Notch Acuity (K_t)	1.0	1.5	2.1	3.1	5.9	9.4	>20
Rupture Time (hours)	394.6	130.4	26.9	20.7	10.9	12.0	11.5
		404.2	141.0	16.4	5.2	1.4	

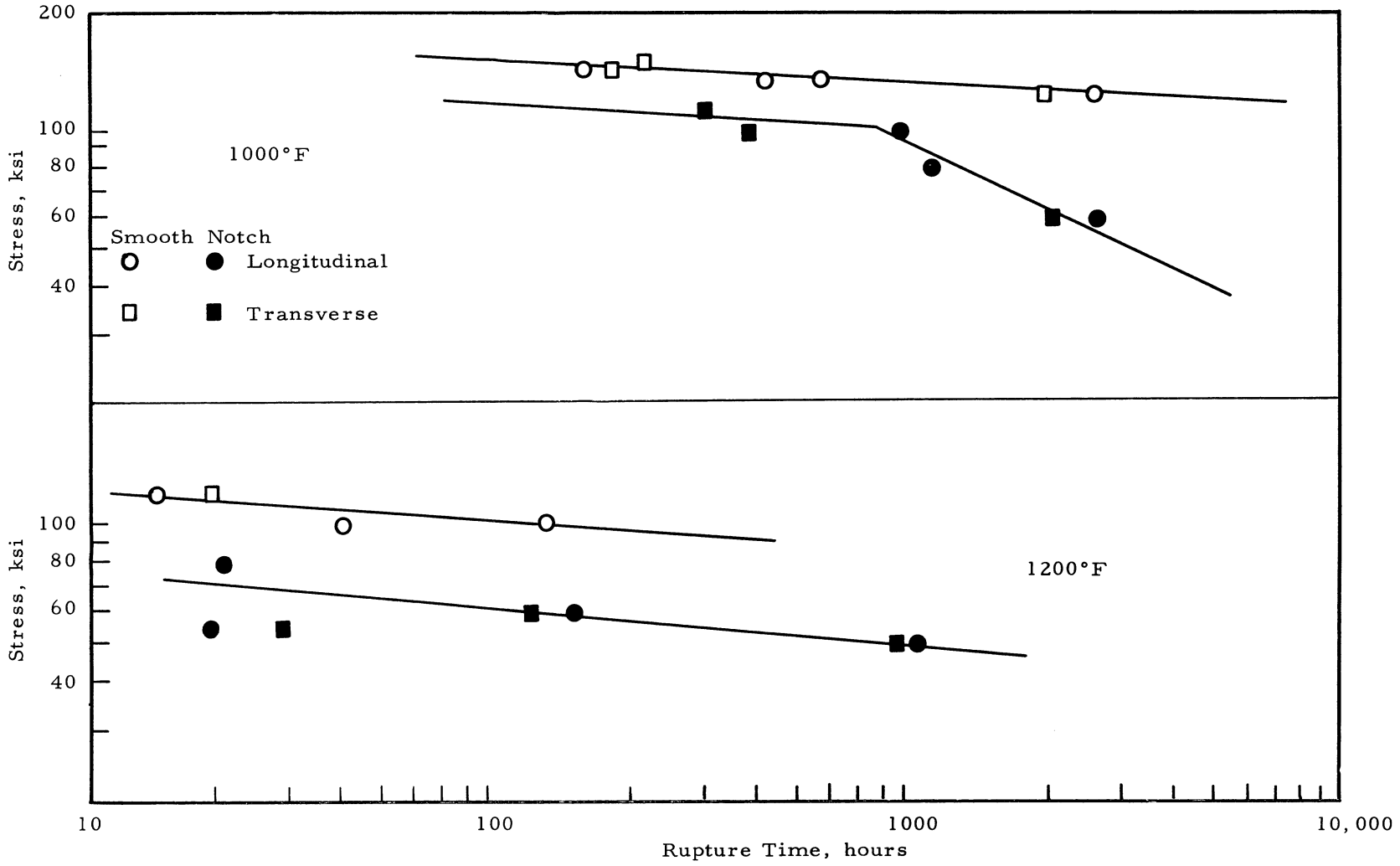

Figure 1. Stress versus rupture time data at 1000° and 1200°F obtained from smooth and notched (K_t = 20) specimens of 0.026-inch thick Waspaloy sheet in the annealed and aged condition (ref. 2).

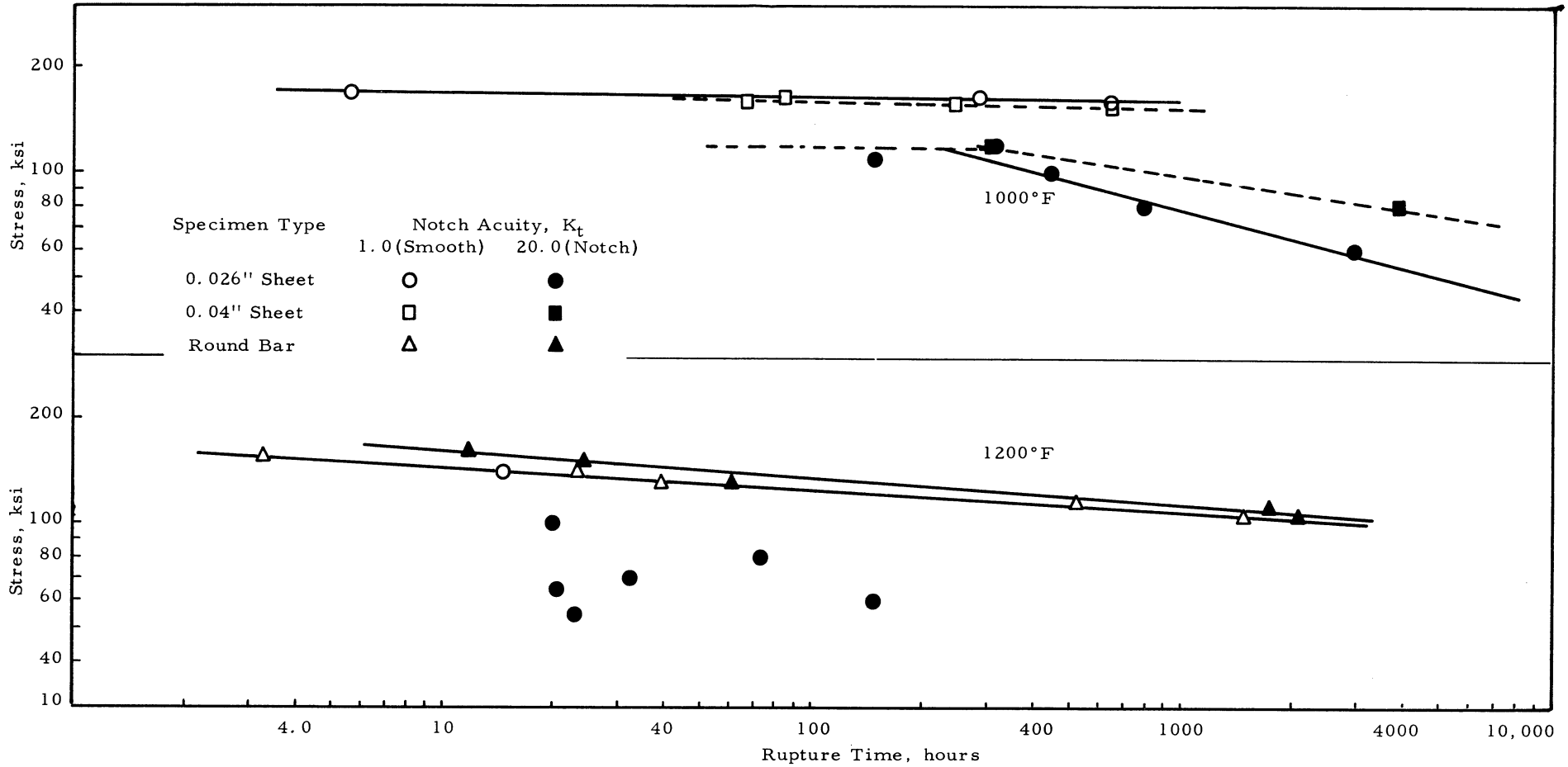

Figure 2. Stress versus rupture time data at 1000° and 1200°F obtained from smooth and notched sheet and round bar specimens of René 41 in the annealed and aged condition.

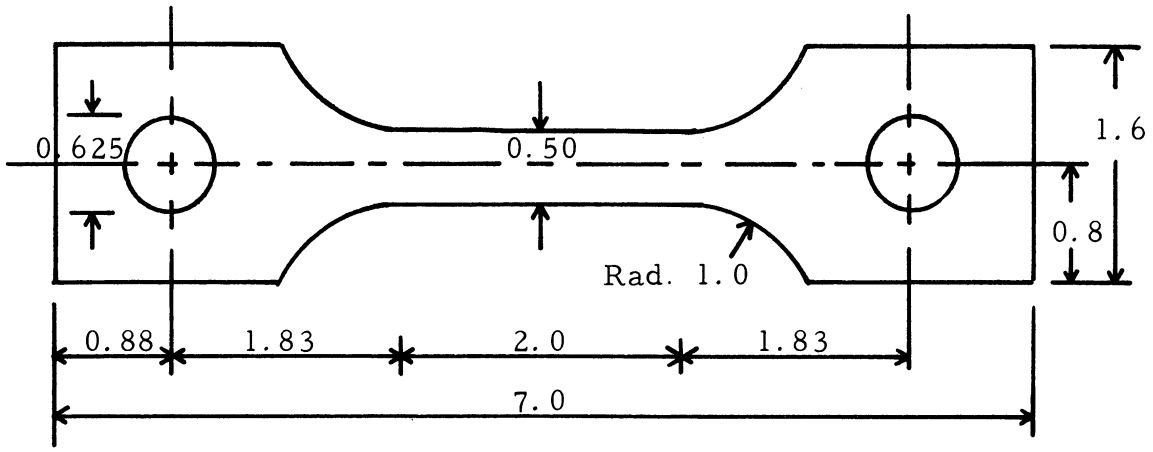

Smooth (unnotched) Specimen ($K_t = 1.0$)

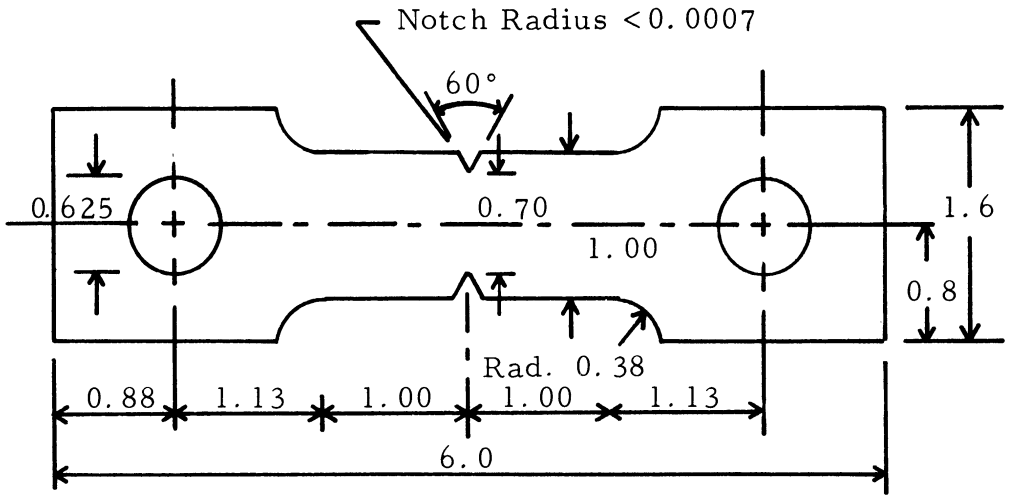

Sharp Edge Notched Specimen ($K_t > 20$)

Figure 3. Types of test specimens (all dimensions in inches).

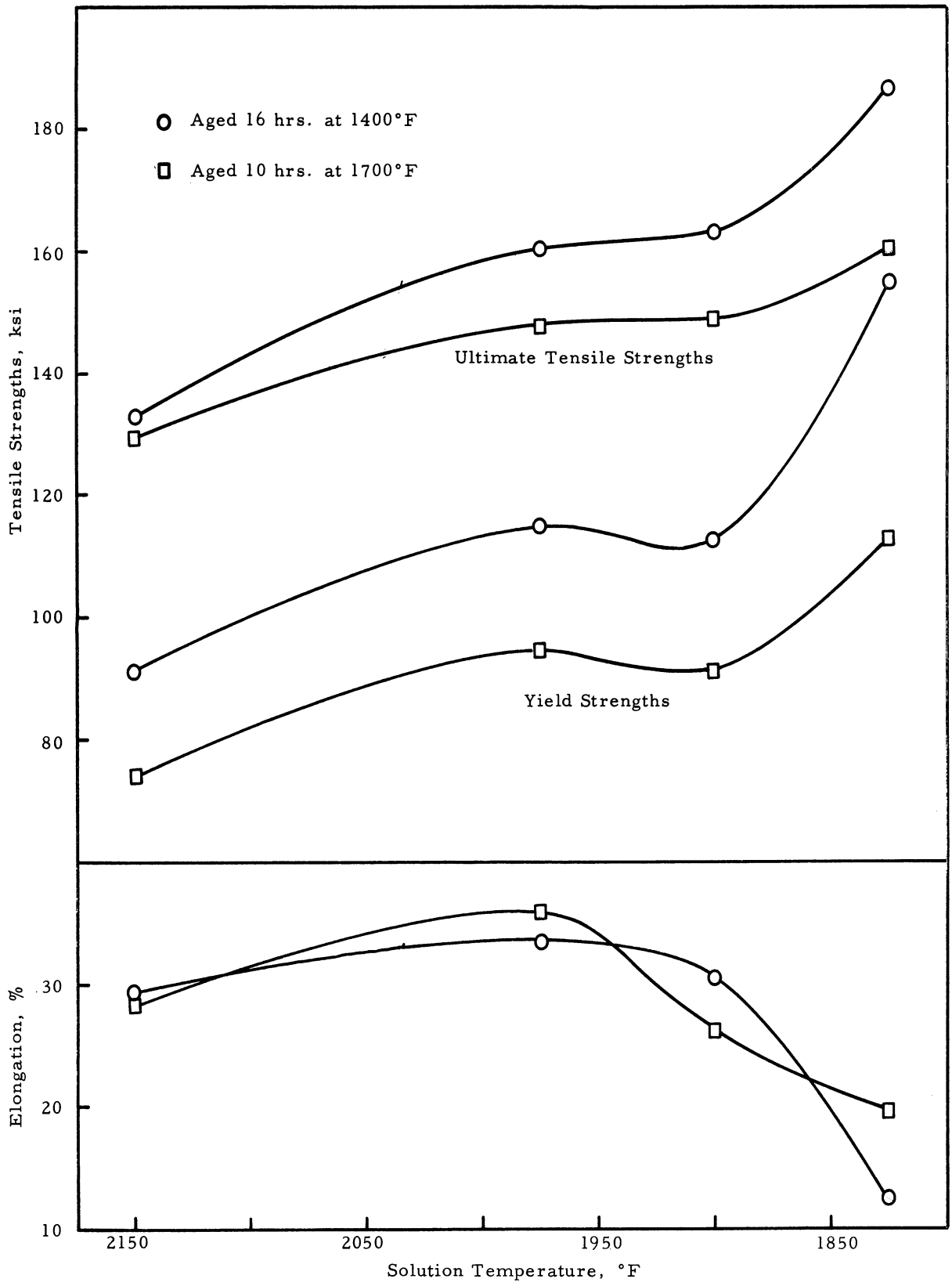

Figure 4. Effect of solution treatment on the tensile properties at 1000°F for Waspaloy in two conditions of aging.

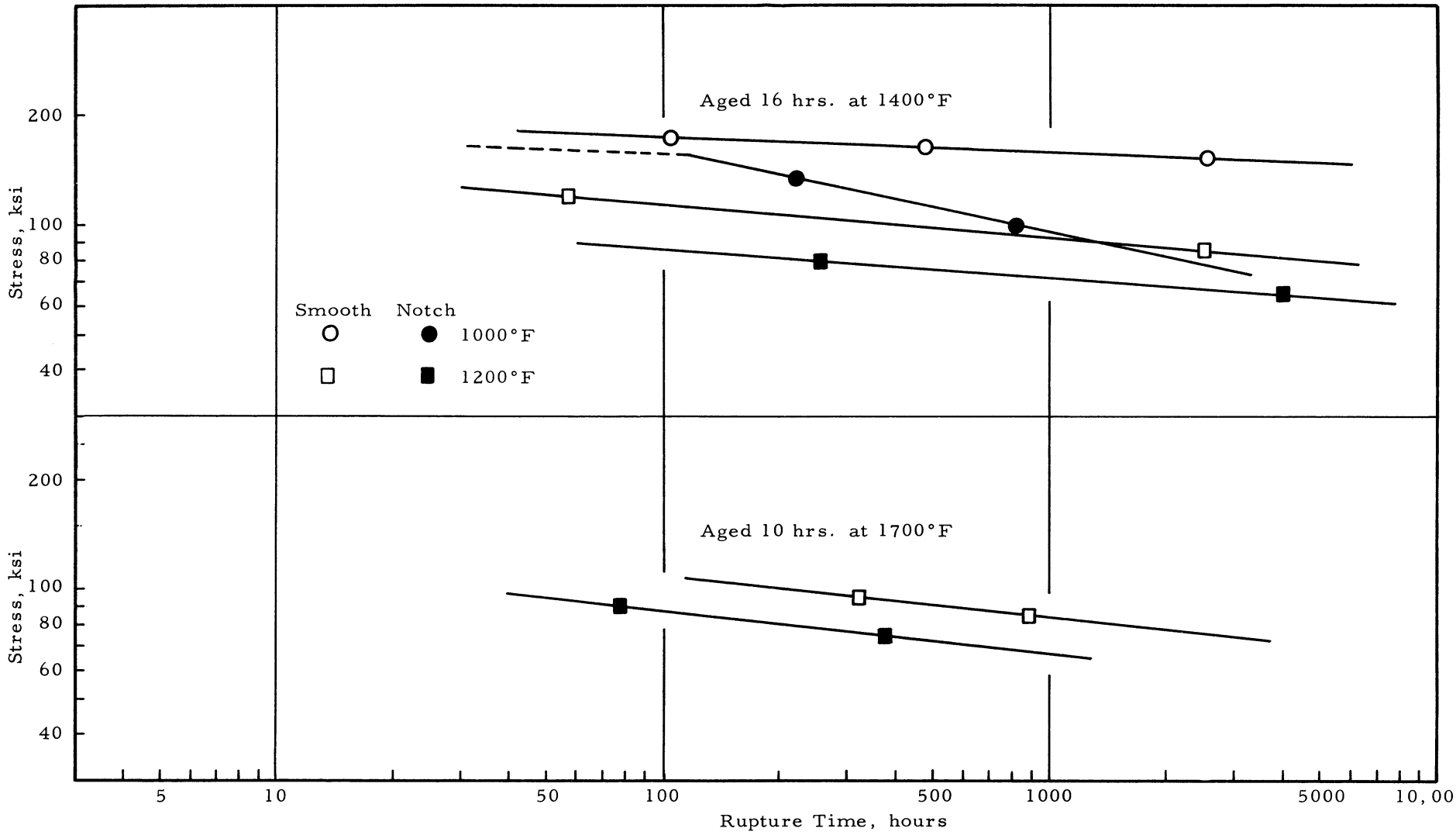

Figure 5. Stress versus rupture time data at 1000° and 1200°F obtained from smooth and notched specimens of 0.026-inch thick Waspaloy sheet heat treated 1/2 hour at 1825°F and aged.

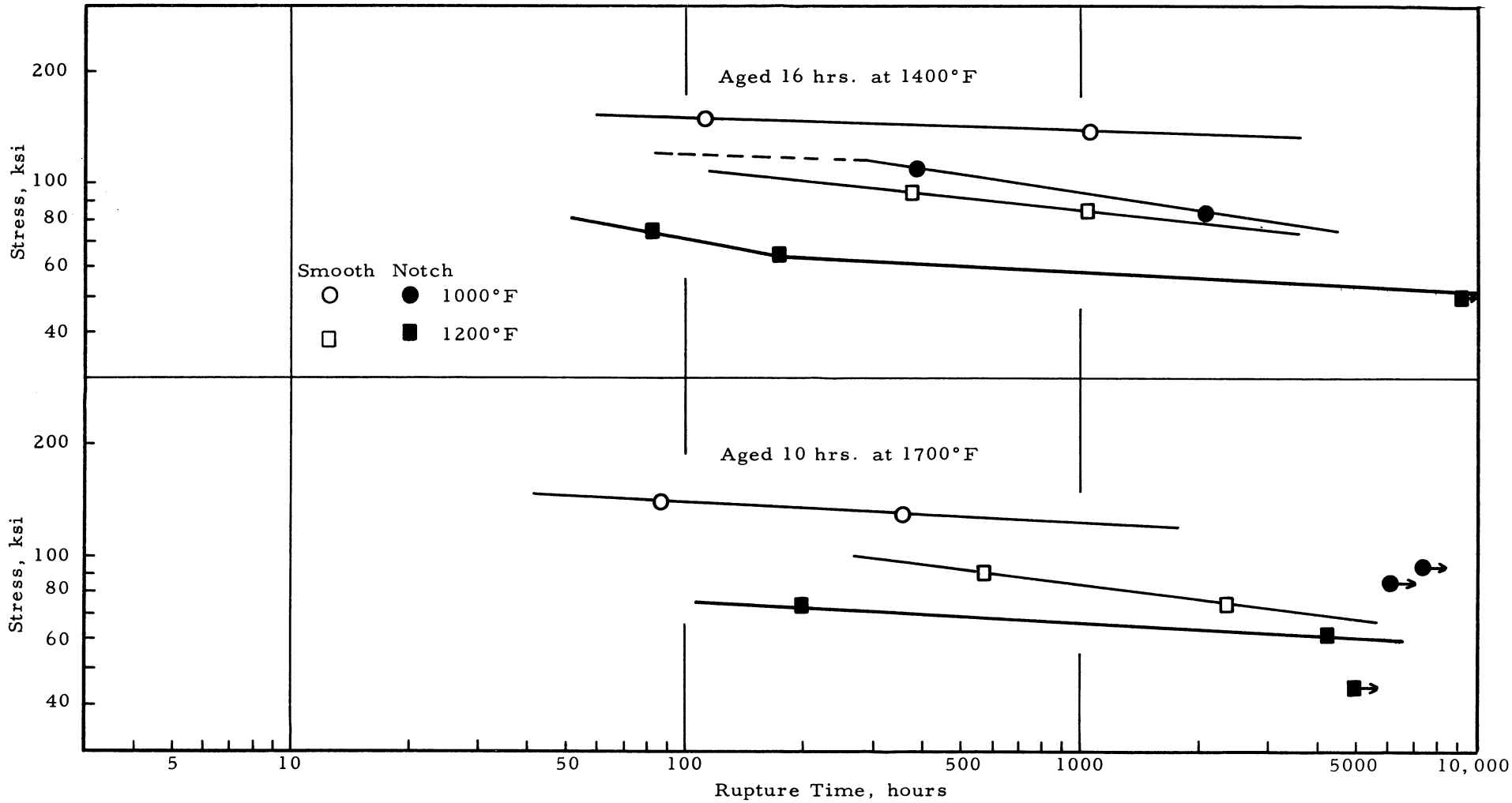

Figure 6. Stress versus rupture time data at 1000° and 1200°F obtained from smooth and notched specimens of 0.026-inch thick Waspaloy sheet heat treated 1/2 hour at 1900°F and aged.

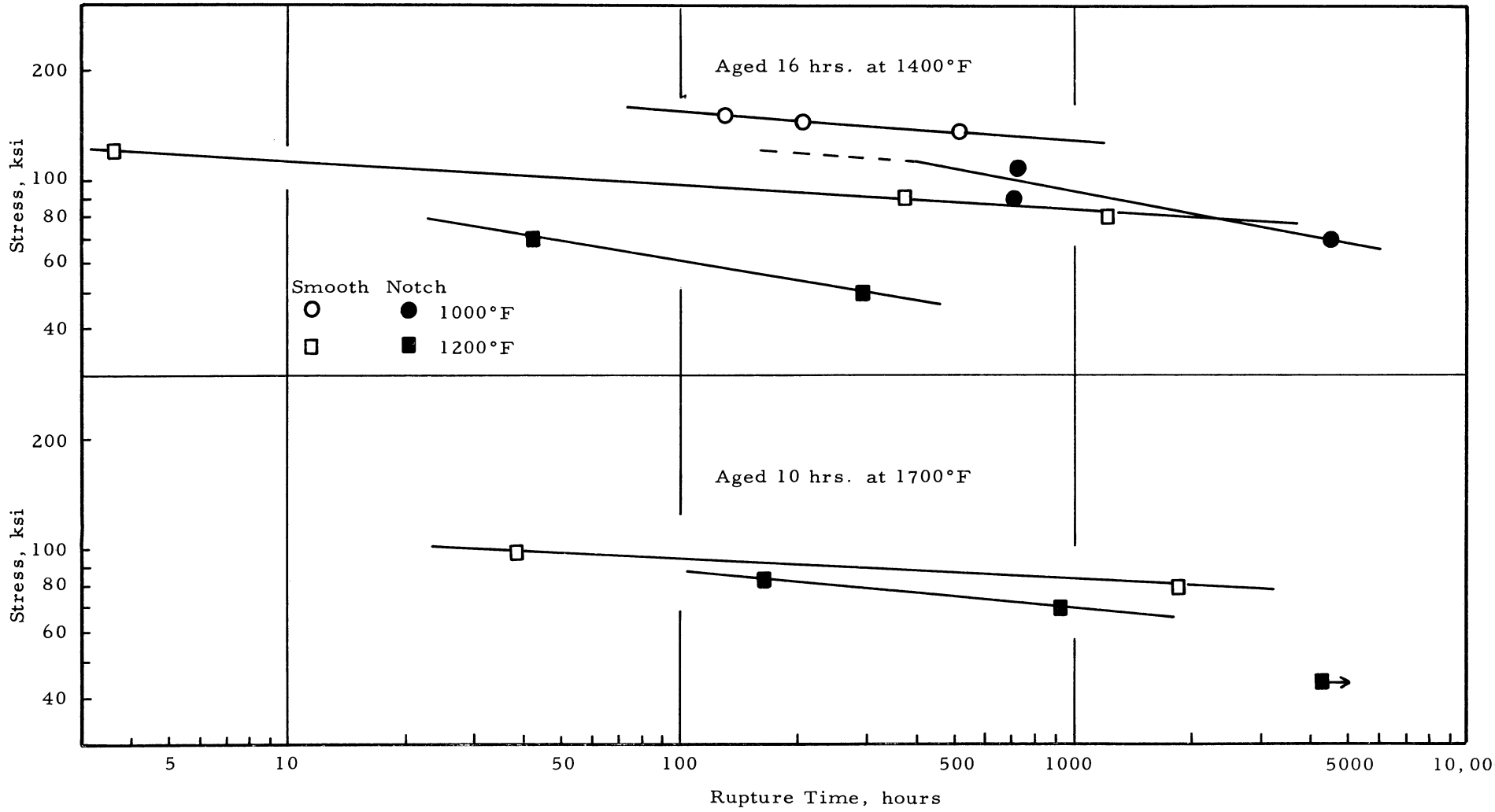

Figure 7. Stress versus rupture time data at 1000° and 1200°F obtained from smooth and notched specimens of 0.026-inch thick Waspaloy sheet heat treated 1/2 hour at 1975°F and aged.

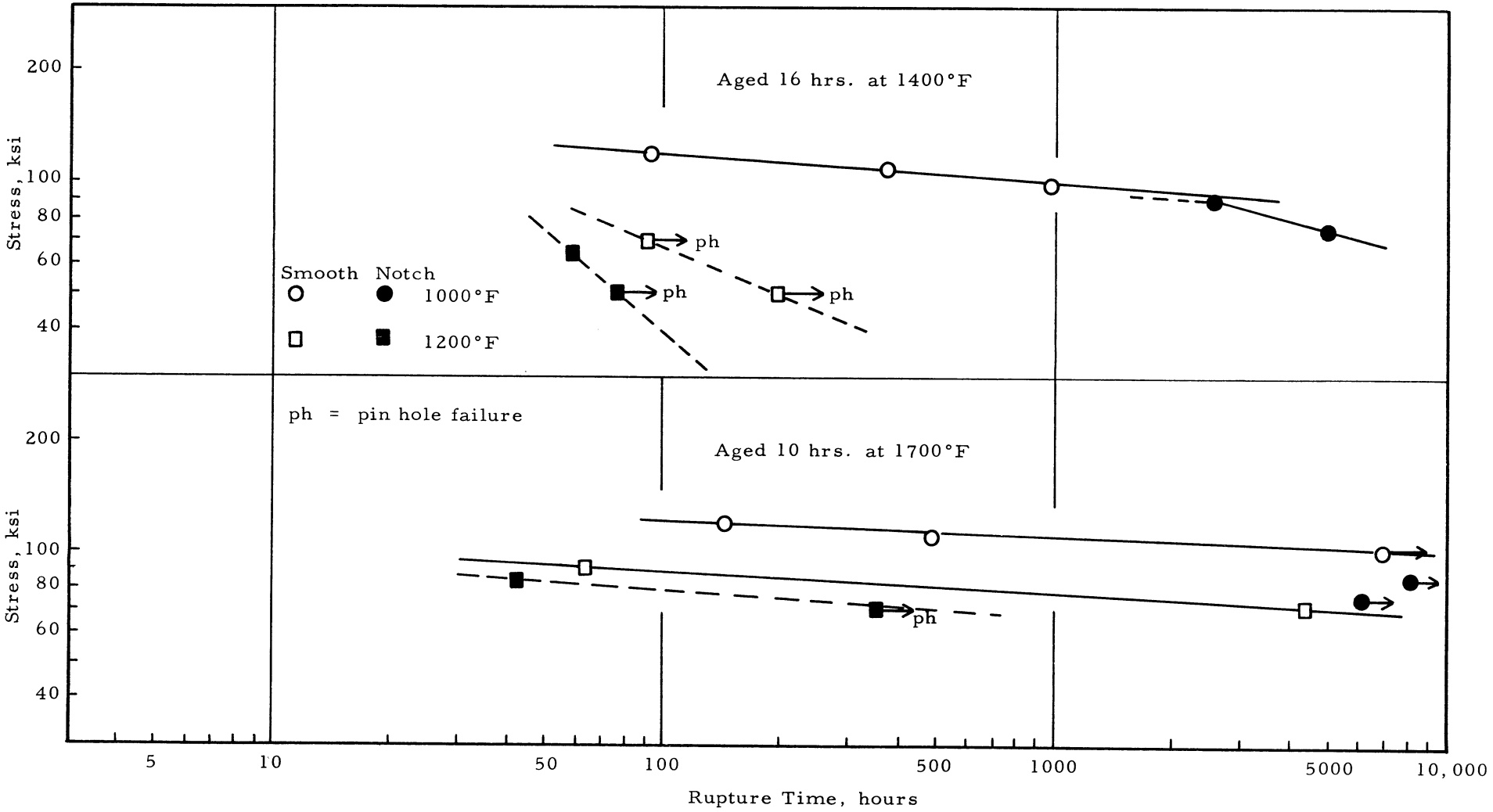

Figure 8. Stress versus rupture time data at 1000° and 1200°F obtained from smooth and notched specimens of 0.026-inch thick Waspaloy sheet heat treated 1/2 hour at 2150°F and aged.

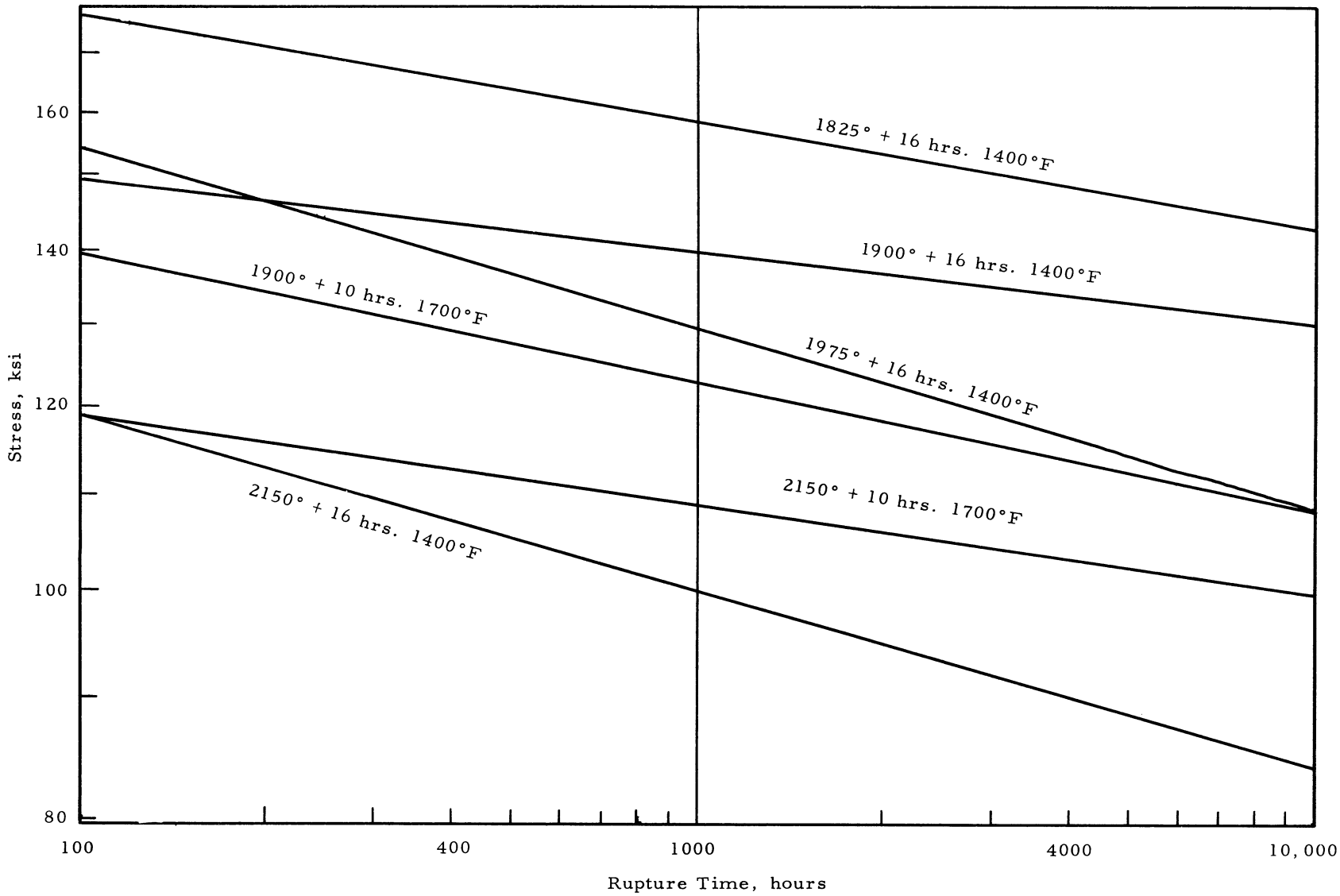

Figure 9. Stress versus rupture time curves at 1000°F for smooth specimens of 0.026-inch thick Waspaloy sheet in the heat treated conditions.

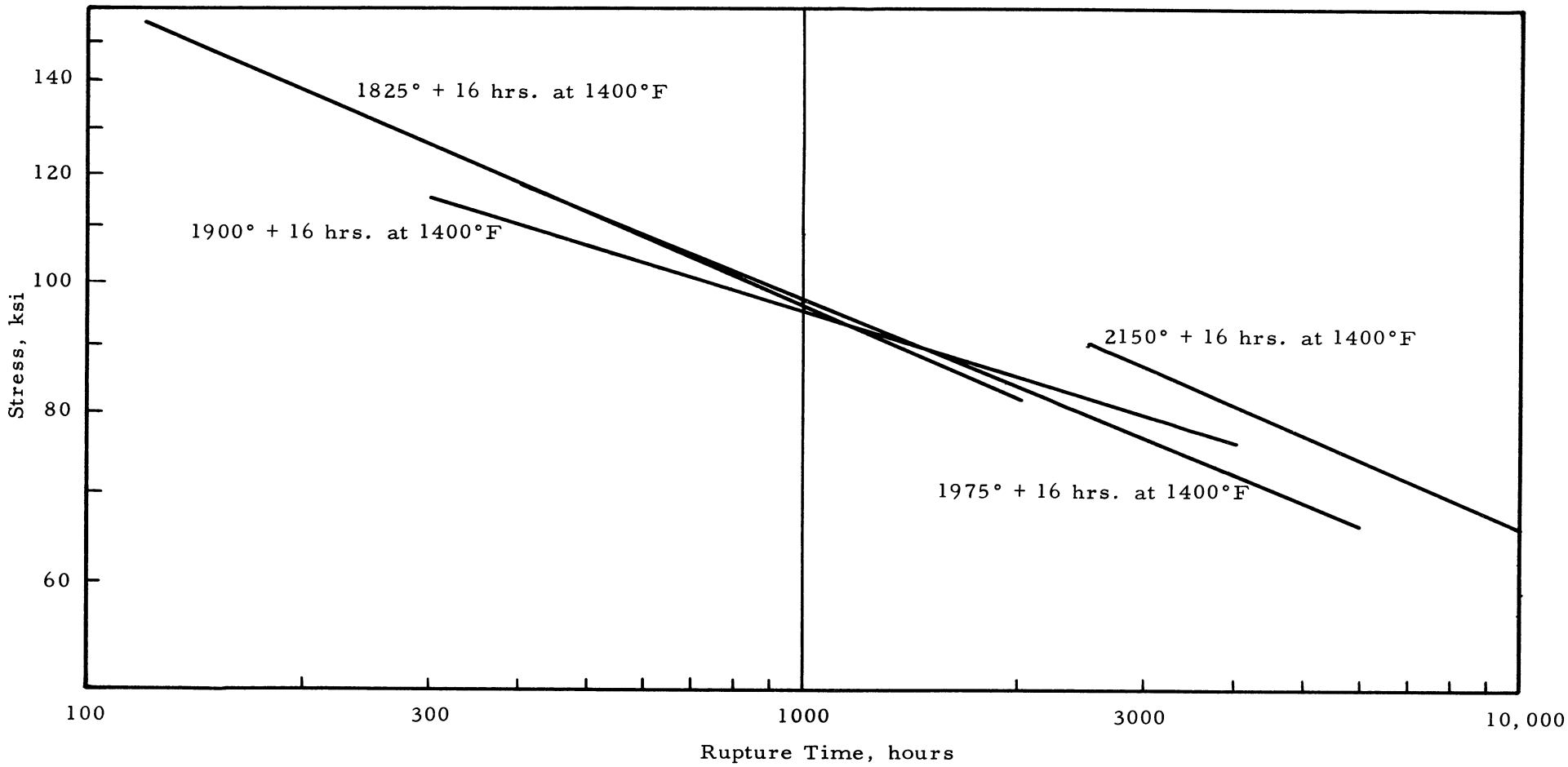

Figure 10. Stress versus rupture time curves at 1000°F for notched specimens of 0.026-inch thick Waspaloy sheet in the heat treated conditions.

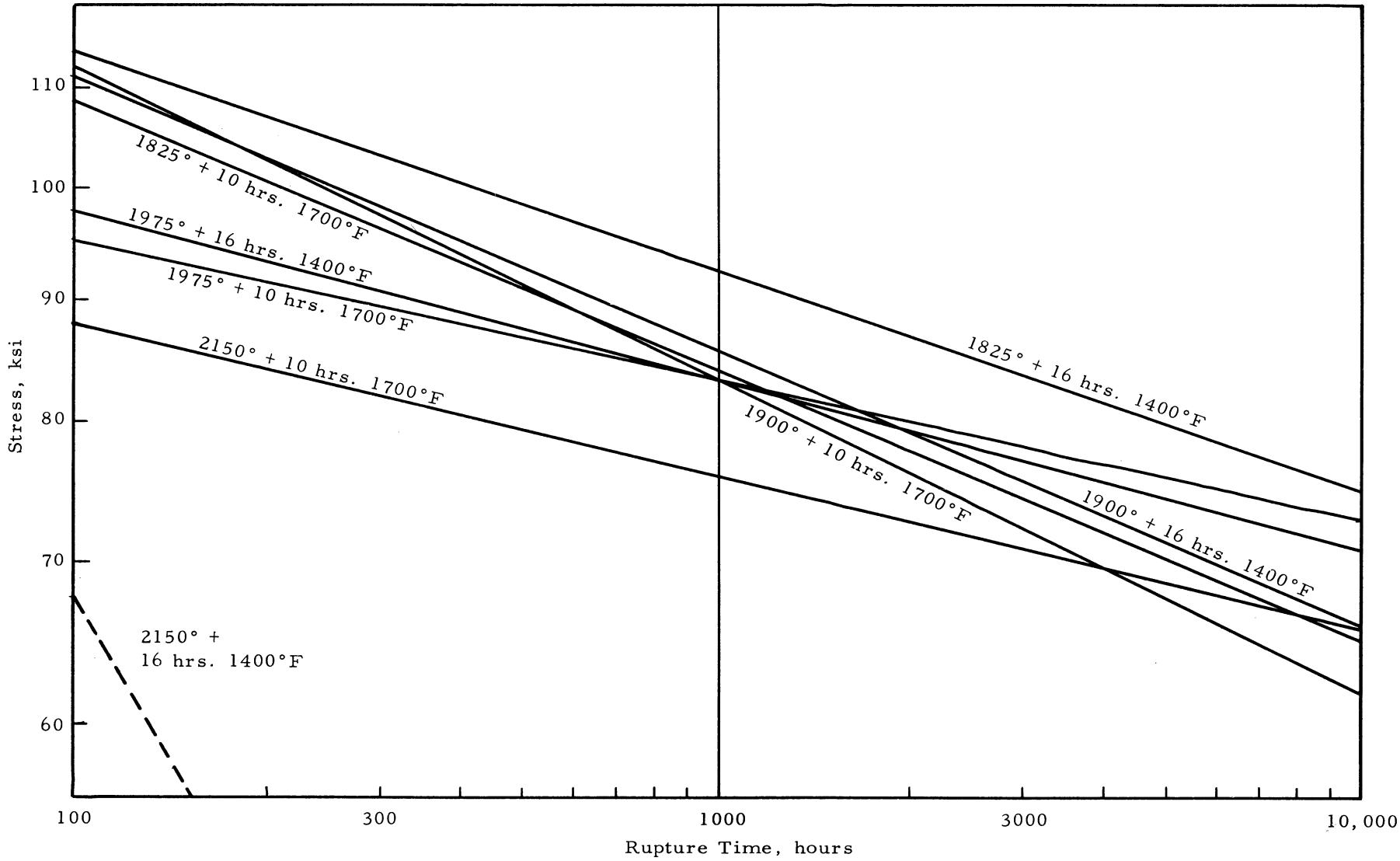

Figure 11. Stress versus rupture time curves at 1200°F for smooth specimens of 0.026-inch thick Waspaloy sheet in the heat treated conditions.

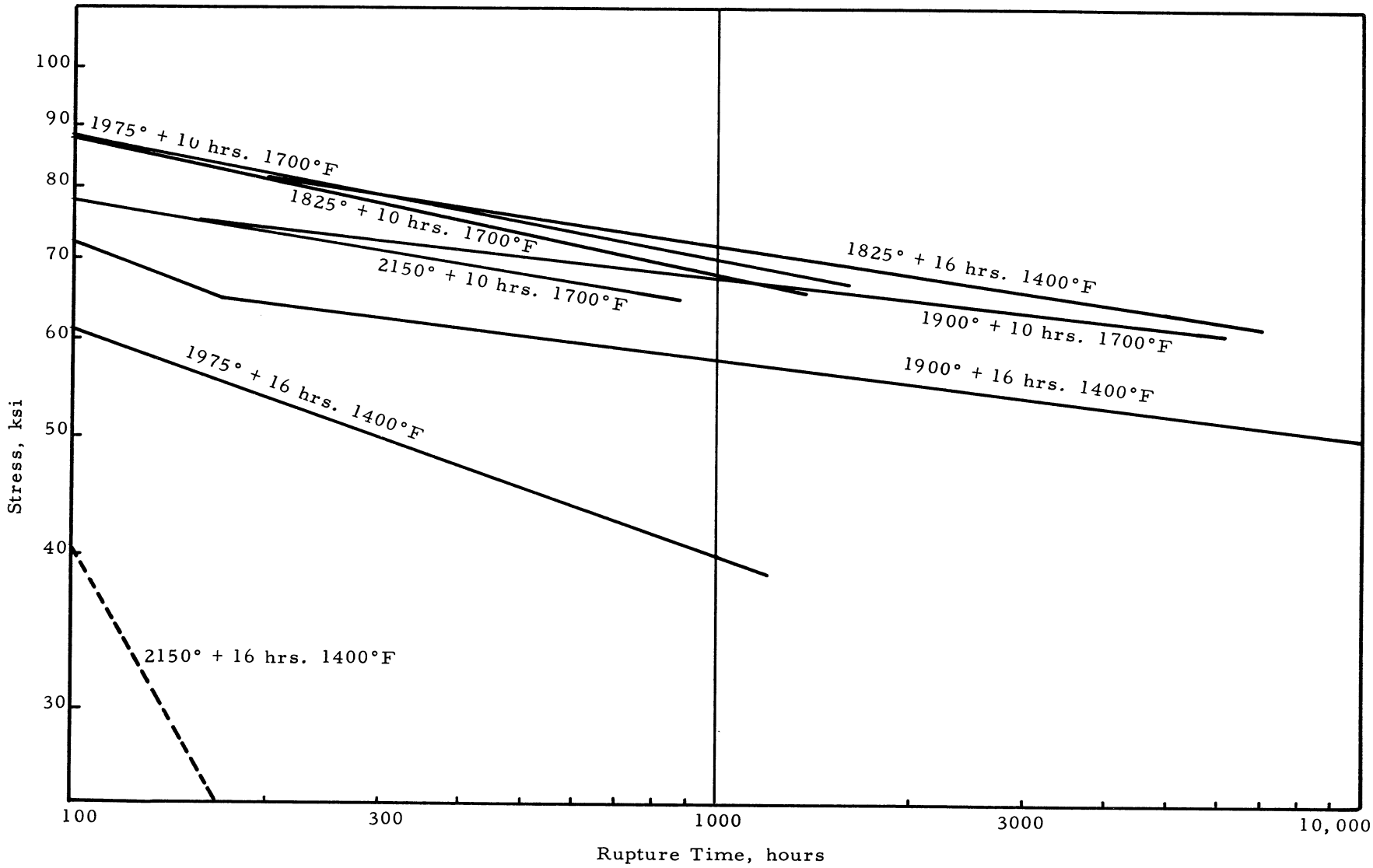

Figure 12. Stress versus rupture time curves at 1200°F for notched specimens of 0.026-inch thick Waspaloy sheet in the heat treated conditions.

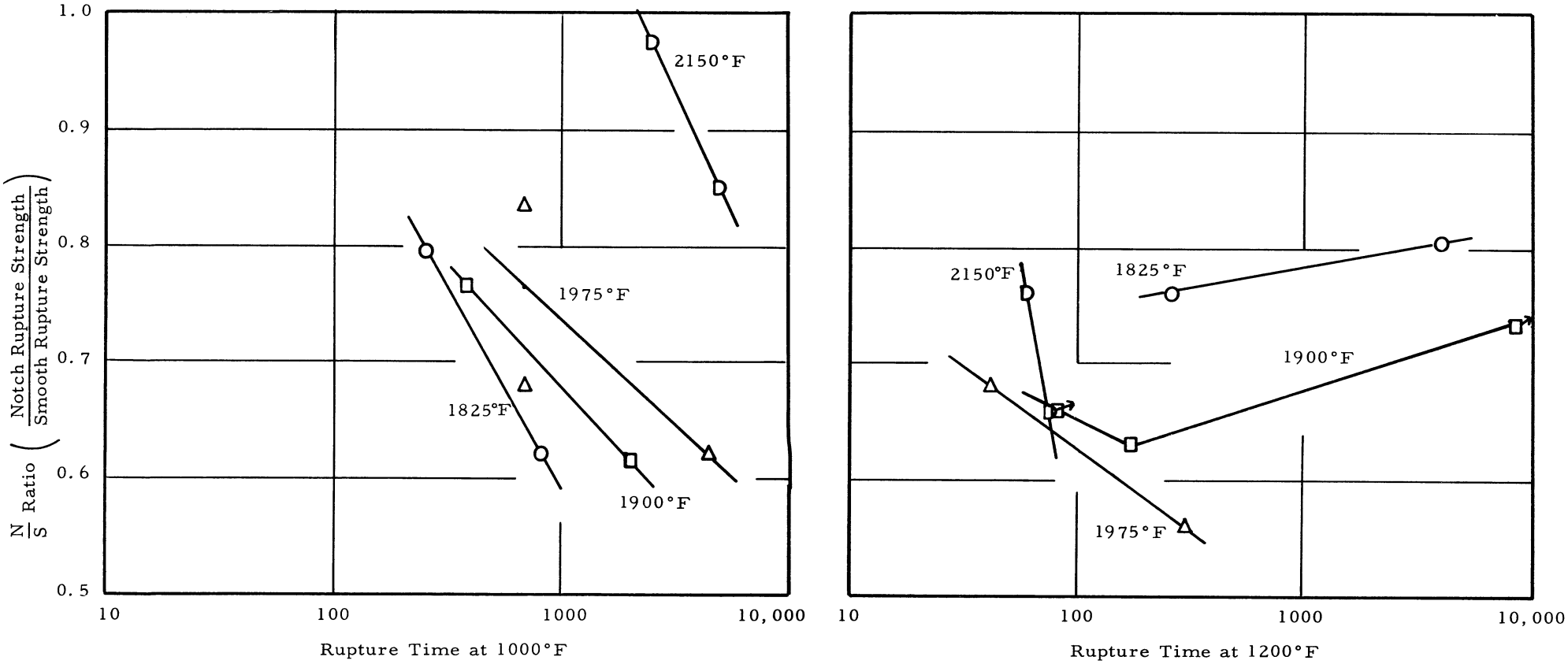

Figure 13. Notch to smooth rupture strength ratios at 1000° and 1200°F obtained from 0.026-inch thick Waspaloy sheet solution treated at temperatures from 1825° to 2150°F and aged at 1400°F.

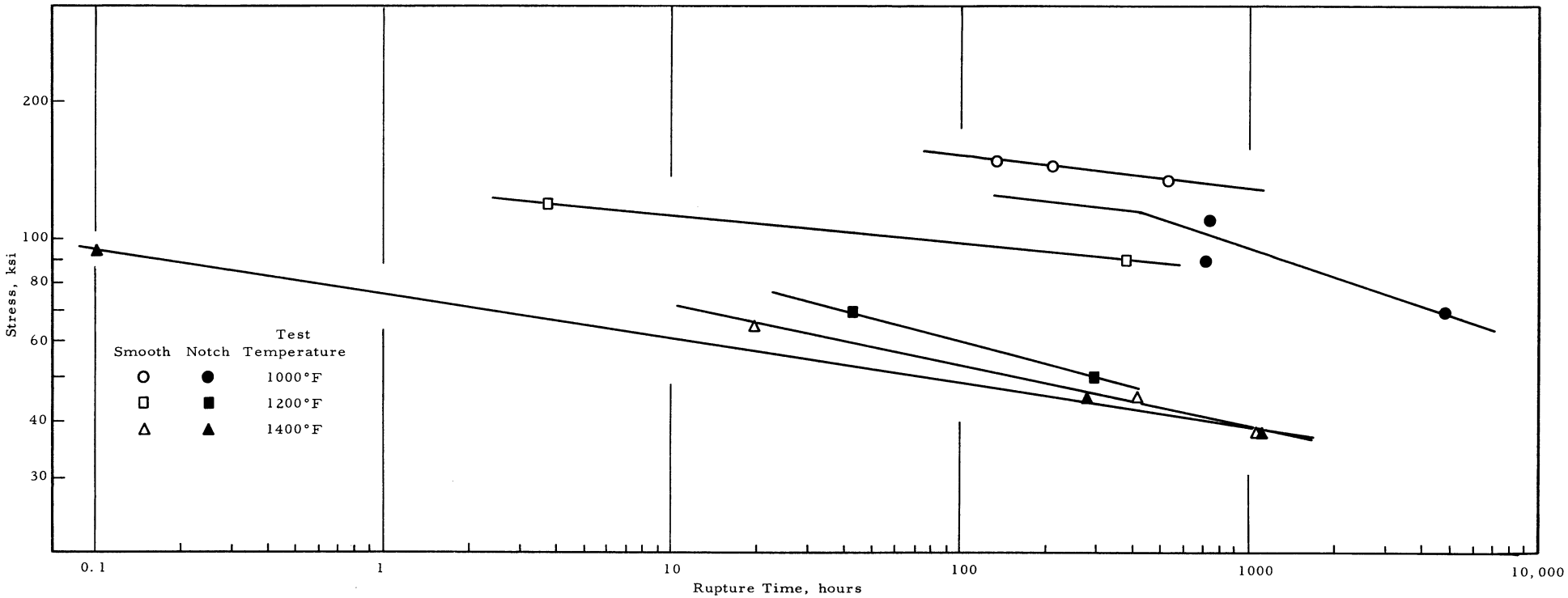

Figure 14. Stress versus rupture time data at 1000°, 1200° and 1400°F obtained from smooth and notched specimens of 0.026-inch thick Waspaloy sheet heat treated at 1975°F and aged at 1400°F.

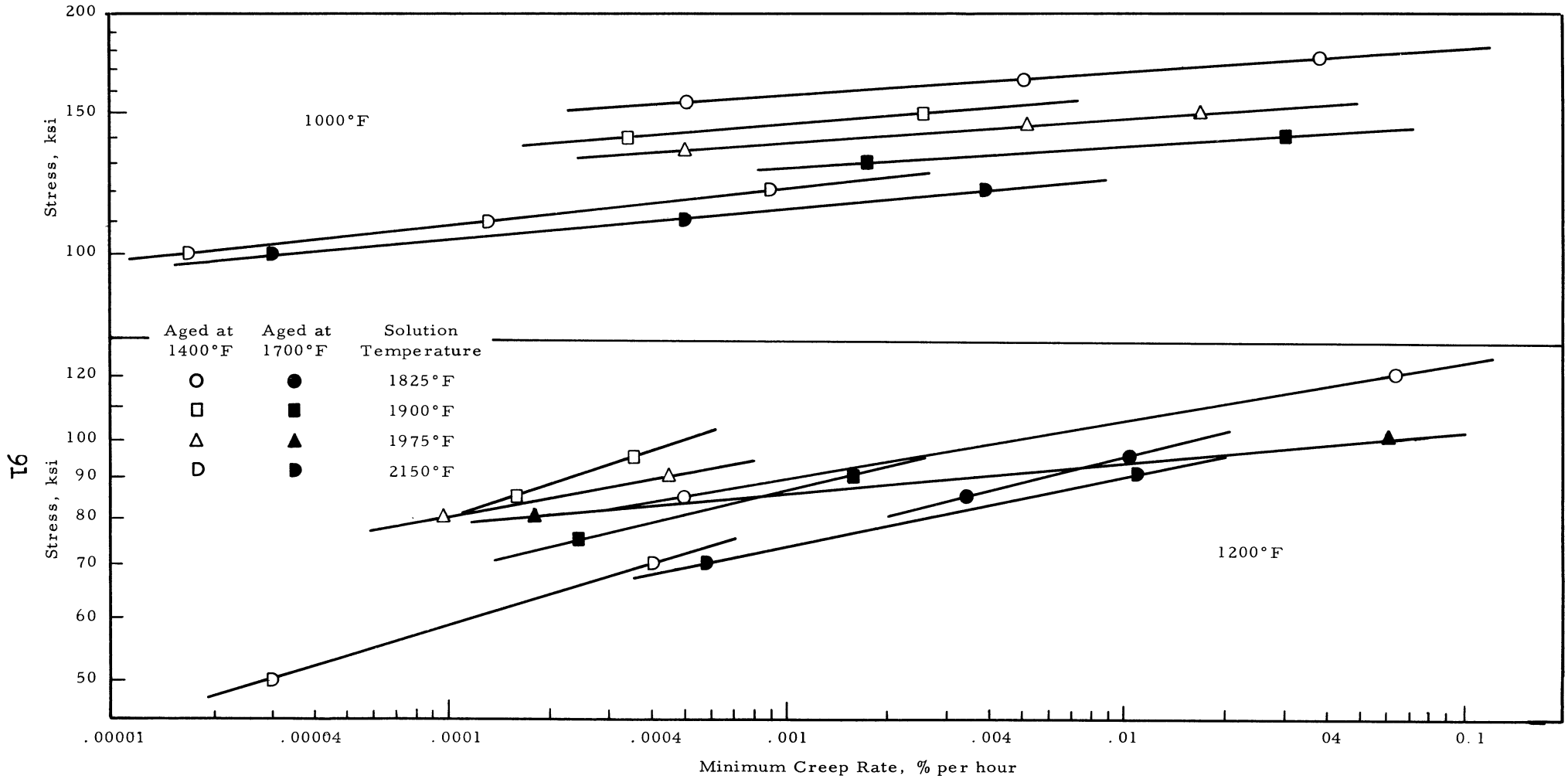

Figure 15. Stress versus minimum creep rate behavior at 1000° and 1200°F for 0.026-inch thick Waspaloy sheet in the heat treated condition.

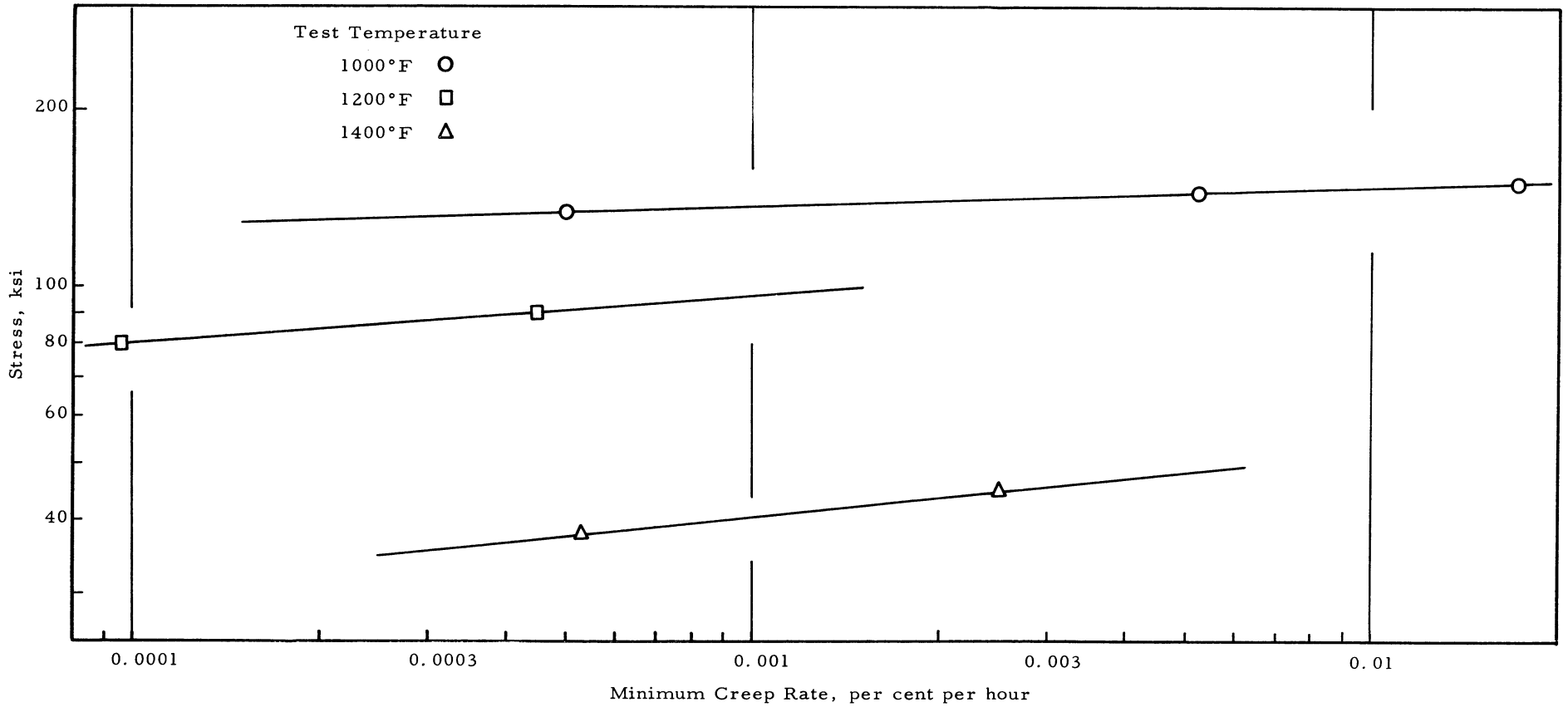

Figure 16. Stress versus minimum creep rate behavior at 1000°, 1200° and 1400°F for 0.026-inch thick Waspaloy sheet heat treated 1/2 hour at 1975°F and aged at 1400°F.

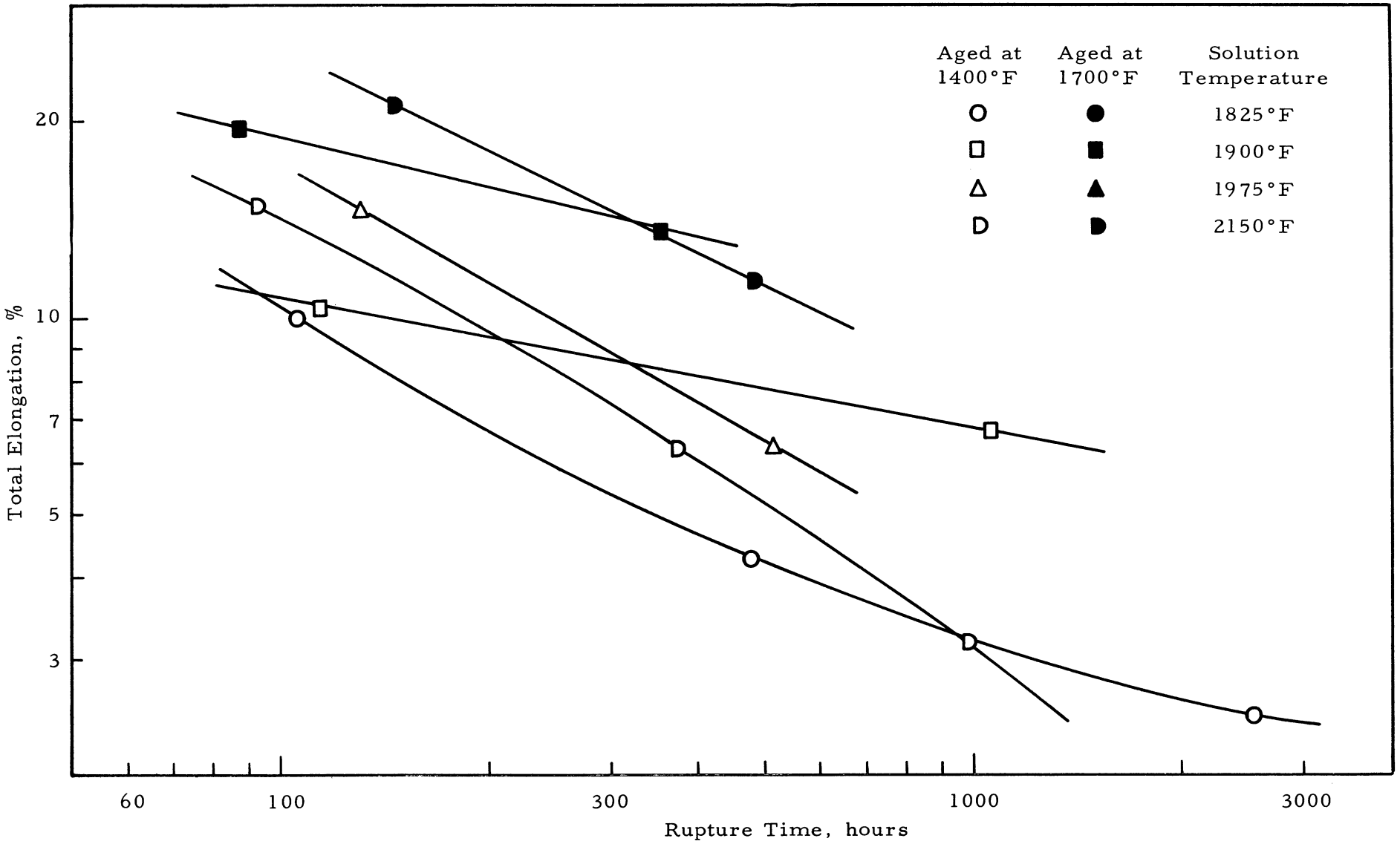

Figure 17. Elongation versus rupture time data at 1000°F for smooth specimens of 0.026-inch thick Waspaloy sheet in the heat treated condition.

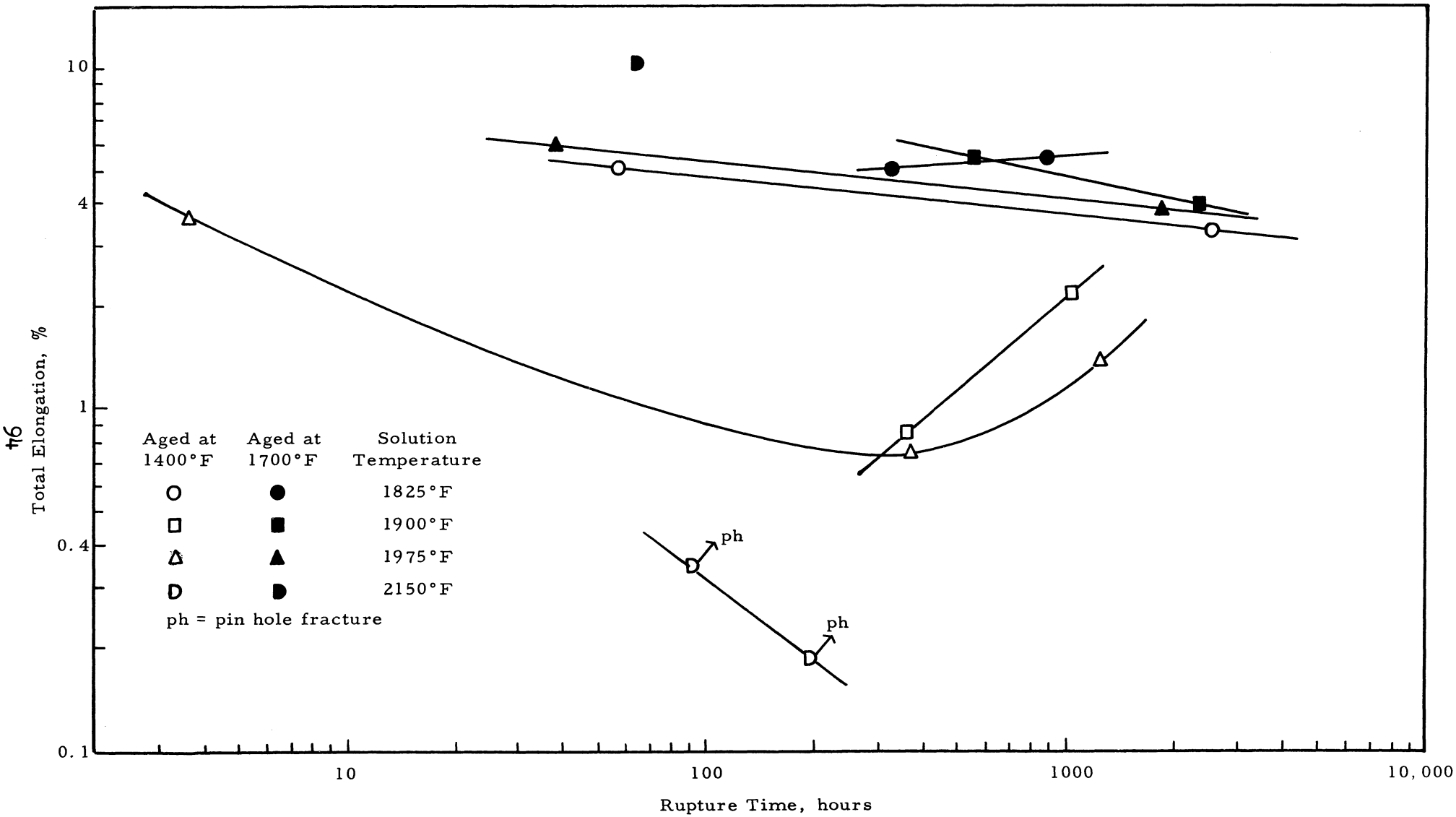

Figure 18. Elongation versus rupture time data at 1200°F for smooth specimens of 0.026-inch thick Waspaloy sheet in the heat treated condition.

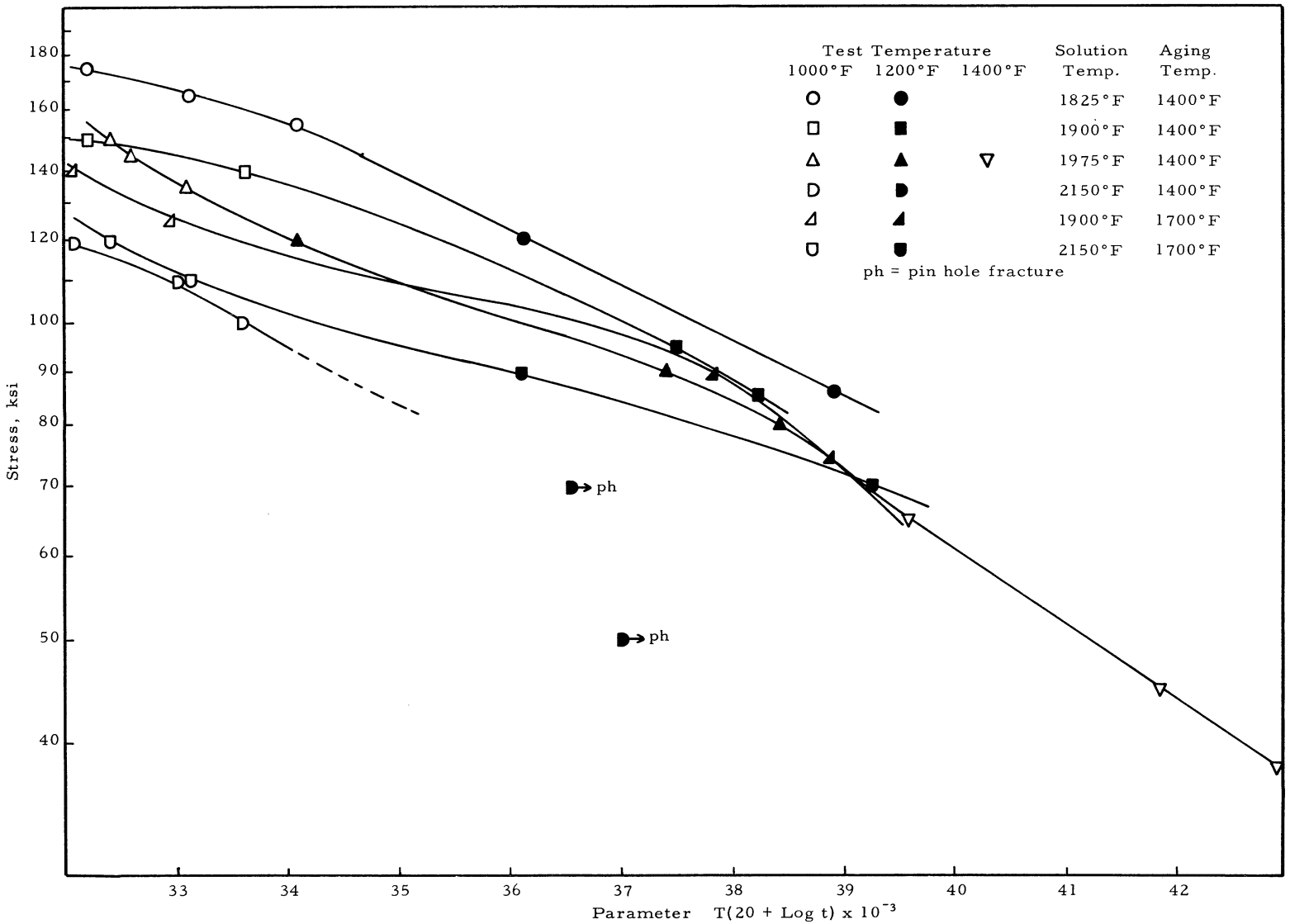

Figure 19. Time-temperature dependence of the rupture strengths at 1000°, 1200° and 1400°F of smooth specimens of 0.026-inch thick Waspaloy sheet in the heat treated condition.

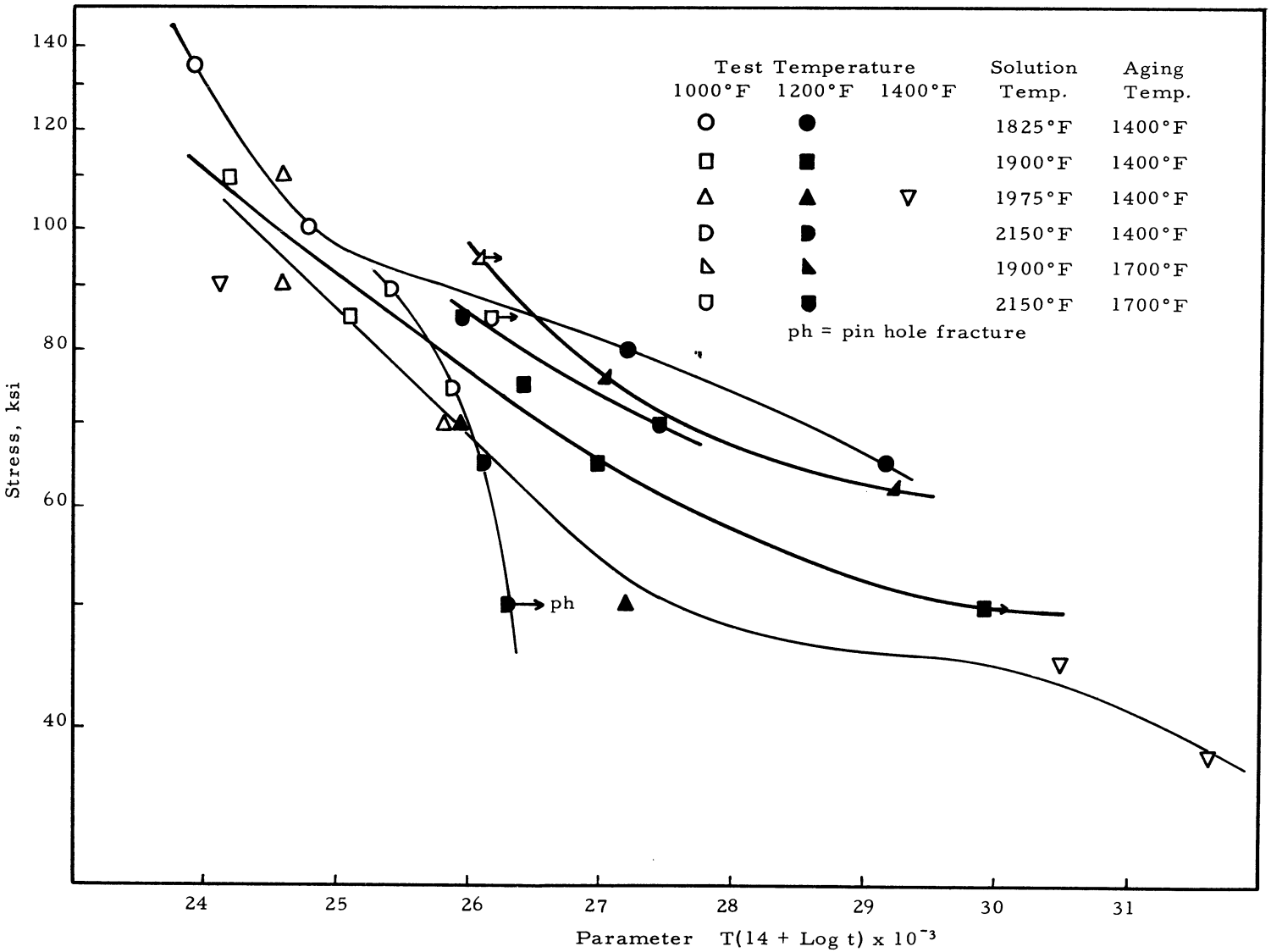

Figure 20. Time-temperature dependence of the rupture strengths at 1000°, 1200° and 1400°F of notched specimens of 0.026-inch thick Waspaloy sheet in the heat treated condition.

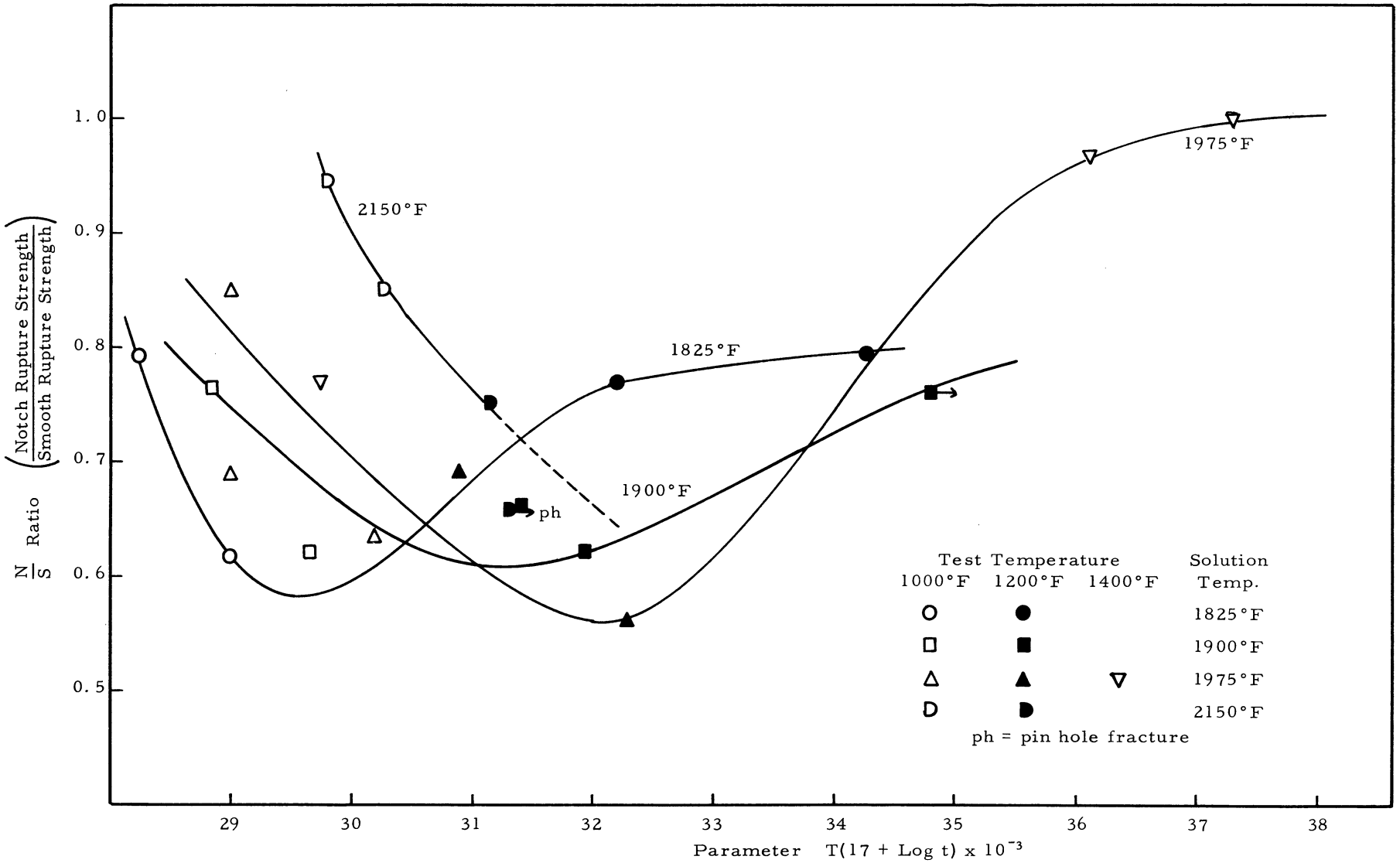

Figure 21. Time-temperature dependence of the notch to smooth rupture strength ratios at 1000°, 1200° and 1400°F for 0.026-inch thick Waspaloy sheet solution treated at temperatures from 1825° to 2150°F and aged at 1400°F.

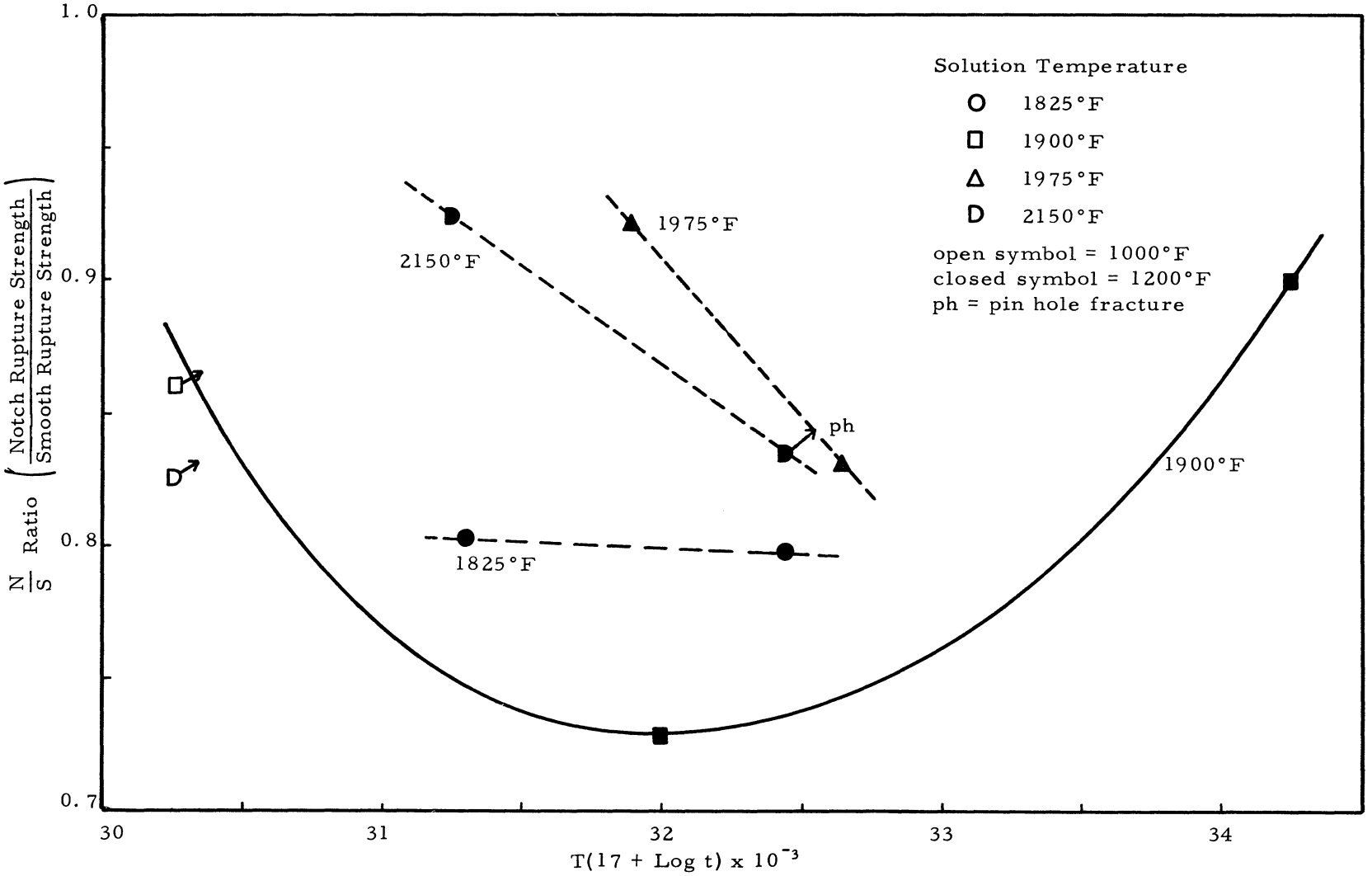

Figure 22. Time-temperature dependence of the notch to smooth rupture strength ratios at 1000°, 1200° and 1400°F for 0.026-inch thick Waspaloy sheet solution treated at temperatures from 1825° to 2150°F and aged at 1700°F.

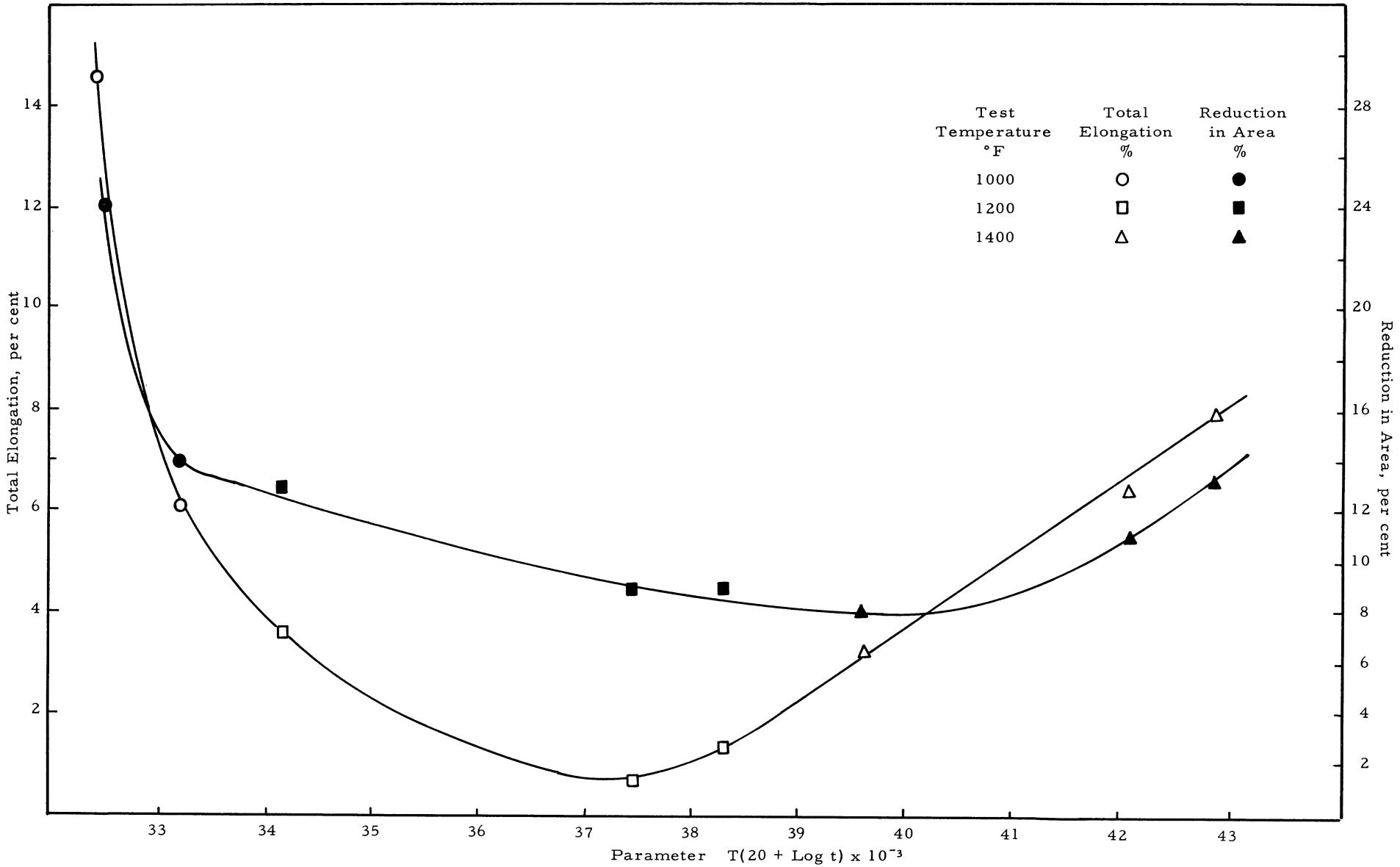

Figure 23. Time-temperature dependence of ductility obtained from smooth specimens of 0.026-inch thick Waspaloy sheet heat treated at 1975°F and aged at 1400°F.

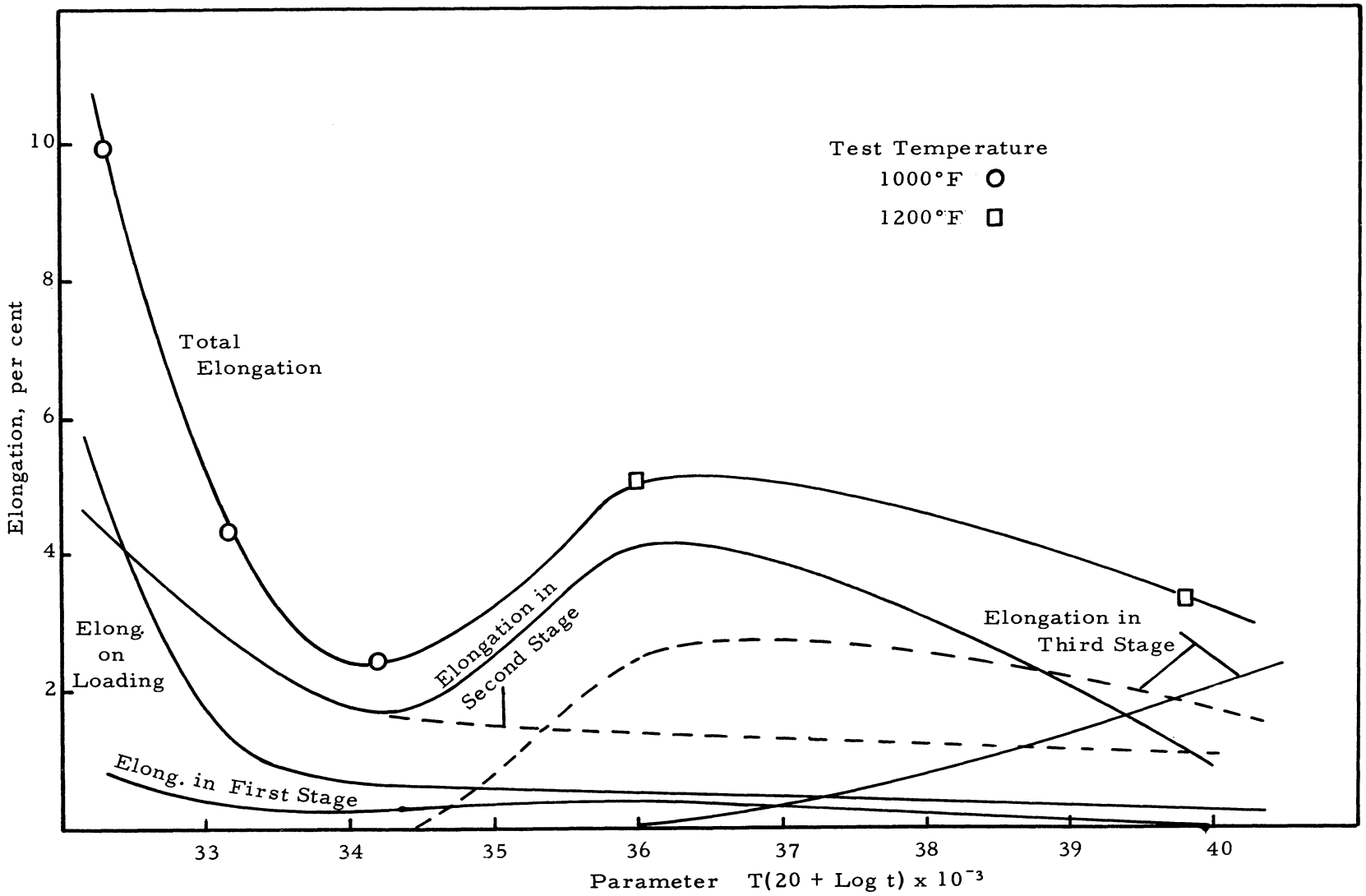

Figure 24. Time-temperature dependence of elongation obtained from smooth specimens of 0.026-inch thick Waspaloy sheet heat treated at 1825°F and aged at 1400°F.

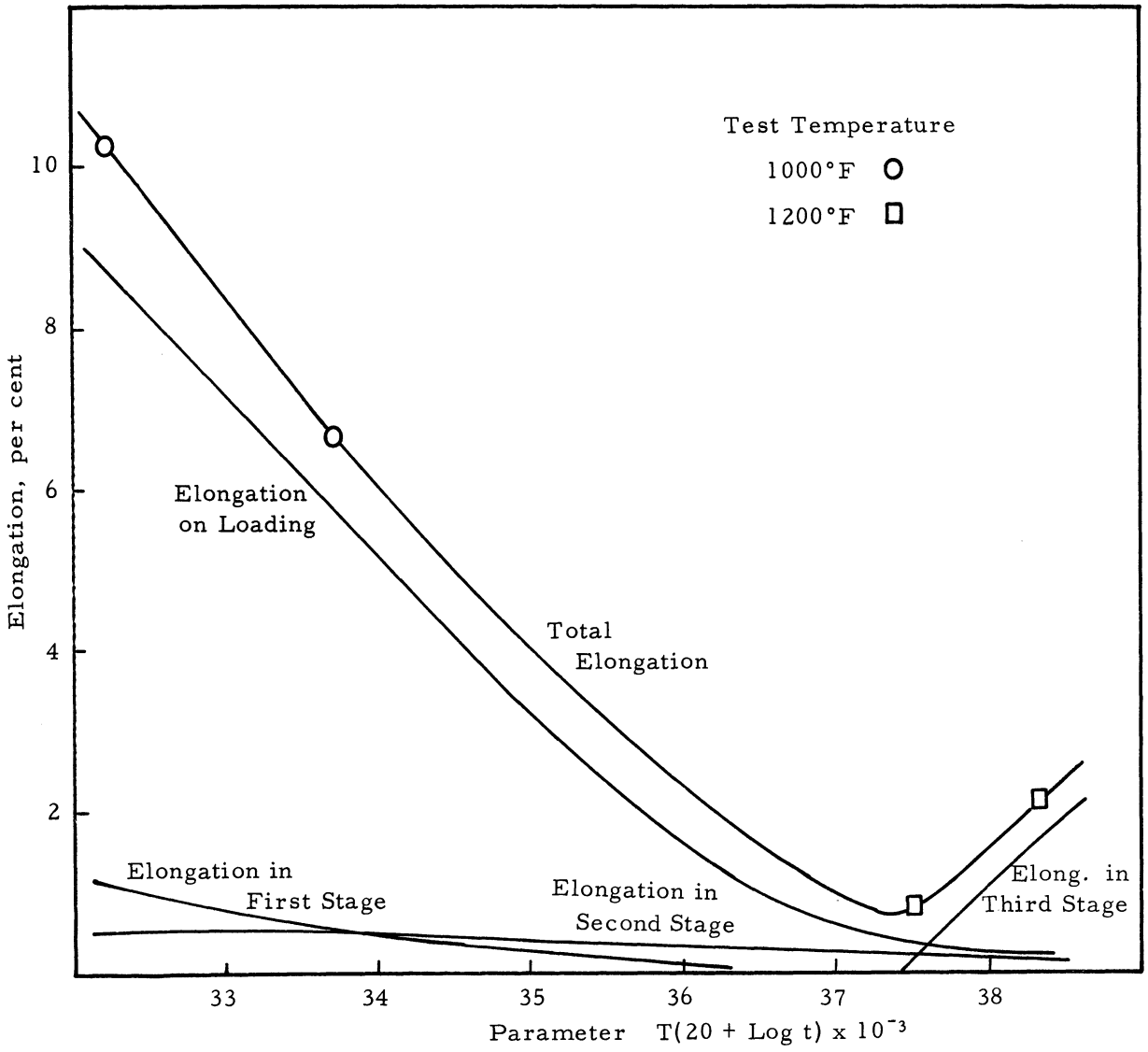

Figure 25. Time-temperature dependence of elongation obtained from smooth specimens of 0.026-inch thick Waspaloy sheet heat treated at 1900°F and aged at 1400°F.

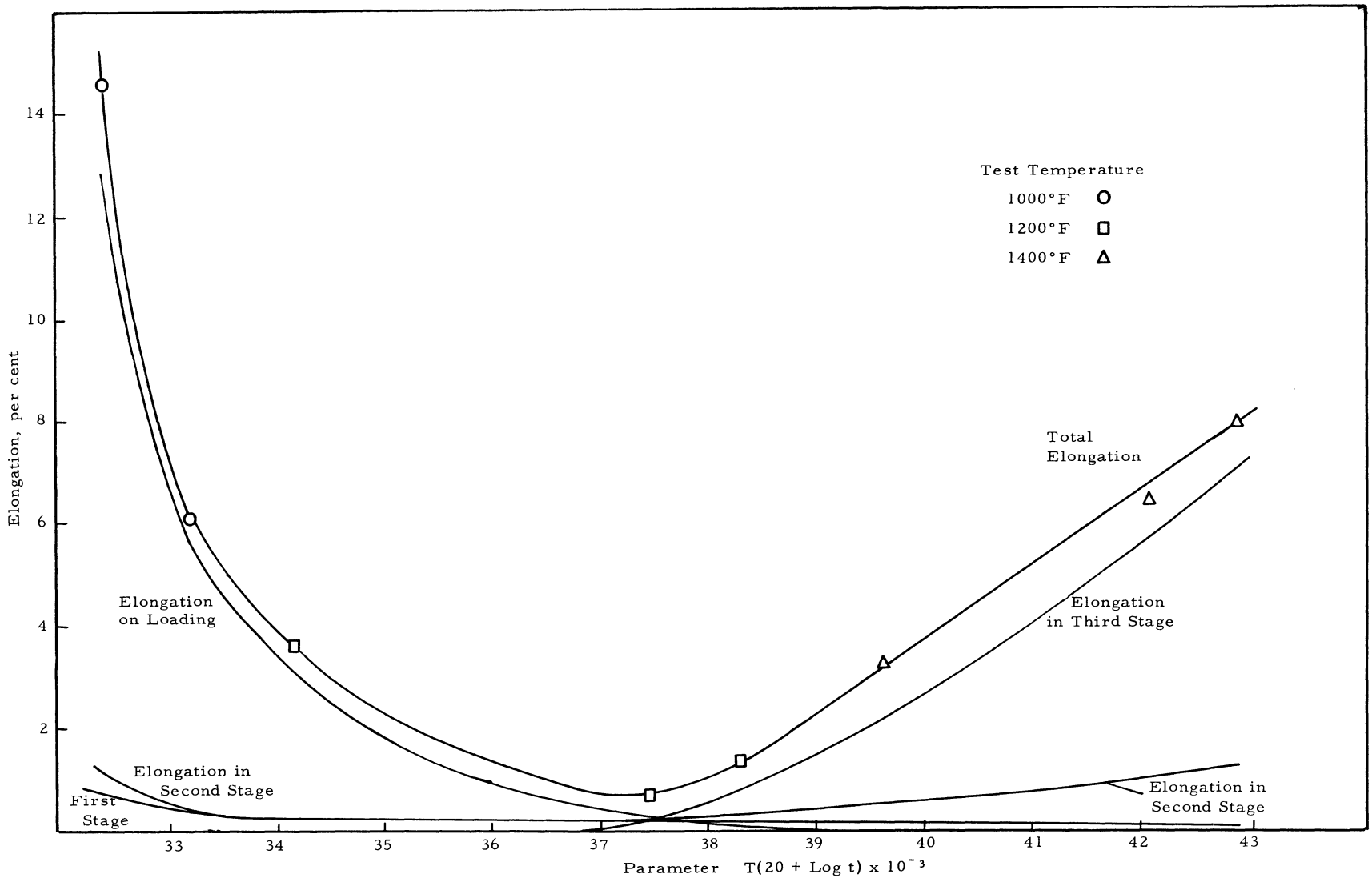

Figure 26. Time-temperature dependence of elongation obtained from smooth specimens of 0.026-inch thick Waspaloy sheet heat treated at 1975°F and aged at 1400°F.

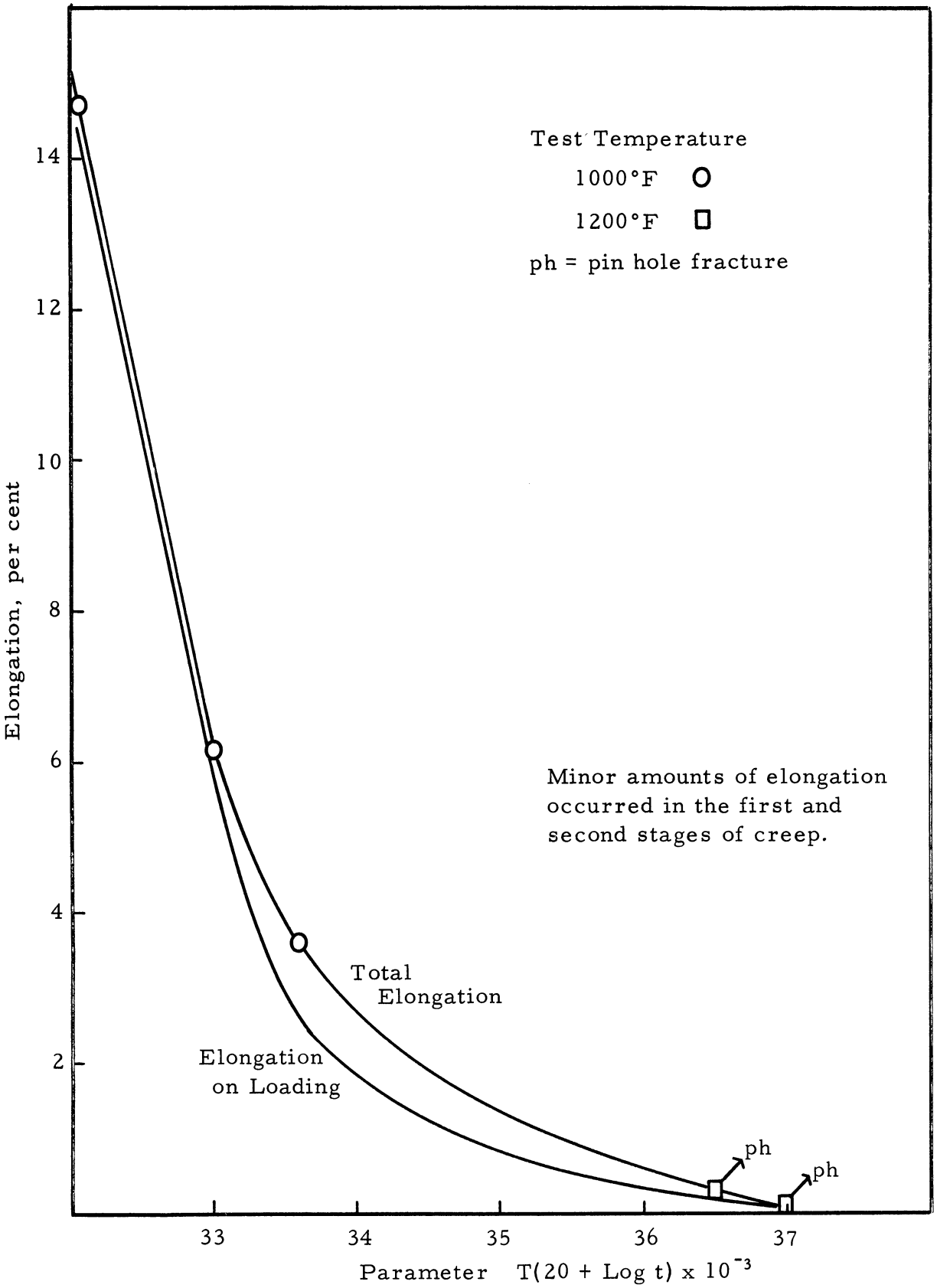

Figure 27. Time-temperature dependence of elongation obtained from smooth specimens of 0.026-inch thick Waspaloy sheet heat treated at 2150°F and aged at 1400°F.

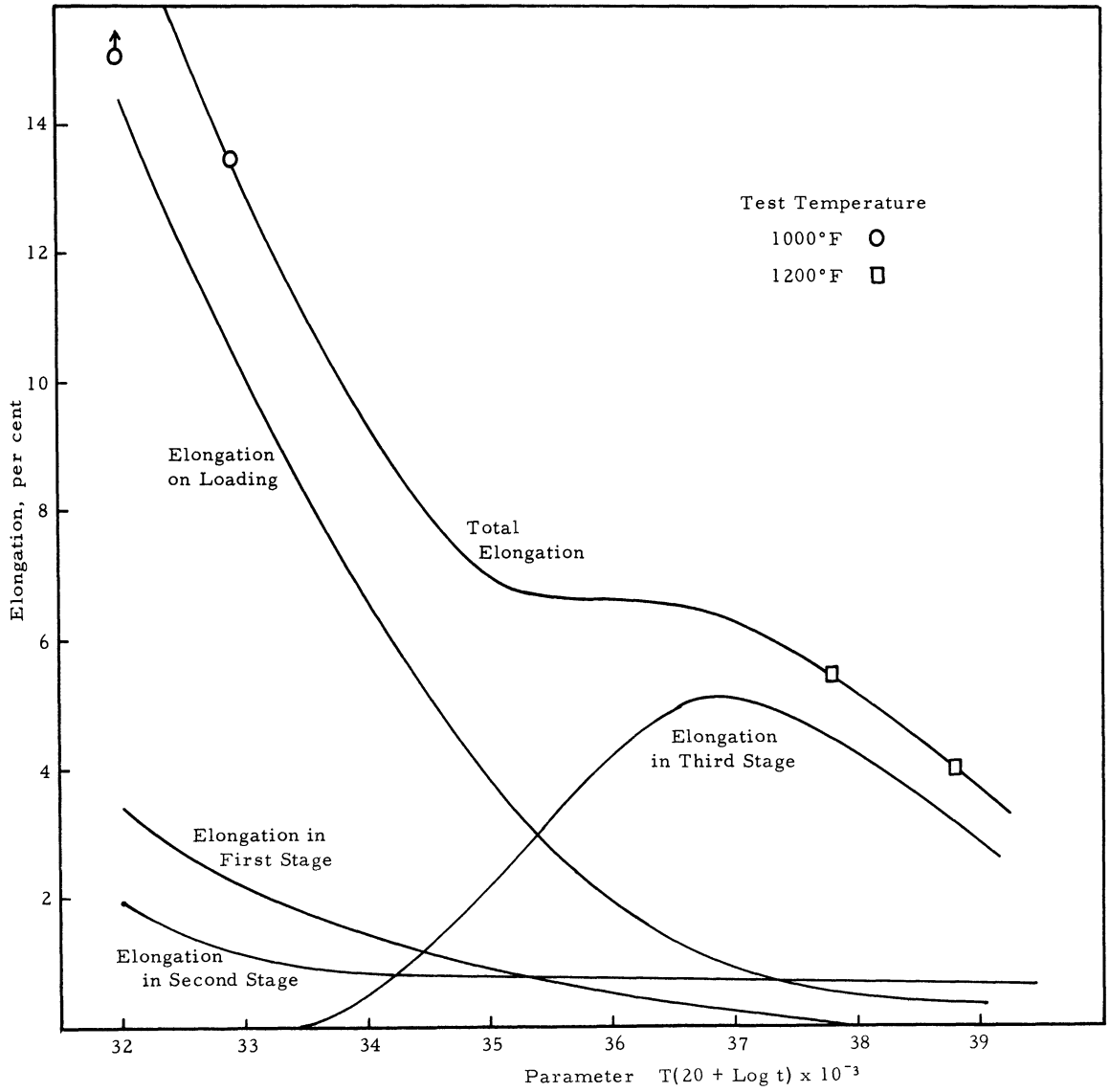

Figure 28. Time-temperature dependence of elongation obtained from smooth specimens of 0.026-inch thick Waspaloy sheet heat treated at 1900°F and aged at 1700°F.

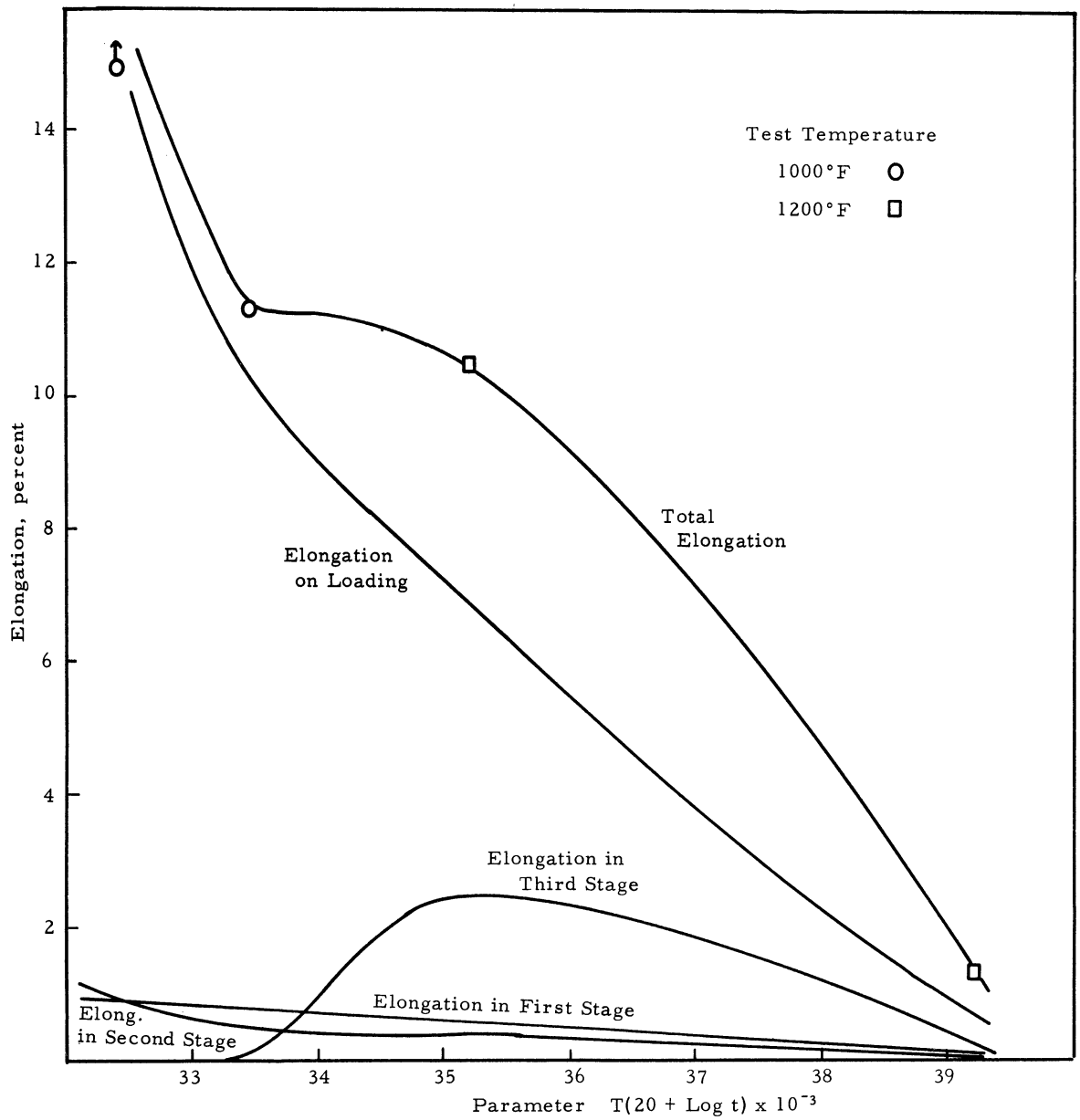

Figure 29. Time-temperature dependence of elongation obtained from smooth specimens of 0.026-inch thick Waspaloy sheet heat treated at 2150°F and aged at 1700°F.

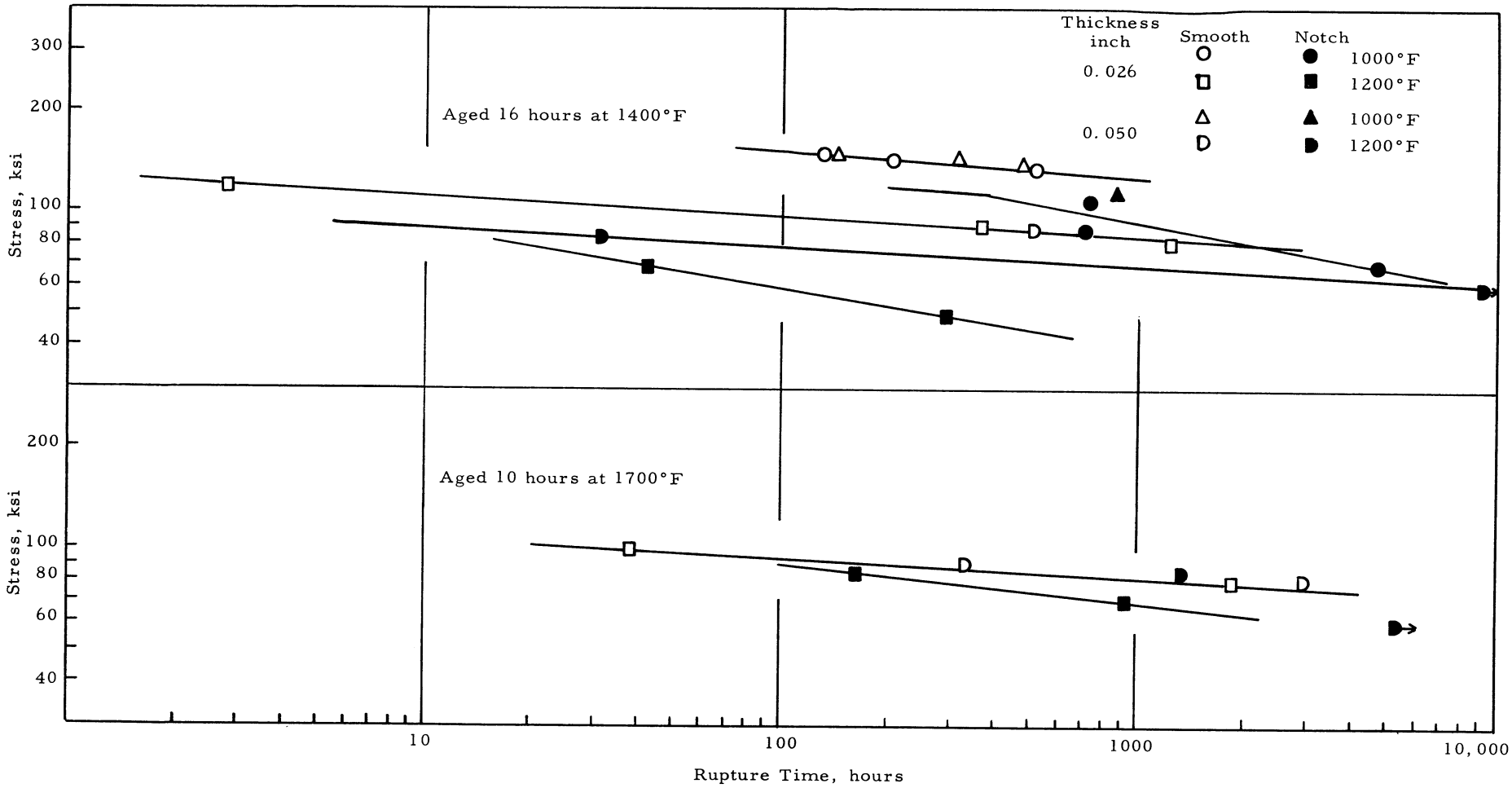

Figure 30. Stress versus rupture time data at 1000° and 1200°F obtained from smooth and notched specimens of 0.026-inch and 0.050-inch thick Waspaloy sheet heat treated at 1975°F and aged.

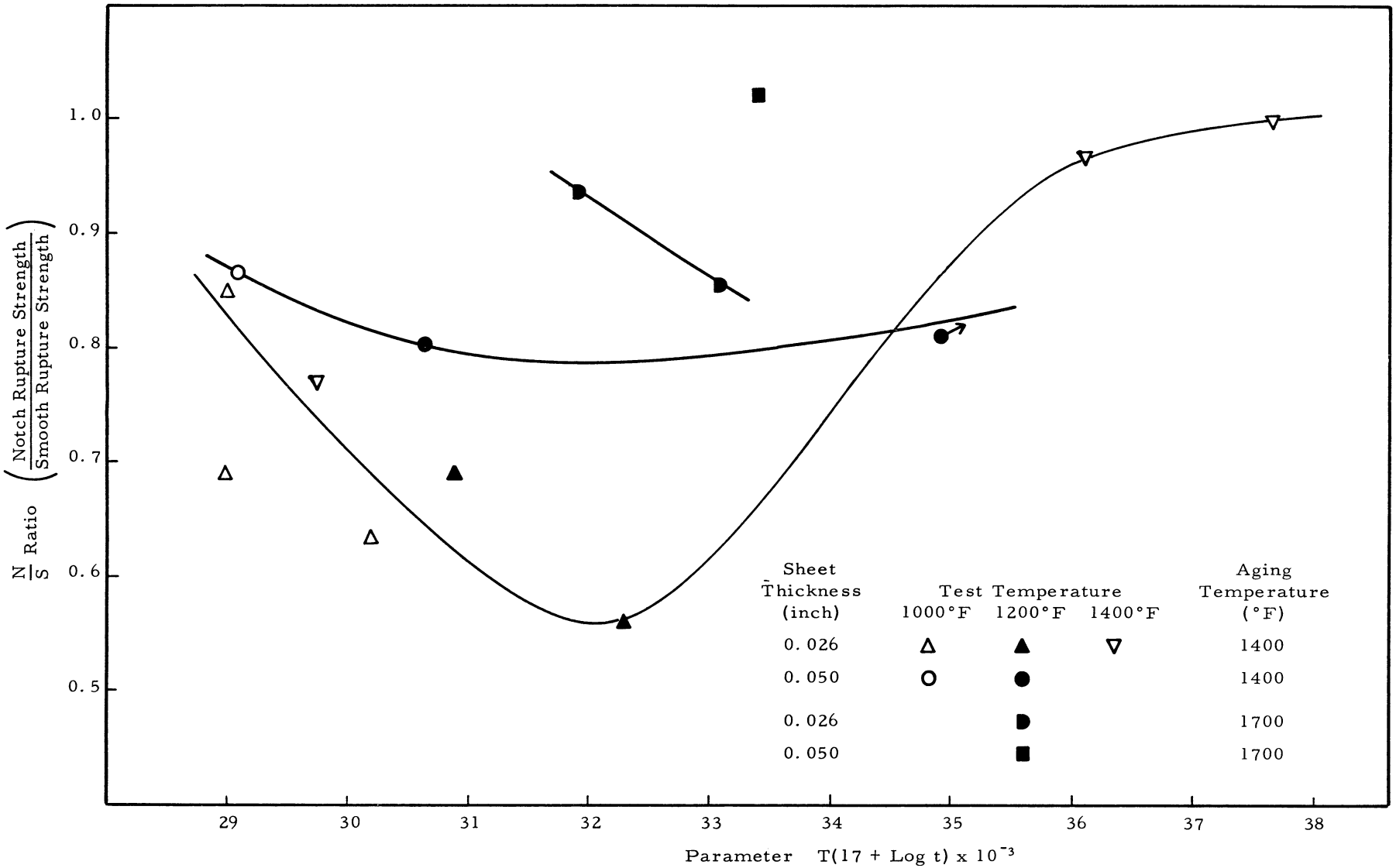

Figure 31. Time-temperature dependence of the notch to smooth rupture strength ratios at 1000°, 1200° and 1400°F for 0.026-inch and 0.050-inch thick Waspaloy sheet solution treated at 1975°F and aged at 1400° or 1700°F.

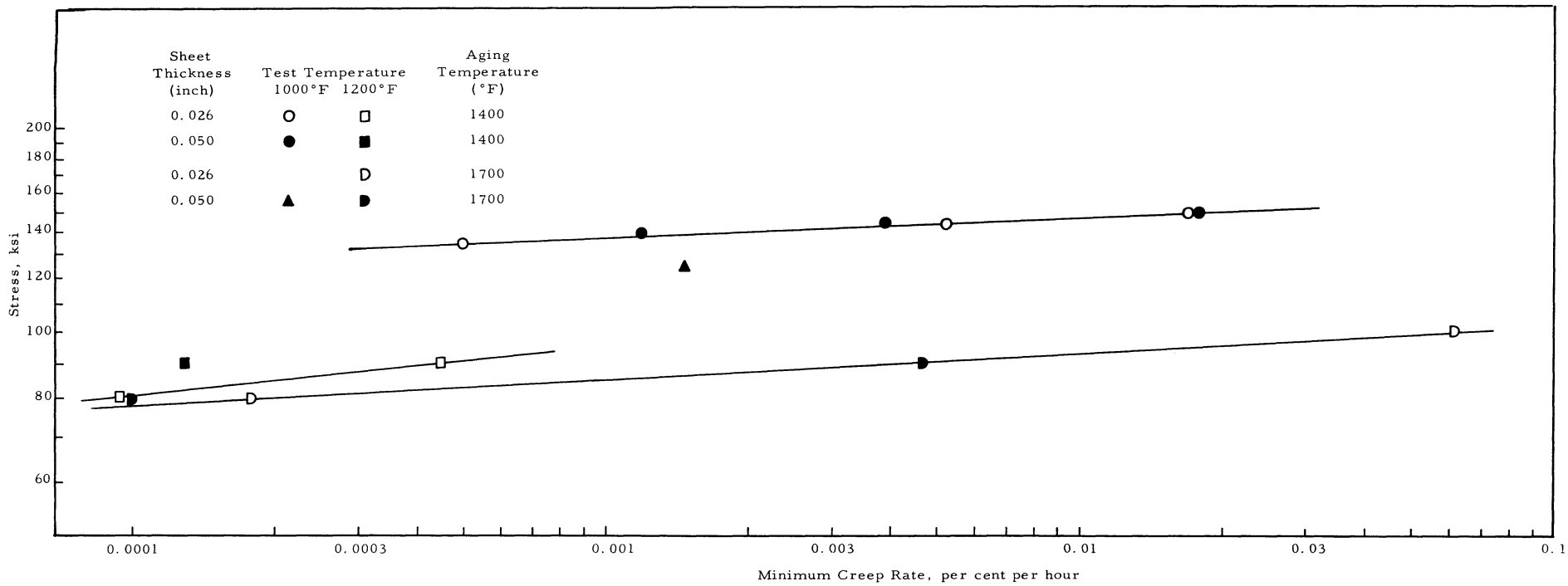

Figure 32. Stress versus minimum creep rate behavior at 1000° and 1200°F for 0.026-inch and 0.050-inch thick Waspaloy sheet heat treated at 1975°F and aged at 1400° or 1700°F.

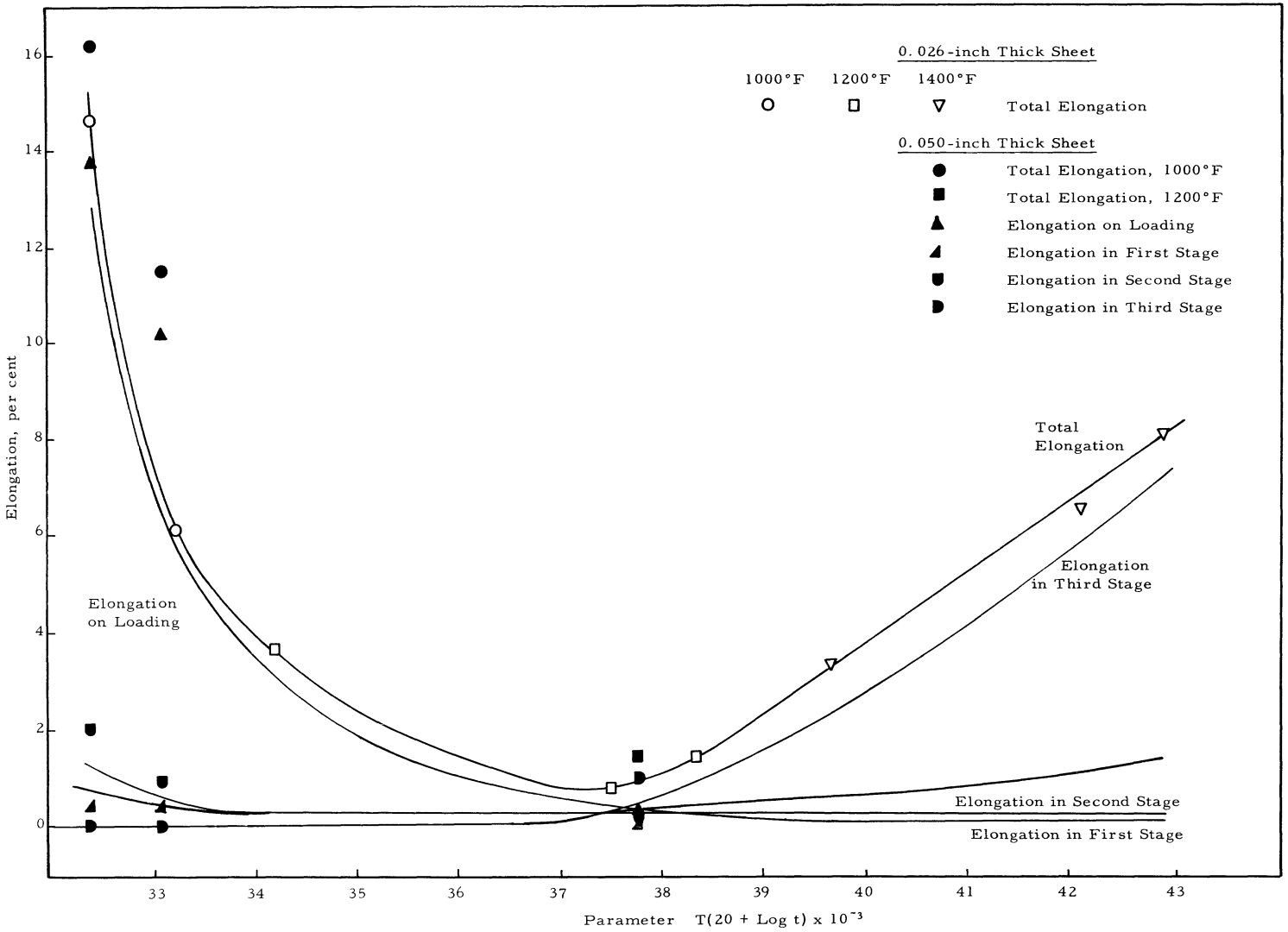

Figure 33. Time-temperature dependence of elongation obtained from smooth specimens of 0.026-inch and 0.050-inch thick Waspaloy sheet heat treated at 1975°F and aged at 1400°F.

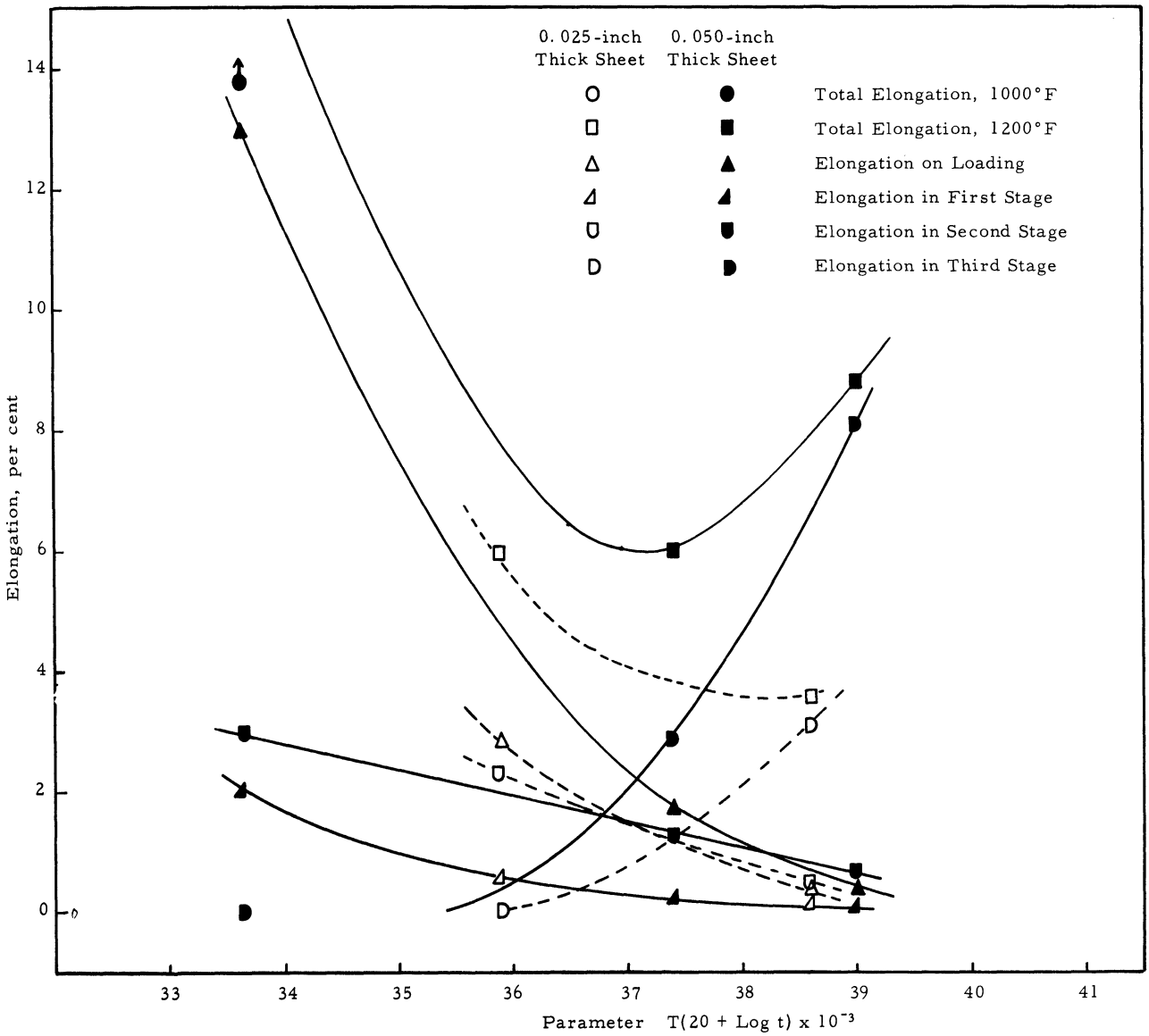

Figure 34. Time-temperature dependence of elongation obtained from smooth specimens of 0.026-inch and 0.050-inch thick Waspaloy sheet heat treated at 1975°F and aged at 1700°F.

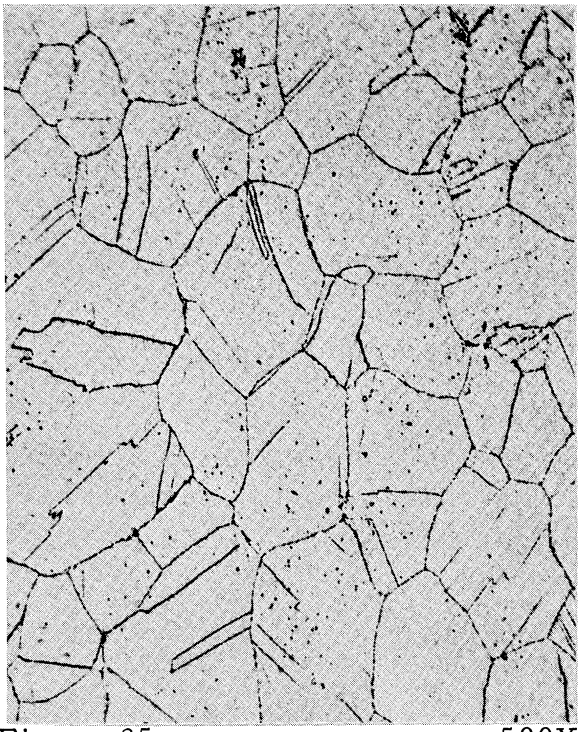

Figure 35. 500X
Aged 16 hours at 1400°F
Solution Treated 1/2-hour at 1825°F

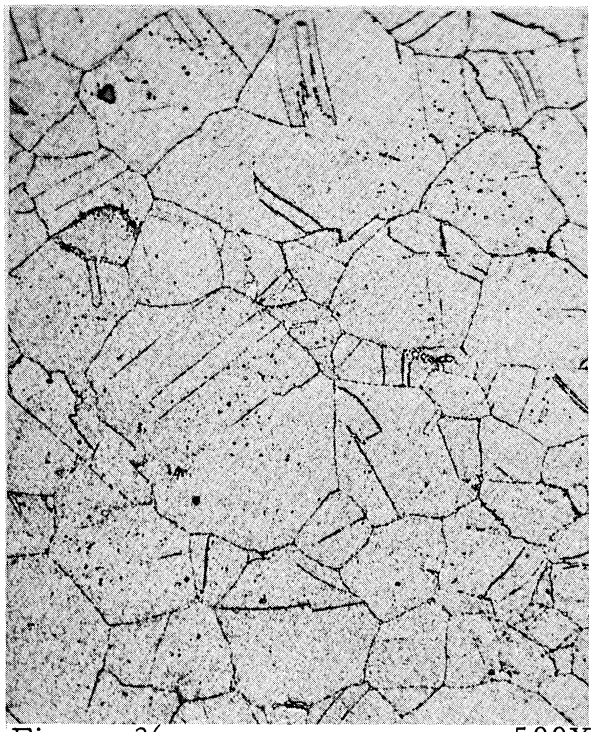

Figure 36. 500X
Aged 10 hours at 1700°F
Solution Treated 1/2-hour at 1825°F

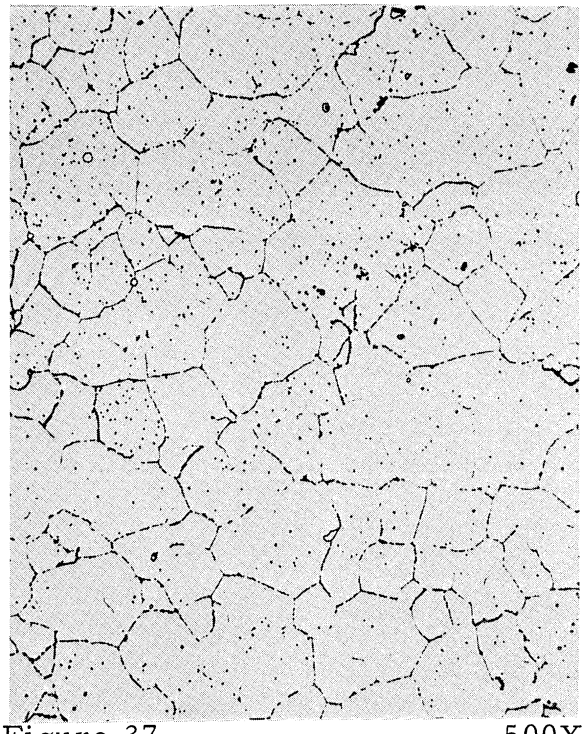

Figure 37. 500X
Aged 16 hours at 1400°F
Solution Treated 1/2-hour at 1900°F

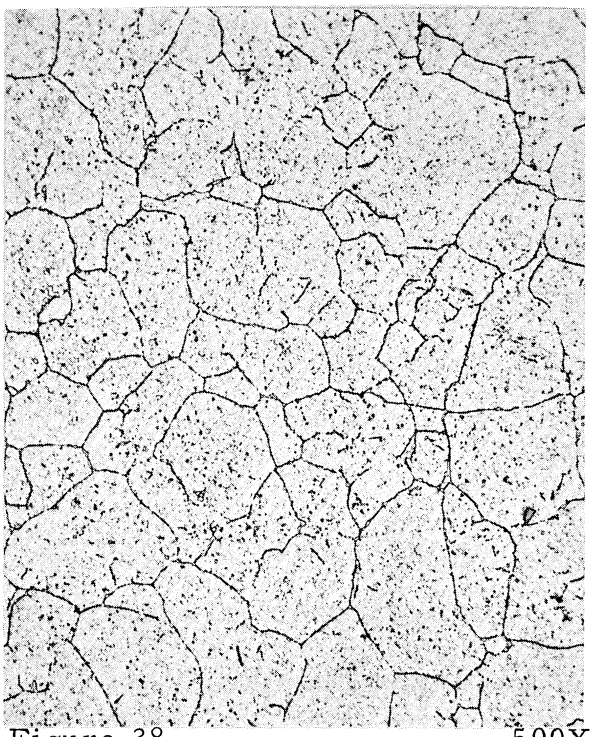

Figure 38. 500X
Aged 10 hours at 1700°F
Solution Treated 1/2-hour at 1900°F

Photomicrographs of 0.026-inch thick Waspaloy sheet
in the as-heat-treated condition.

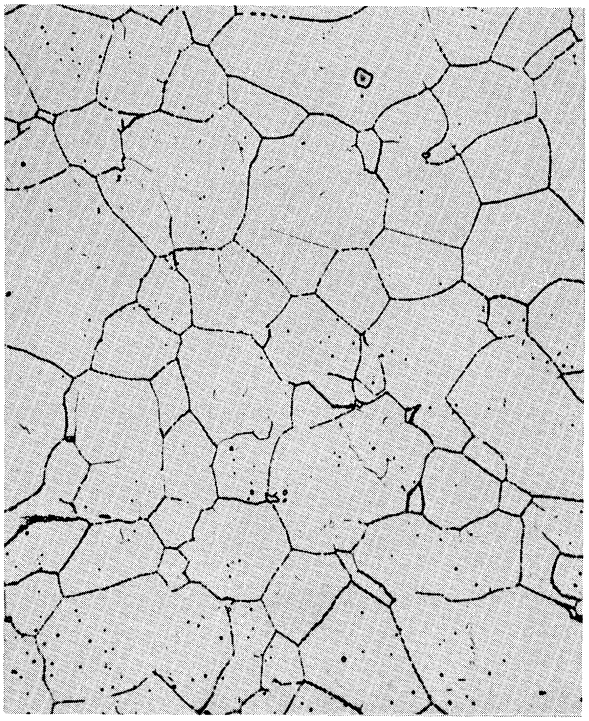

Figure 39. 500X
Aged 16 hours at 1400°F
Solution Treated 1/2-hour at 1975°F

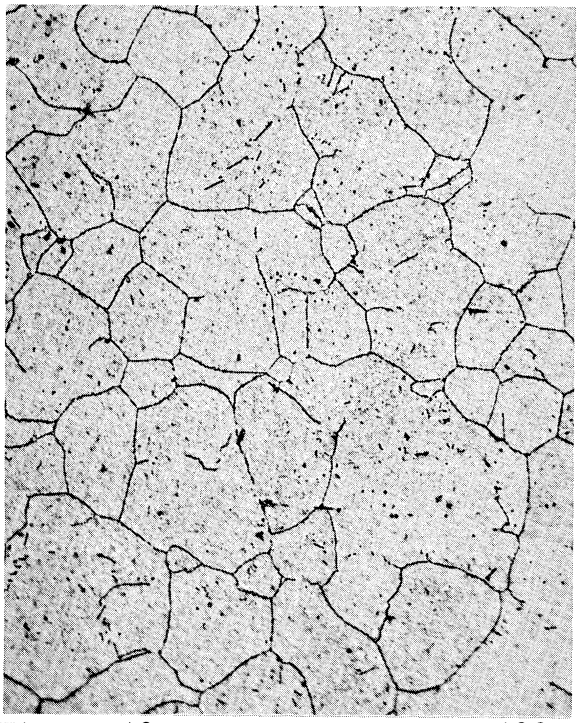

Figure 40. 500X
Aged 10 hours at 1700°F
Solution Treated 1/2-hour at 1975°F

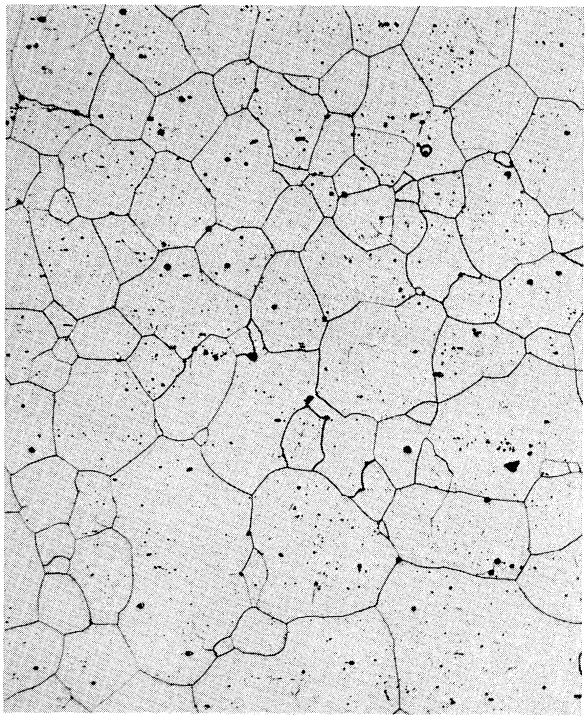

Figure 41. 100X
Aged 16 hours at 1400°F
Solution Treated 1/2-hour at 2150°F

Figure 42. 100X
Aged 10 hours at 1700°F
Solution Treated 1/2-hour at 2150°F

Photomicrographs of 0.026-inch thick Waspaloy sheet
in the as-heat-treated condition.

Figure 43. 5,400X
Aged 16 hours at 1400°F

Figure 44. 5,400X
Aged 10 hours at 1700°F

Solution Treated 1/2-hour at 1825°F

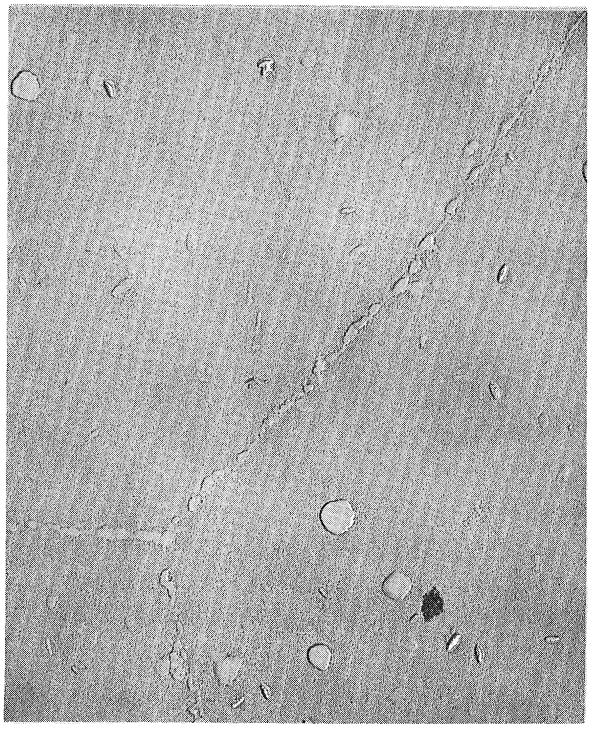

Figure 45. 5,400X
Aged 16 hours at 1400°F

Figure 46. 5,400X
Aged 10 hours at 1700°F

Solution Treated 1/2-hour at 1900°F

Electron micrographs of 0.026-inch thick Waspaloy sheet in the as-heat-treated condition.

Figure 47. 5,400X
Aged 16 hours at 1400°F

Figure 48. 5,400X
Aged 10 hours at 1700°F

Solution Treated 1/2-hour at 1975°F

Figure 49. 5,400X
Aged 16 hours at 1400°F

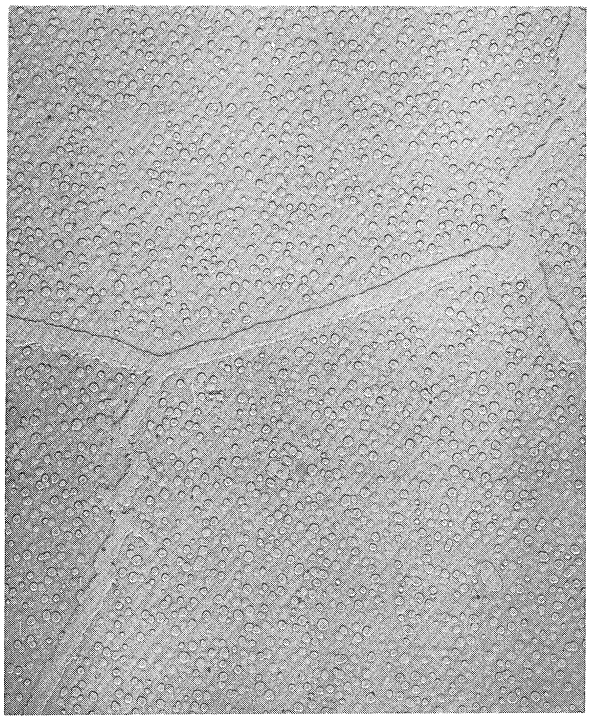

Figure 50. 5,400X
Aged 10 hours at 1700°F

Solution Treated 1/2-hour at 2150°F

Electron micrographs of 0.026-inch thick Waspaloy sheet in the as-heat-treated condition.

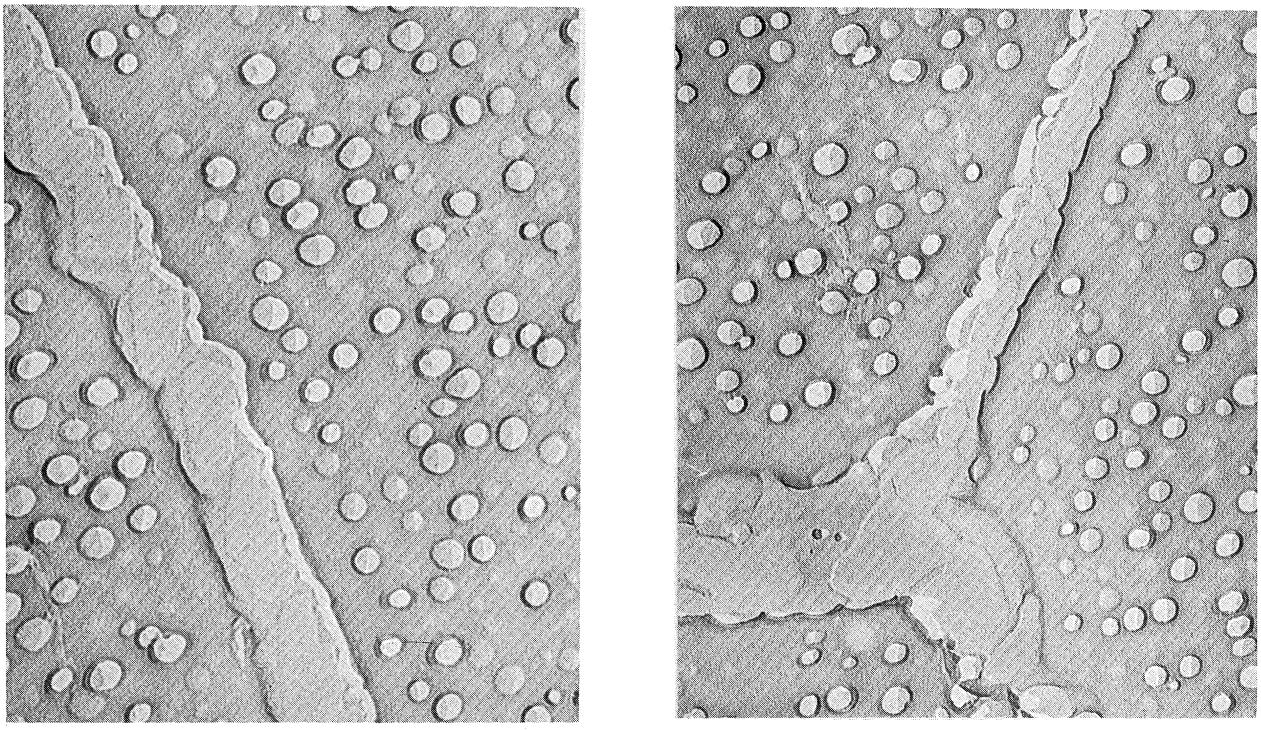

16,000X 14,000X

Figure 51. Electron micrographs showing γ' and carbide precipitates in the grain boundary of 0.026-inch thick Waspaloy sheet solution treated 1/2-hour at 2150°F and aged 10 hours at 1700°F.

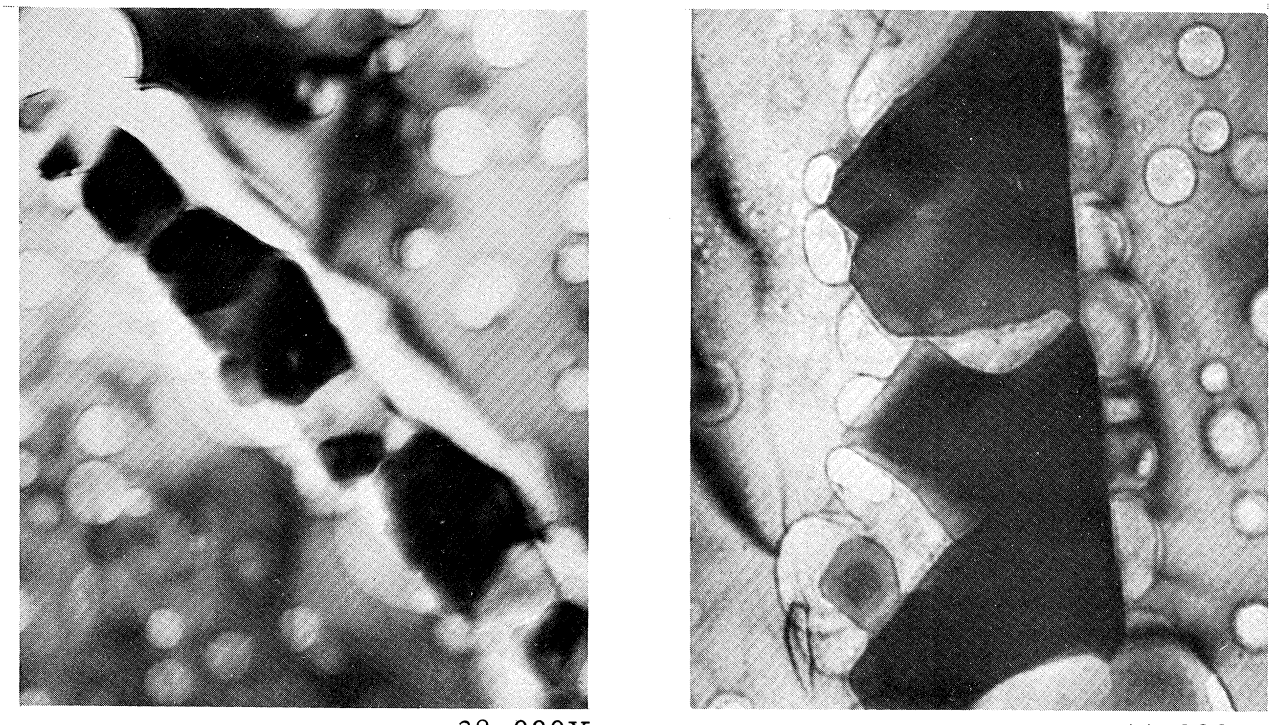

38,000X 44,000X

Figure 52. Transmission electron micrographs showing γ' and carbide precipitates in the grain boundary of 0.026-inch thick Waspaloy sheet solution treated 1/2-hour at 2150°F and aged 10 hours at 1700°F.

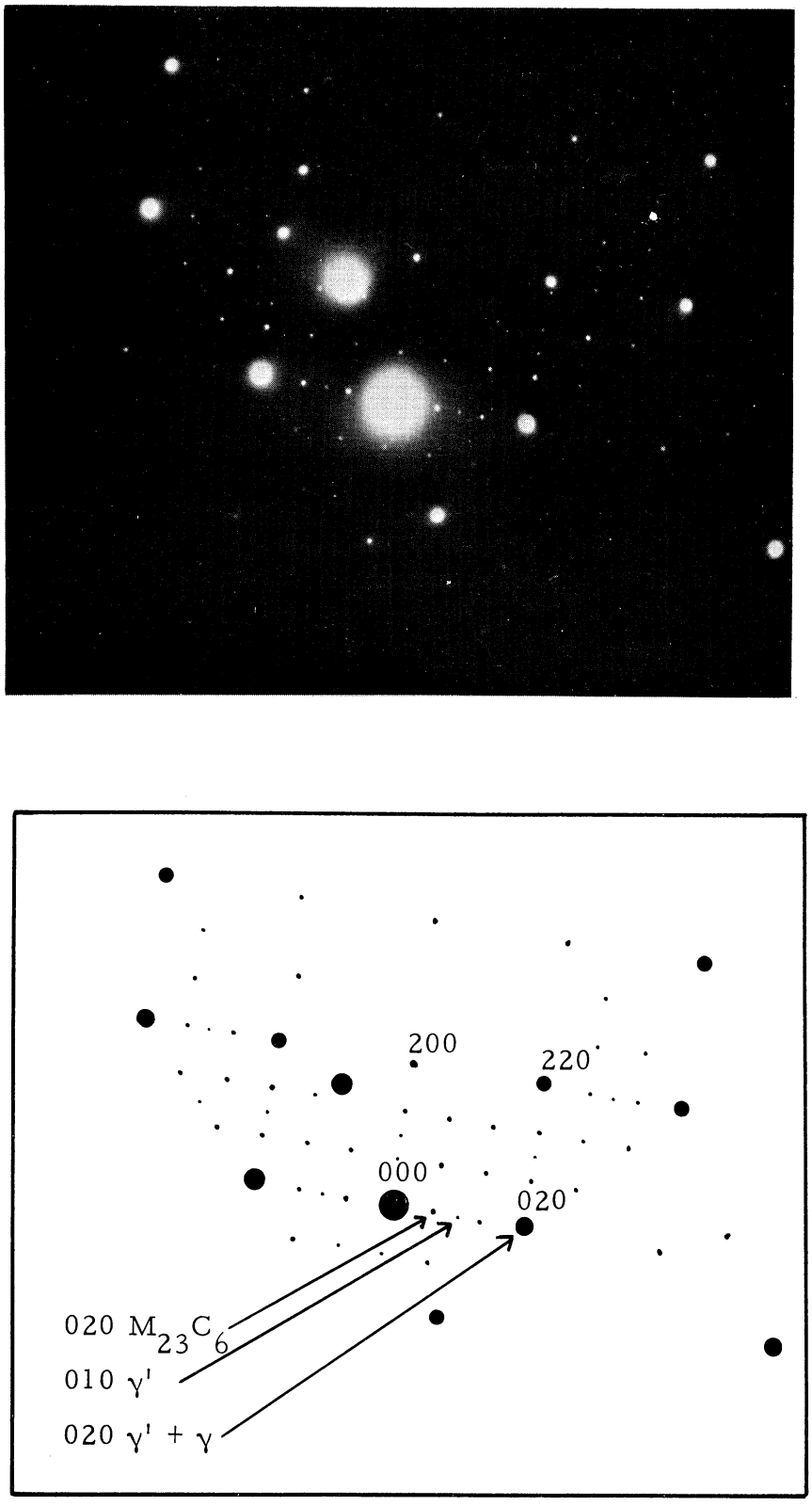

Figure 53. Selected area diffraction pattern of a grain boundary (0.026-inch thick Waspaloy sheet solution treated 1/2-hour at 2150°F and aged 16 hours at 1400°F) showing identical orientations of $M_{23}C_6$ and the matrix on one side of the boundary.

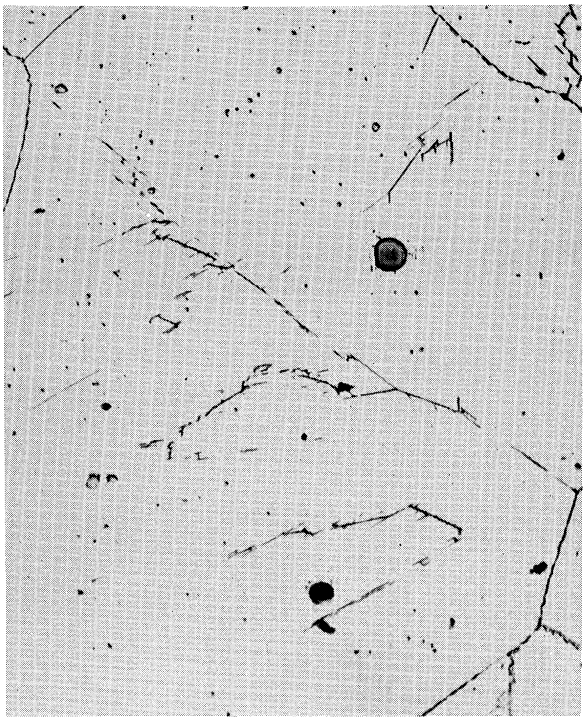

Optical Micrograph 1,000X

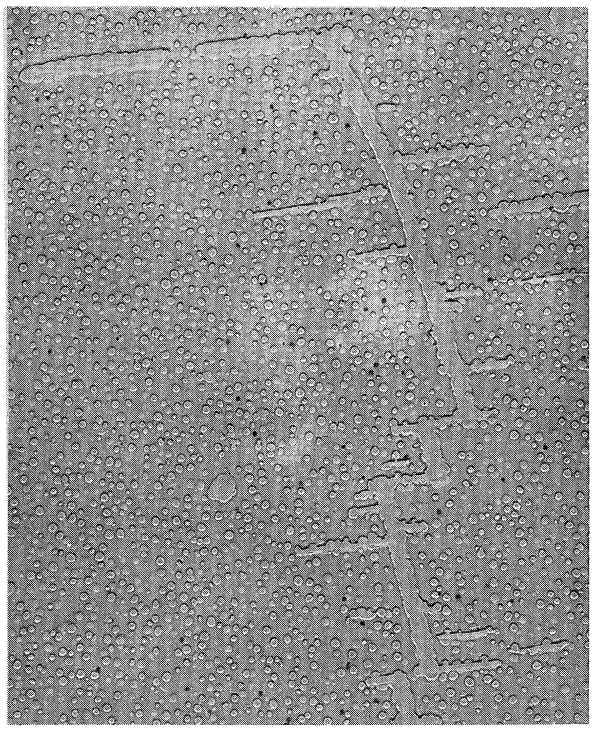

Electron Micrograph 5,400X

Figure 54.

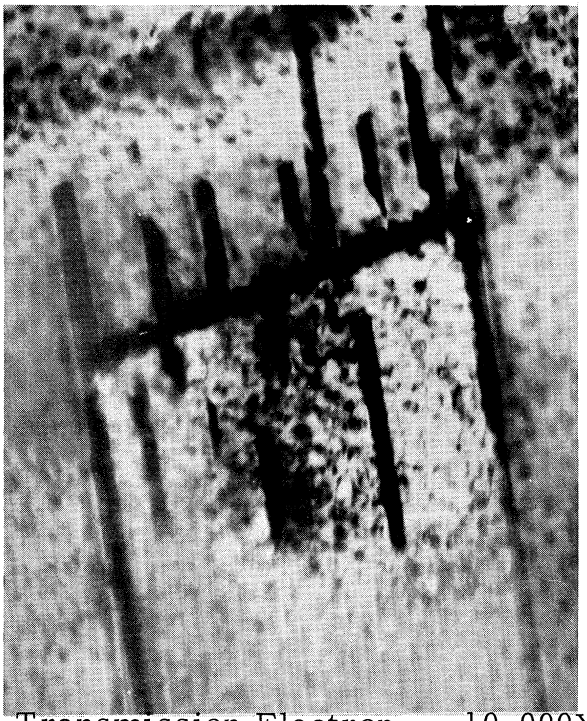

Transmission Electron Micrograph 10,000X

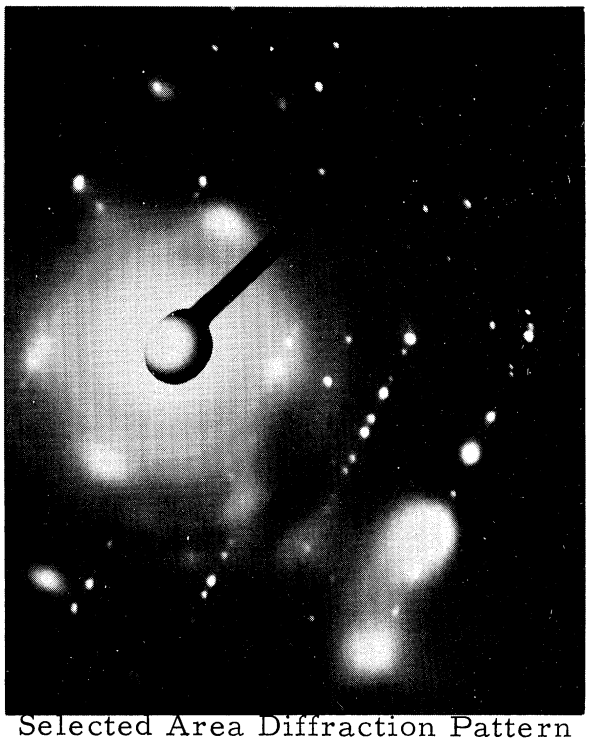

Selected Area Diffraction Pattern

Figure 55.

Micrographs of $M_{23}C_6$ phase present in a "Chinese Script" form in 0.026-inch thick Waspaloy sheet solution treated 1/2-hour at 2150°F and aged 10 hours at 1700°F.

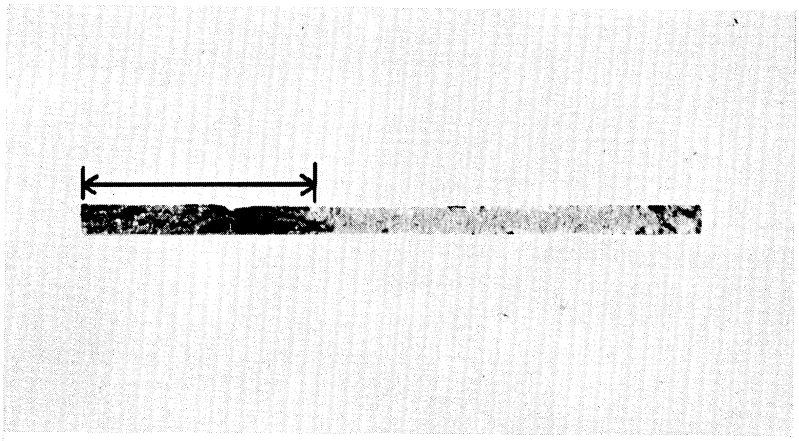

16X

Smooth specimen of 0.026-inch thick Waspaloy sheet. (Material solution treated at 1825°F and aged at 1700°F; tested at 1200°F at 85 ksi; ruptured in 894.5 hours).

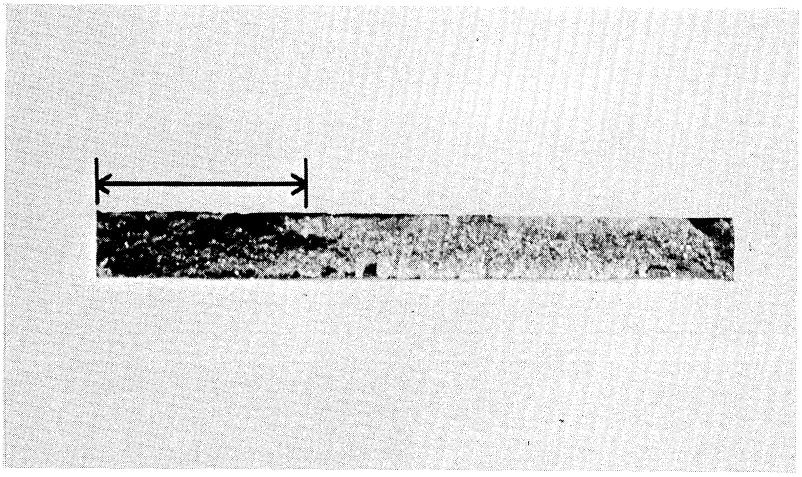

16X

Smooth specimen of 0.050-inch thick Waspaloy sheet. (Material solution treated at 1975°F and aged at 1400°F; tested at 1200°F at 90 ksi; ruptured in 513.1 hours).

Figure 56. Fracture surfaces of ruptured specimens. (Slow intergranular crack propagation region indicated by arrows).

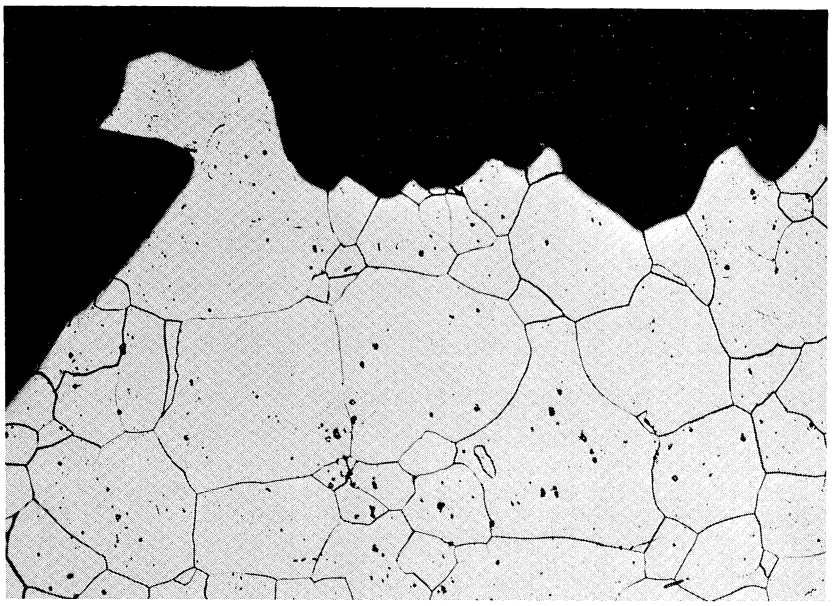

Figure 57. Fracture Traverse at 50X. Solution treated at 2150° and aged at 1400°F. (Notched specimen tested at 1200°F at 65 ksi, ruptured in 59.1 hours.)

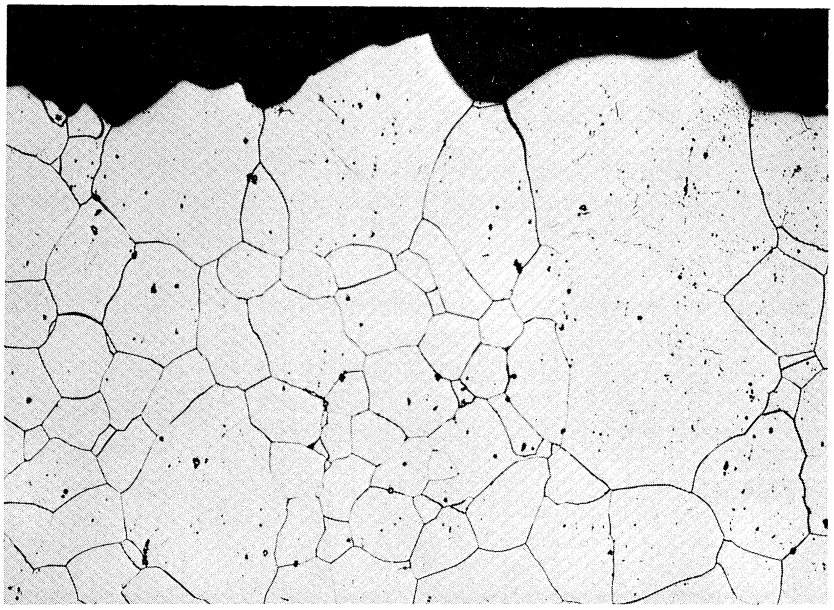

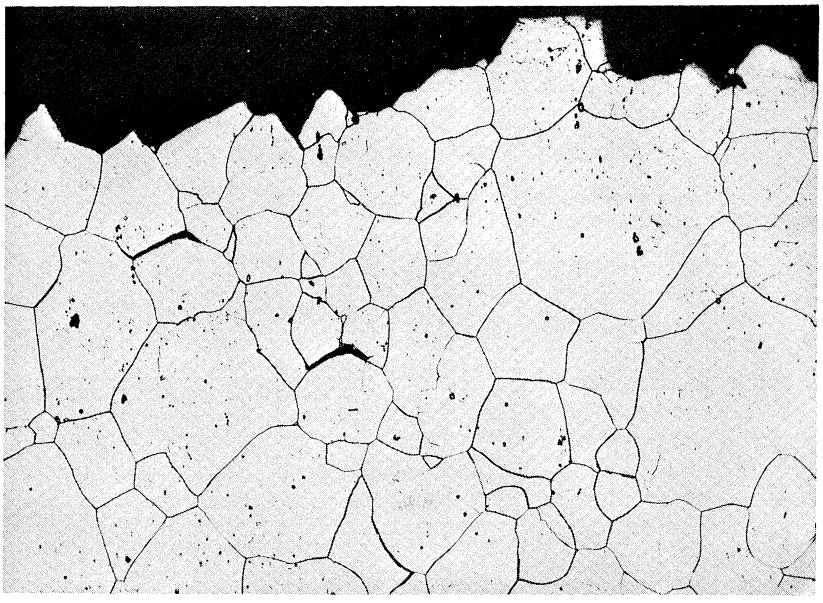

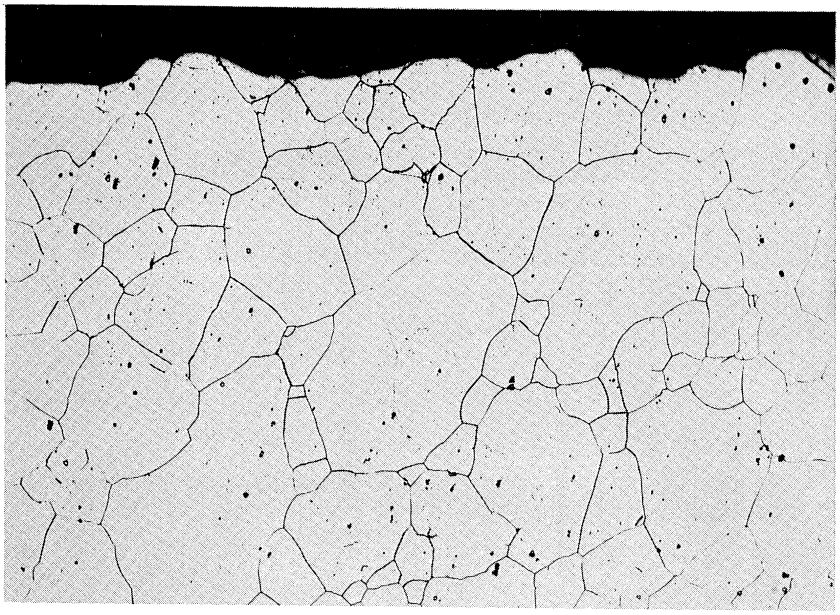

Figure 57 continued.

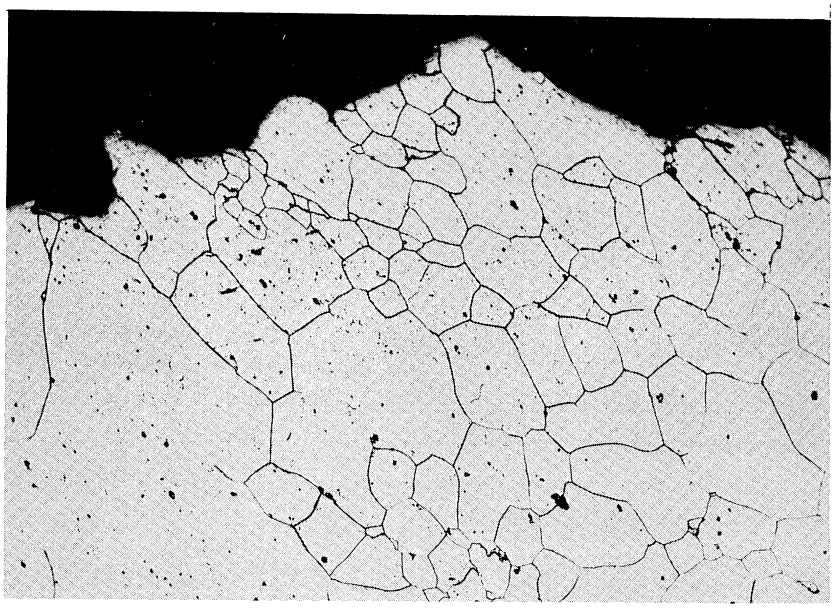

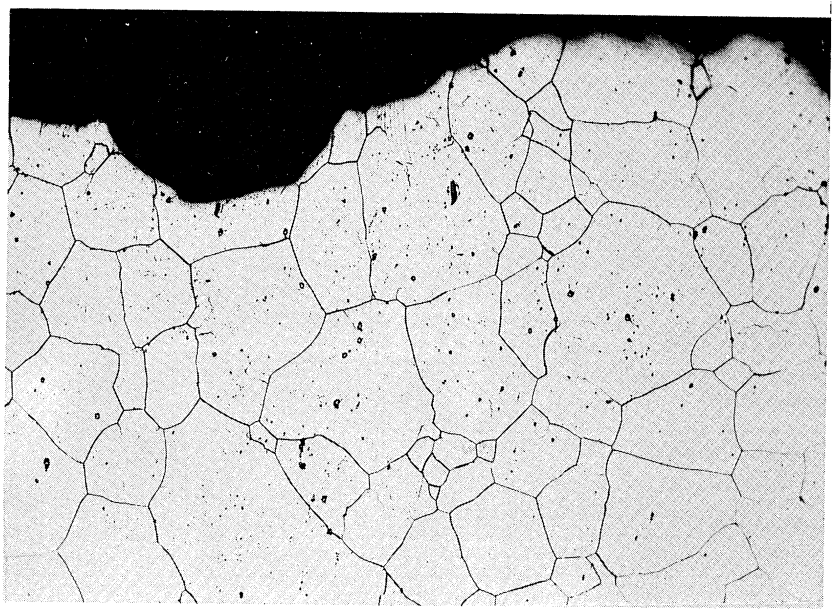

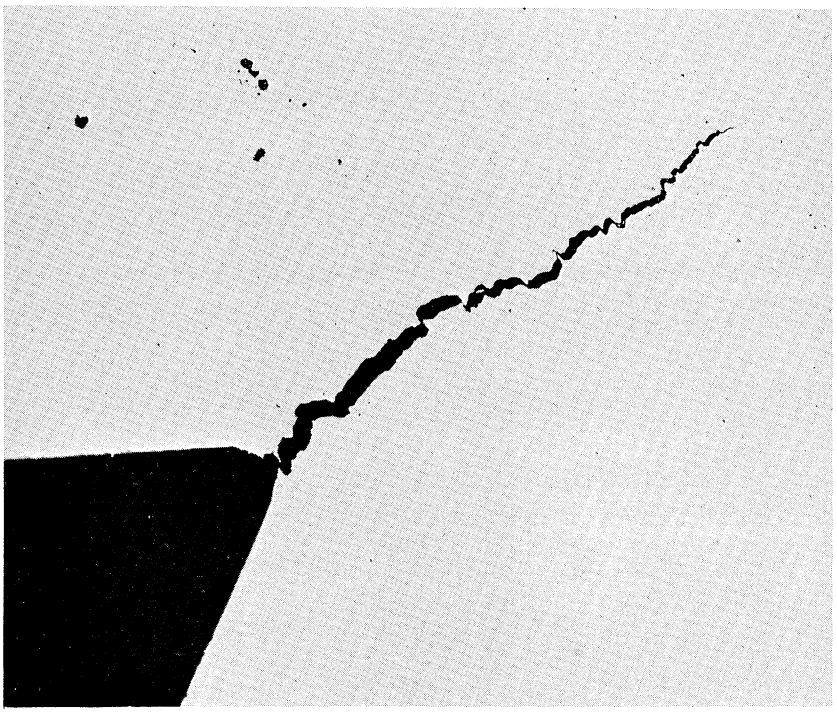

50X

Figure 58. Photomicrograph showing an intergranular crack developing from a machined notch (K_t=20). (0.026-inch thick Waspaloy sheet solution treated at 1900°F and aged at 1700°F; tested at 1000°F at 85 ksi; discontinued after 6147 hours.)

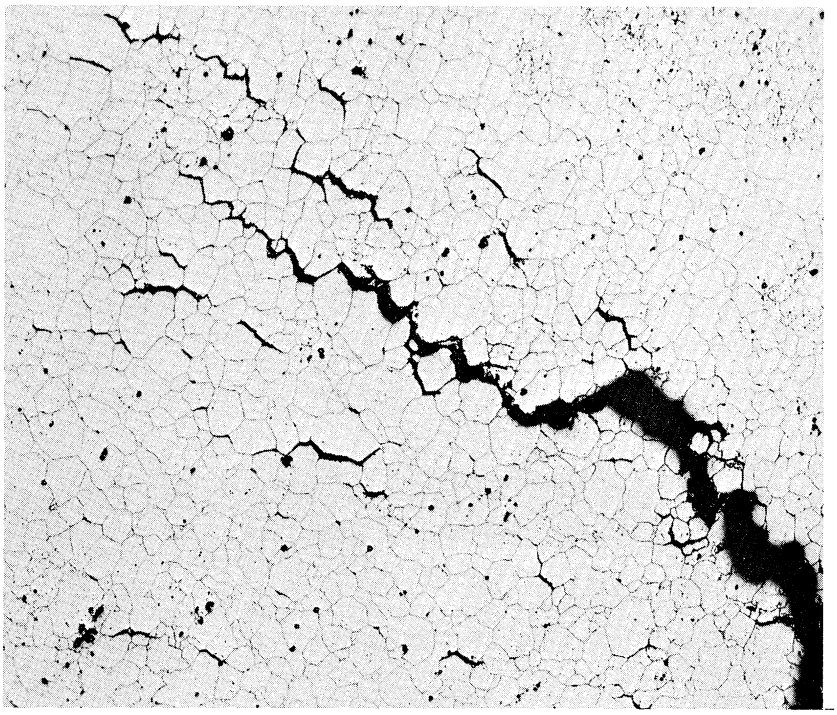

100X

Figure 59. Photomicrograph showing subsidiary cracking in the region of the major intergranular crack. (0.026-inch thick Waspaloy sheet notched specimen solution treated at 1975°F and aged at 1400°F; tested at 1400°F at 45 ksi; ruptured in 260 hours in the pin holes.)

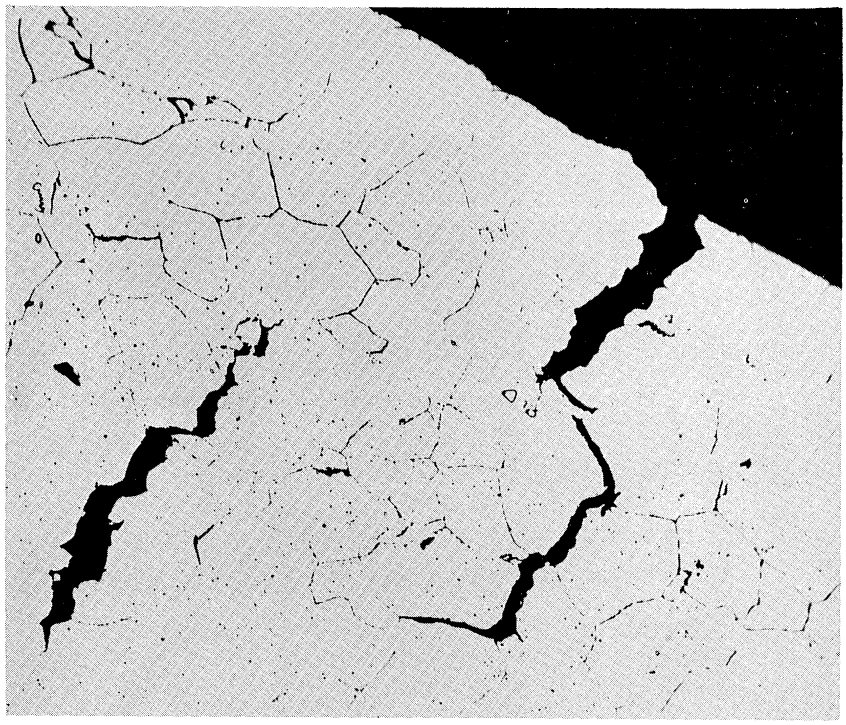

500X

Figure 60. Photomicrograph showing subsidiary cracking in a smooth specimen. (0.026-inch thick Waspaloy sheet solution treated at 1975°F and aged at 1400°F; tensile tested at 1200°F.)

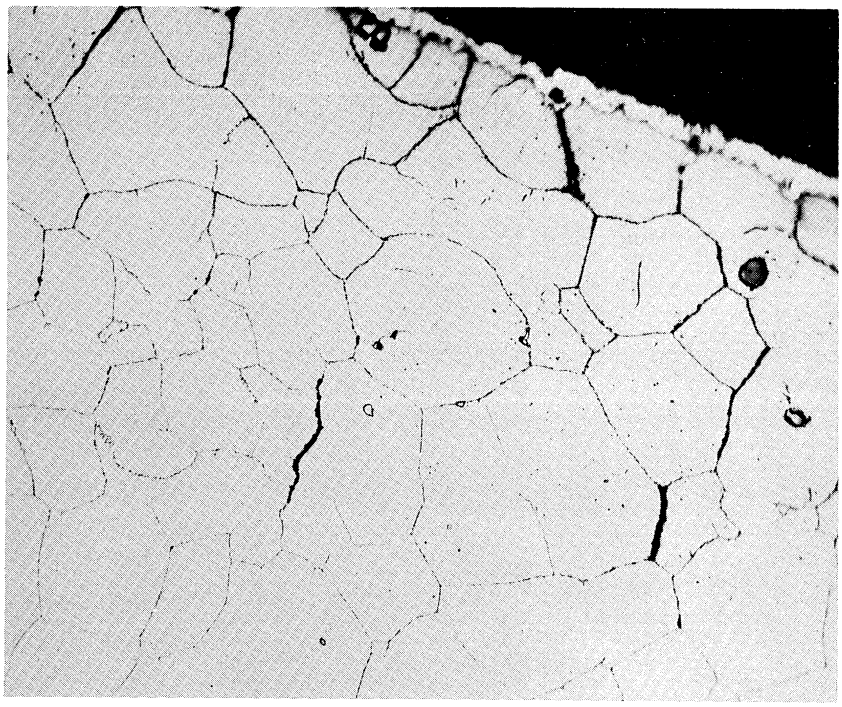

500X

Figure 61. Photomicrograph showing subsidiary cracking in a smooth specimen. (0.026-inch thick Waspaloy sheet solution treated at 1975°F and aged at 1700°F; tested at 1200°F at 80 ksi; ruptured in 1,870 hours.)

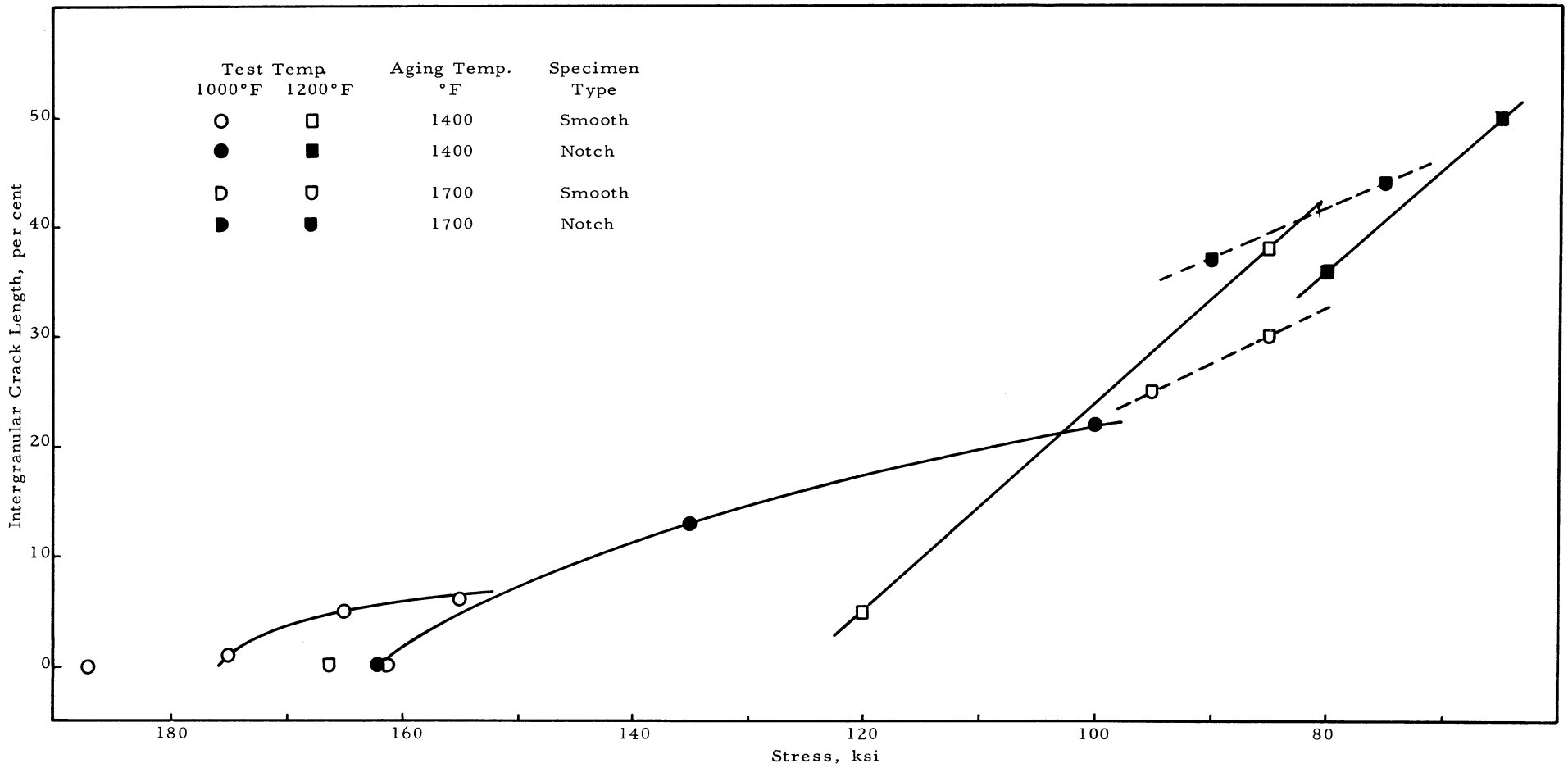

Figure 62. Intergranular crack length versus initial loading stress at 1000° and 1200°F obtained from smooth and notched specimens of 0.026-inch thick Waspaloy sheet heat treated at 1825°F and aged at 1400° or 1700°F.

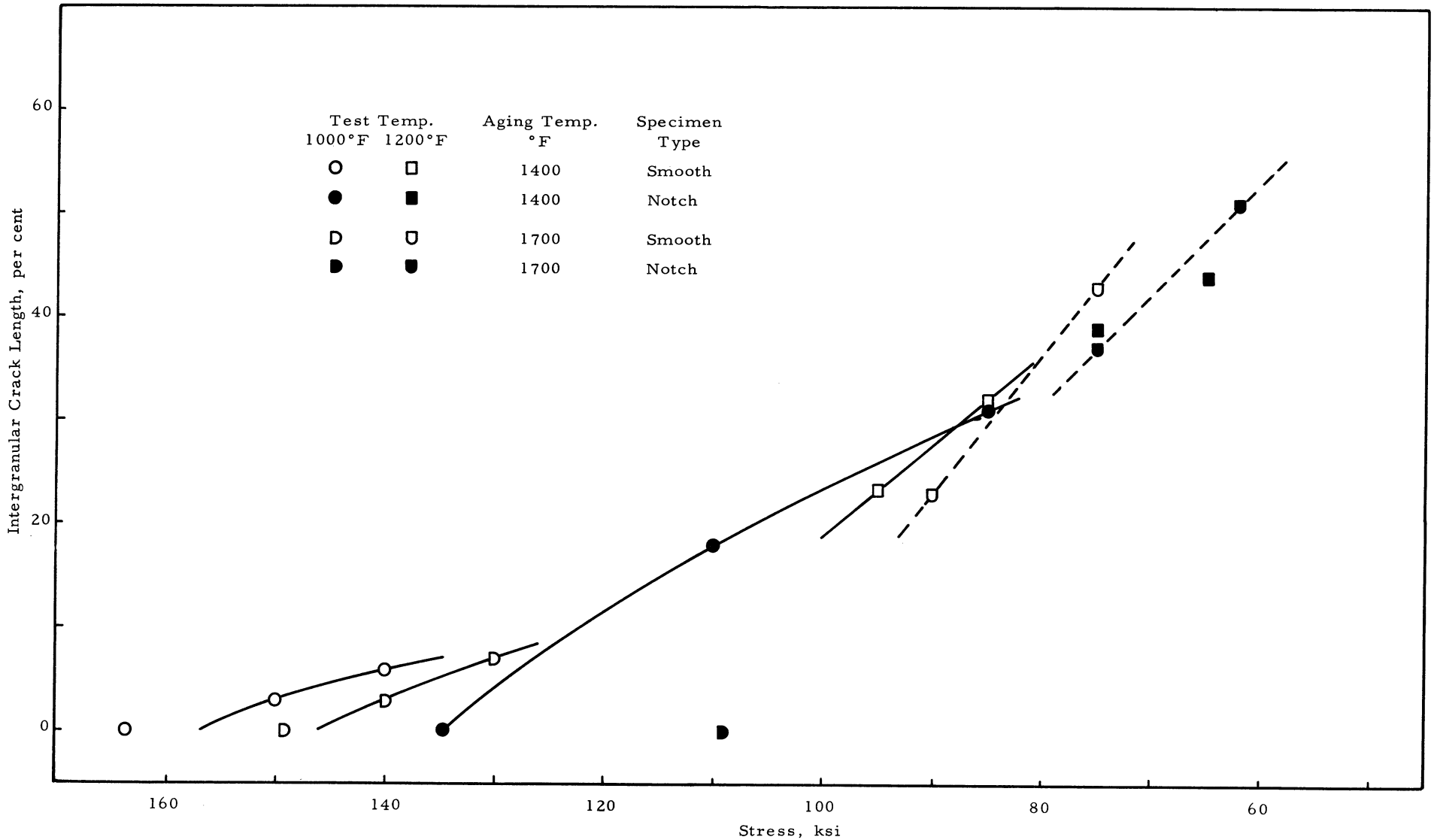

Figure 63. Intergranular crack length versus initial loading stress at 1000° and 1200°F obtained from smooth and notched specimens of 0.026-inch thick Waspaloy sheet heat treated at 1900°F and aged at 1400° or 1700°F.

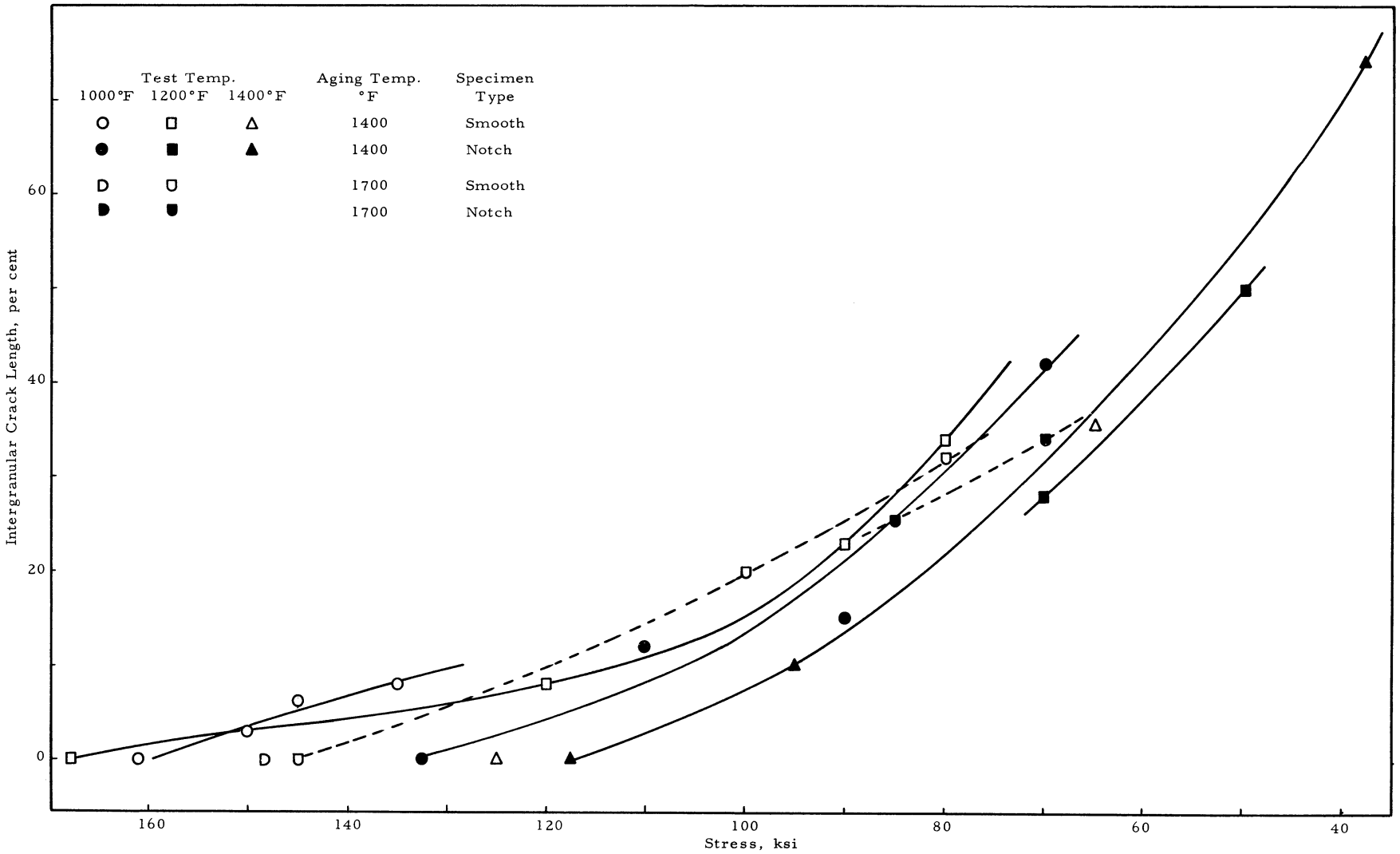

Figure 64. Intergranular crack length versus initial loading stress at 1000°, 1200° and 1400°F obtained from smooth and notched specimens of 0.026-inch thick Waspaloy sheet heat treated at 1975°F and aged at 1400° or 1700°F.

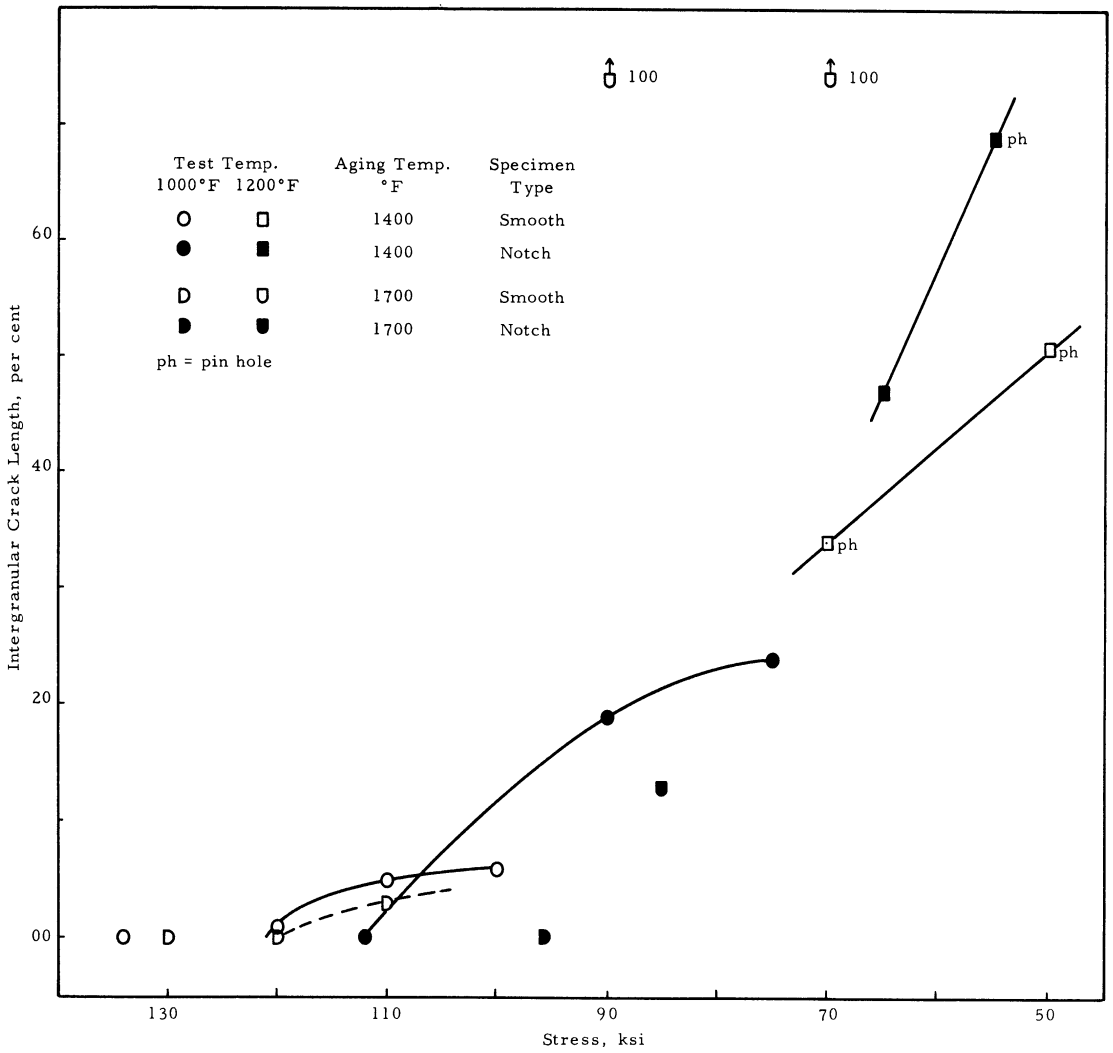

Figure 65. Intergranular crack length versus initial loading stress at 1000° and 1200°F obtained from smooth and notched specimens of 0.026-inch thick Waspaloy sheet heat treated at 2150°F and aged at 1400° or 1700°F.

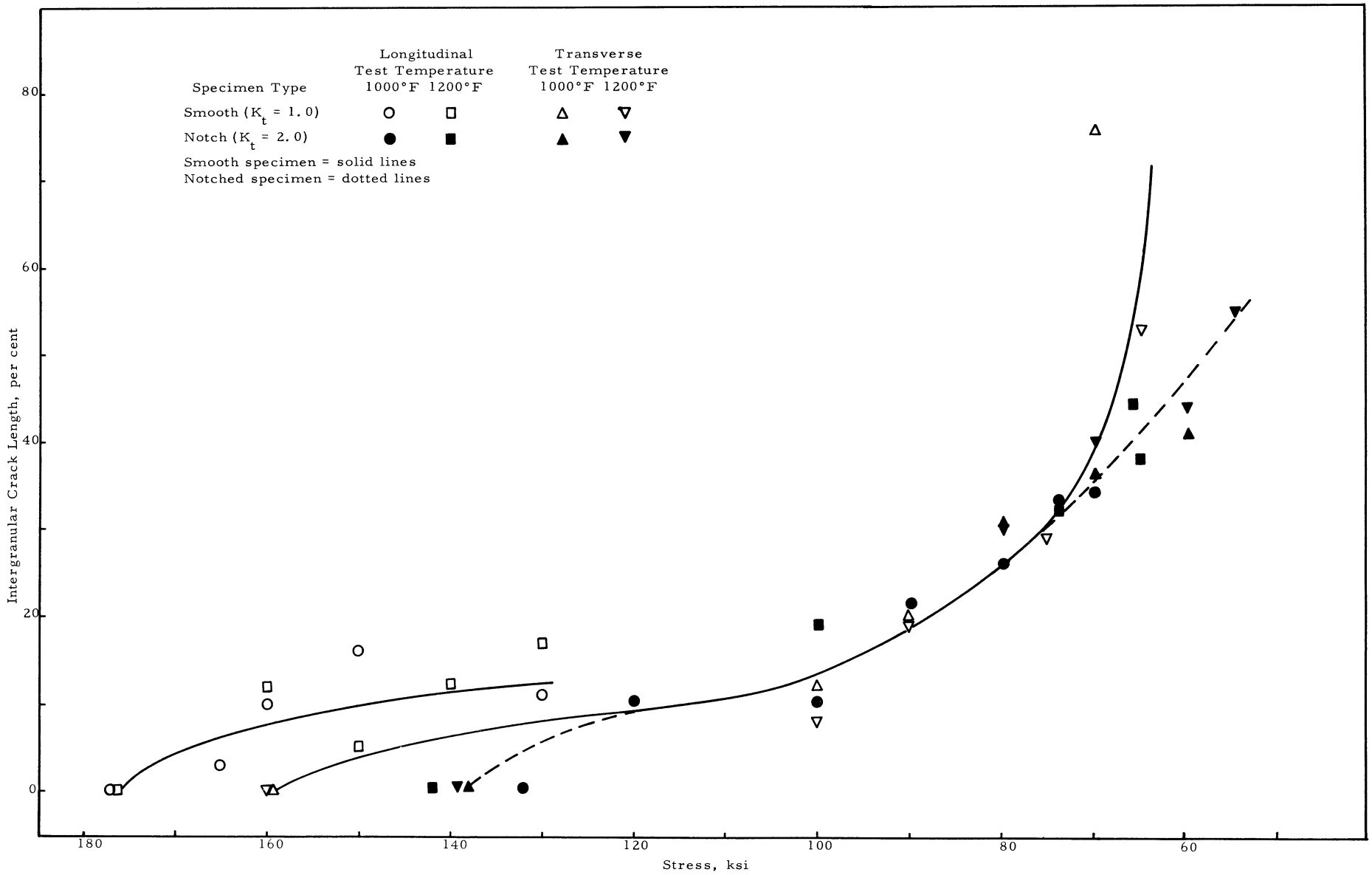

Figure 66. Intergranular crack length versus initial loading stress at 1000° and 1200°F obtained from smooth and notched specimens of 0.026-inch thick Inconel 718 sheet annealed at 1750°F and aged.

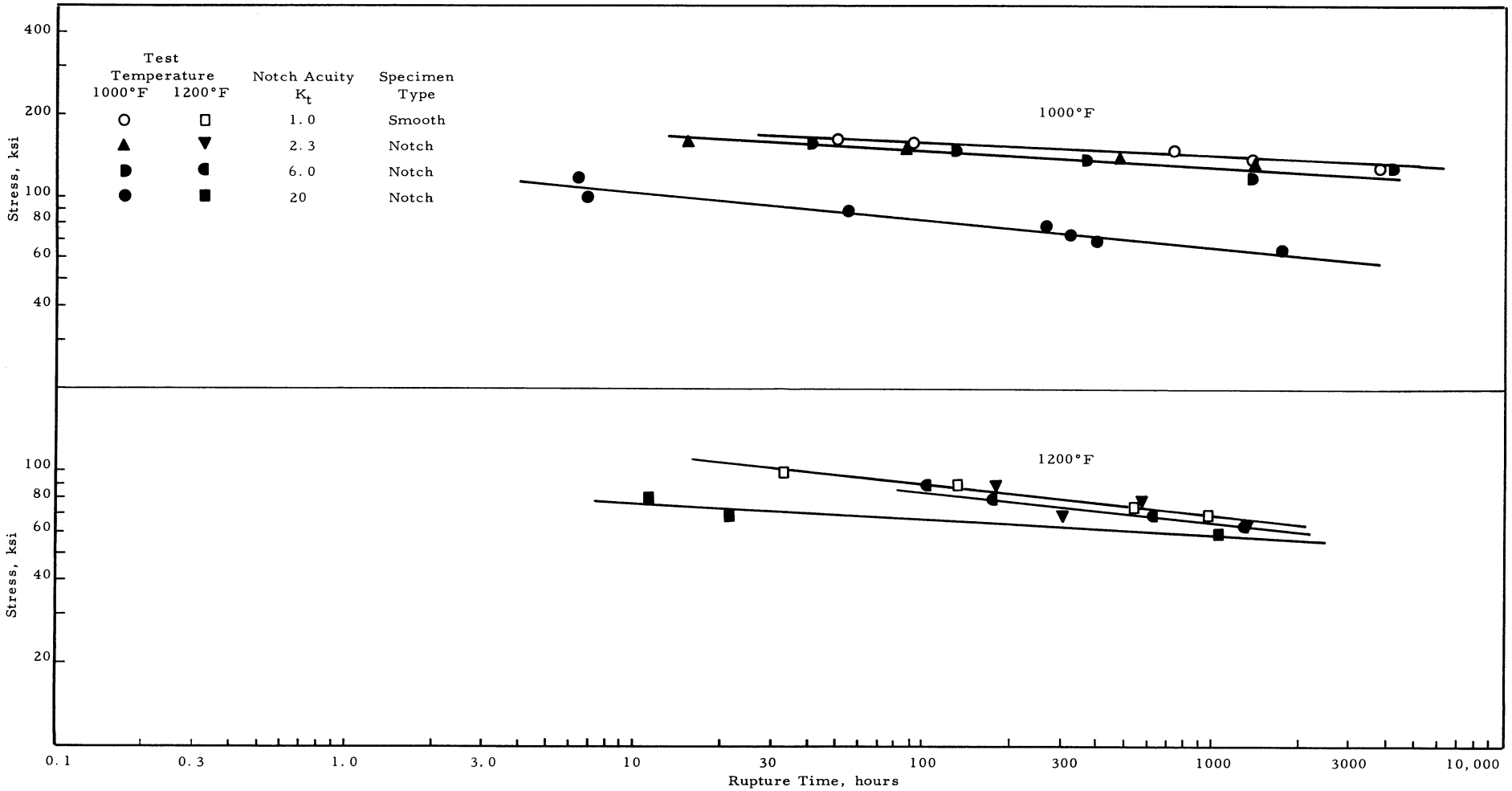

Figure 67. Stress versus rupture time data at 1000° and 1200°F for smooth and notched specimens (K_t's 2.3, 6.0, 20) for 0.026-inch thick Inconel 718 sheet annealed at 1750°F and aged (ref. 3).

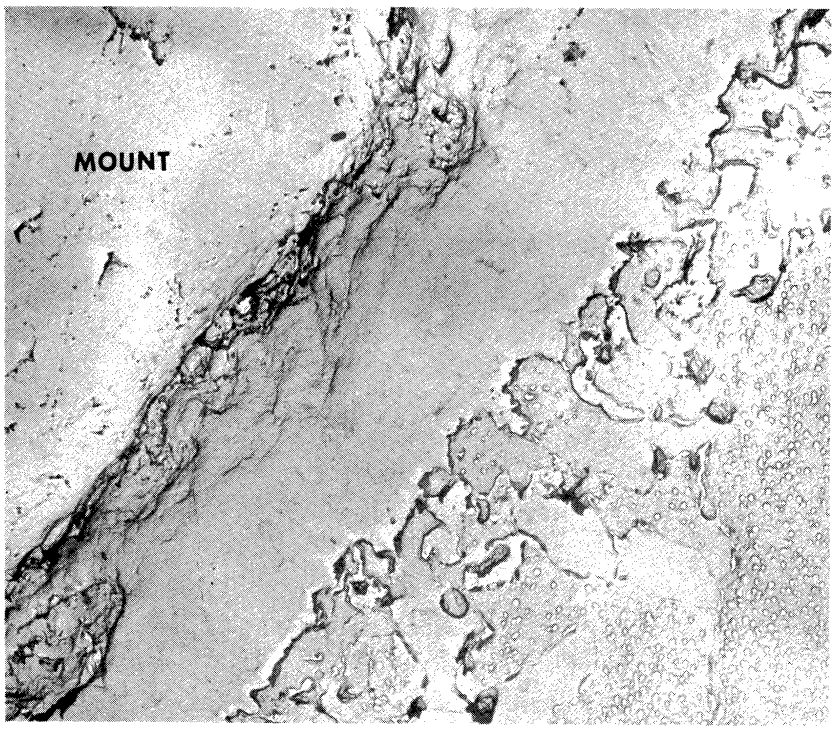

4,000X

Figure 68a. Electron micrograph showing surface effects. (0.026-inch thick Waspaloy sheet smooth specimen solution treated at 1975°F and aged at 1700°F; tested at 1200°F at 80 ksi; ruptured in 1,870 hours.)

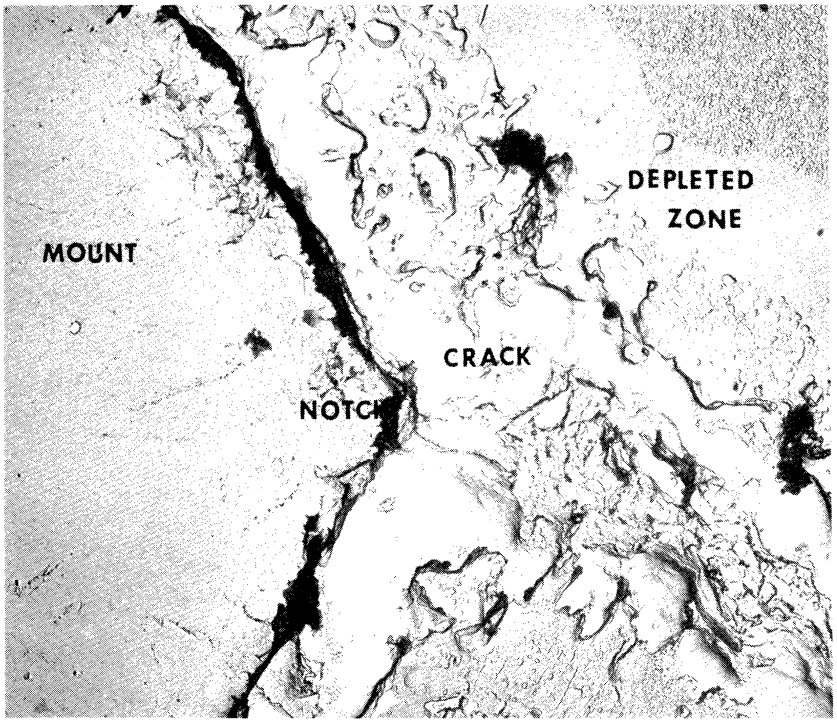

4,000X

Figure 68b. Electron micrograph showing surface effects. (0.026-inch thick Waspaloy sheet notched specimen solution treated at 1975°F and aged at 1400°F; tested at 1400°F at 45 ksi; ruptured in 260 hours at the pin holes.)